

# IDŐJÁRÁS

## QUARTERLY JOURNAL OF THE HUNGARIAN METEOROLOGICAL SERVICE

*Special Issue: Meteorological aspects of water management*  
*Guest Editors: Sándor Szalai*

### CONTENTS

<i>Editorial</i> .....	I
<u>Judit Gerhátné Kerényi</u> : Application of remote sensing for the determination of water management parameters, Hydrology SAF .....	1
<i>Zoltán Gribovszki</i> : Validation of diurnal soil moisture dynamic-based evapotranspiration estimation methods.....	15
<i>Márton Jolánkai, Katalin Kassai M., Ákos Tarnawa, Barnabás Pósa, and Márta Birkás</i> : Impact of precipitation and temperature on the grain and protein yield of wheat ( <i>Triticum aestivum</i> L) varieties .....	31
<i>Angéla Anda, Brigitta Simon, Gábor Soós, and Tamás Kucserka</i> : Estimation of natural water body's evaporation based on Class A pan measurements in comparison to reference evapotranspiration .....	41
<i>István Ihász, Amarilla Mátrai, Balázs Szintai, Mihály Szűcs, and Imre Bonta</i> : Application of European numerical weather prediction models for hydrological purposes.....	59
<i>Péter Csáki, Márton Miklós Szinetár, András Herceg, Péter Kalicz, and Zoltán Gribovszki</i> : Climate Change Impacts on the Water Balance - Case Studies in Hungarian Watersheds.....	81

# IDŐJÁRÁS

*Quarterly Journal of the Hungarian Meteorological Service*

*Editor-in-Chief*  
**LÁSZLÓ BOZÓ**

*Executive Editor*  
**MÁRTA T. PUSKÁS**

## EDITORIAL BOARD

- |                                       |  |
|---------------------------------------|--|
| ANTAL, E. (Budapest, Hungary)         | MIKA, J. (Eger, Hungary)                   |
| BARTHOLY, J. (Budapest, Hungary)      | MERSICH, I. (Budapest, Hungary)            |
| BATCHVAROVA, E. (Sofia, Bulgaria)     | MÖLLER, D. (Berlin, Germany)               |
| BRIMBLECOMBE, P. (Hong Kong, SAR)     | PINTO, J. (Res. Triangle Park, NC, U.S.A.) |
| CZELNAI, R. (Dörgicse, Hungary)       | PRÁGER, T. (Budapest, Hungary)             |
| DUNKEL, Z. (Budapest, Hungary)        | PROBÁLD, F. (Budapest, Hungary)            |
| FERENCZI, Z. (Budapest, Hungary)      | RADNÓTI, G. (Reading, U.K.)                |
| GERESDI, I. (Pécs, Hungary)           | S. BURÁNSZKI, M. (Budapest, Hungary)       |
| HASZPRA, L. (Budapest, Hungary)       | SZALAI, S. (Budapest, Hungary)             |
| HORVÁTH, Á. (Siófok, Hungary)         | SZEIDL, L. (Budapest, Hungary)             |
| HORVÁTH, L. (Budapest, Hungary)       | SZUNYOGH, I. (College Station, TX, U.S.A.) |
| HUNKÁR, M. (Keszthely, Hungary)       | TAR, K. (Debrecen, Hungary)                |
| LASZLO, I. (Camp Springs, MD, U.S.A.) | TÁNCZER, T. (Budapest, Hungary)            |
| MAJOR, G. (Budapest, Hungary)         | TOTH, Z. (Camp Springs, MD, U.S.A.)        |
| MÉSZÁROS, E. (Veszprém, Hungary)      | VALI, G. (Laramie, WY, U.S.A.)             |
| MÉSZÁROS, R. (Budapest, Hungary)      | WEIDINGER, T. (Budapest, Hungary)          |

*Editorial Office: Kitaibel P.u. 1, H-1024 Budapest, Hungary*

*P.O. Box 38, H-1525 Budapest, Hungary*

*E-mail: [journal.idojaras@met.hu](mailto:journal.idojaras@met.hu)*

*Fax: (36-1) 346-4669*

---

**Indexed and abstracted in Science Citation Index Expanded™ and  
Journal Citation Reports/Science Edition**

**Covered in the abstract and citation database SCOPUS®**

**Included in EBSCO's databases**

---

*Subscription by mail:*

*IDŐJÁRÁS, P.O. Box 38, H-1525 Budapest, Hungary*

*E-mail: [journal.idojaras@met.hu](mailto:journal.idojaras@met.hu)*

## *Special Issue: Meteorological aspects of water management*

Precipitation climatology has a very high variability in Hungary. The absolute maximum daily precipitation is equal with the absolute minimum annual precipitation. It can happen flood and drought in the same year and place. Regular event is the excess water, which can cover more than hundred thousand hectares of arable land. But water is not only a limiting factor in the agriculture, source of natural disasters, but could cause problems on other areas of our life, too. Hungary is geographically on the border of the future precipitation change. Depending on climate models and scenarios, increasing or decreasing yearly precipitation sum or no significant change can happen. This uncertainty makes the climate change adaptation difficult. The seasonal changes could have even different sign of tendencies affecting the frequency of water connected extreme meteorological and climatological events.

According to the climate change, qualitative changes in precipitation are mosaic, but rarely significant because of its high variability. Many indicators show the increasing precipitation intensity in Hungary. Therefore, increasing erosion, more frequent flash floods, decreasing available water are expected in the future. Municipality water management faces troubles because of increasing number of heavy precipitation. All these facts request developments in the measurement technique (both in-situ and remote sensing), especially on the area of short term intensity, improved climate, forecast, and applied models. Narrow cooperation is needed among the organizations dealing with water issue. The continuous scientific development in meteorology and climatology has to be applied in other disciplines and used in the strategic planning processes. Only a flexible and cooperative approach makes the effective adaptation actions and the best available cost/benefit ratio possible.

That was the reason why the Hungarian Meteorological Service dedicated the Meteorological Scientific Days to the water management in 2016. This topic is very broad, only a general overview could be given in this time. Multidisciplinarity, problems, and results were shown in the presentations. The sessions dealt with regional and national overviews, meteorological extreme events, measurements techniques, and applications to climate change. The poster session supported the deeper insight into the topics. This volume gives a small part of the presentations, but describes important areas of the connection between the meteorology, water management, and other topics.

The main result of the events was to make evident the increasing requirement of cooperation among the disciplines on scientific, among the organizations on administrative, and among the countries on international level. Without this cooperation we cannot solve even our present problems, which are expected to be larger in the future in the Danube catchment region.

*Sándor Szalai*  
Guest Editor

# IDŐJÁRÁS

*Quarterly Journal of the Hungarian Meteorological Service  
Vol. 122, No. 1, January – March, 2018, pp. 1–13*

## **Application of remote sensing for the determination of water management parameters, Hydrology SAF**

**Judit Gerhátné Kerényi**

*Hungarian Meteorological Service  
P.O.Box 38, H-1525 Budapest, Hungary*

*Author E-mail: muhold@met.hu*

*(Manuscript received in final form March 27, 2017)*

**Abstract**—The European Organisation for the Exploitation of Meteorological Satellite (EUMETSAT) established the Satellite Application Facility on Support to Operational Hydrology and Water management (H-SAF) on July 2005. The aim of the H-SAF is to derive parameters which are important for hydrology, for hydrological models. H-SAF derives precipitation, soil moisture, and snow products based on satellite information, and makes hydrological validation. The Hungarian Meteorological Service takes part in the product validation work.

In this paper we describe the different products, then the validation activities are shown including some examples.

*Key-words:* hydrology, satellite, H-SAF, precipitation, snow, soil moisture, product validation, hydrological validation, flood, drought

### **1. Introduction**

In recent years, severe and catastrophic flood events occurred frequently in many parts of the world. These events demonstrate the importance of improving the flood forecasting and flood warning system. In Hungary, in the last 20 years, flood records were broken along 21 rivers, 3 times at Danube, 5 times at Tisza River.

Another type of meteorological events, the droughts have also caused large problems in the recent years. For example, in 2015, the long warm period during summer and the low precipitation caused drought in some areas of Hungary.

Large number of techniques were developed to derive hydrological parameters from ground and satellite measurements in the last 50 years. EUMETSAT supplies weather and climate-related satellite data, images, and products – 24 hours a day, 365 days a year – to the National Meteorological Services of the EUMETSAT Member and Cooperating States in Europe, and other users worldwide. EUMETSAT established eight Satellite Application Facilities (SAFs) to derive several meteorological parameters, and they also distribute software packages. The various SAFs were established at different times between 1997 and 2005, starting with the Development Phase (DP), which held for 5-years. The activities are now in the Continuous Development and Operations Phases (CDOP). The CDOP-2 period finished in February 2017, and the new 5 year period, the CDOP-3 has started in March 2017.

One of these SAFs is the Support to Operational Hydrology and Water management SAF (H-SAF or Hydrology SAF). The H-SAF was established by the EUMETSAT Council on July 3, 2005. The aim of the H-SAF is to generate and archive high-quality datasets and products for operational hydrological applications. The leading entity of the H-SAF is the Italian Meteorological Service, and the consortium members are eleven European countries (Austria, Belgium, Bulgaria, Finland, France, Germany, Hungary, Italy, Poland, Slovakia, and Turkey) and the ECMWF.

The H-SAF objectives are:

1. to provide new satellite-derived products from existing and future satellites for operational hydrology, as follows:
  - a. precipitation (instantaneous, accumulated),
  - b. soil moisture,
  - c. snow parameter;
2. to perform independent validation of the products by
  - a. statistical calculation using radar and rain-gauge dataset,
  - b. case studies;
3. investigation of the products at hydrological model application.

The Hungarian Meteorological Service takes part as consortium member in the precipitation product validation.

In this paper, first we give information about the precipitation products, after that we describe the snow products. In the third part, we show the soil moisture products.

In Section 5, we detail the validation activity by OMSZ, and some results. Finally, we show some example for the hydrological validation, including Hungarian validation as well.

## 2. Precipitation products

Six different precipitation products (PR-OBS-x, where PR refers to the precipitation, x is the serial number of the product, also referred as Hx) have been developed during the first 5-year period (Mugnai *et al.*, 2013). Since then, one of them was withdrawn. Two of these products are based on passive microwave (MW) measurements received from polar orbiting satellites, while the other 3 products are derived as a combination of infrared and microwave measurements. The MW radiation is sensitive to changes in rain and cloud droplet size distributions due to scattering and emission/absorption processes in clouds. The infrared (IR) data are received from the EUMETSAT geostationary satellites. The infrared measurement gives information about the temperature of the cloud top and the surface of the Earth.

*Fig. 1* shows the spatial coverage of the precipitation products based on the different measurements.

The H01 precipitation product is derived from SSM/I or SSM/I/S passive MW instruments onboard of polar orbiting DMSP satellites (DMSP F17, DMSP F18). Cloud microphysical properties are retrieved by a cloud resolving and a radiative transfer model. *Fig. 2* shows the different precipitation products compared to radar measurements.

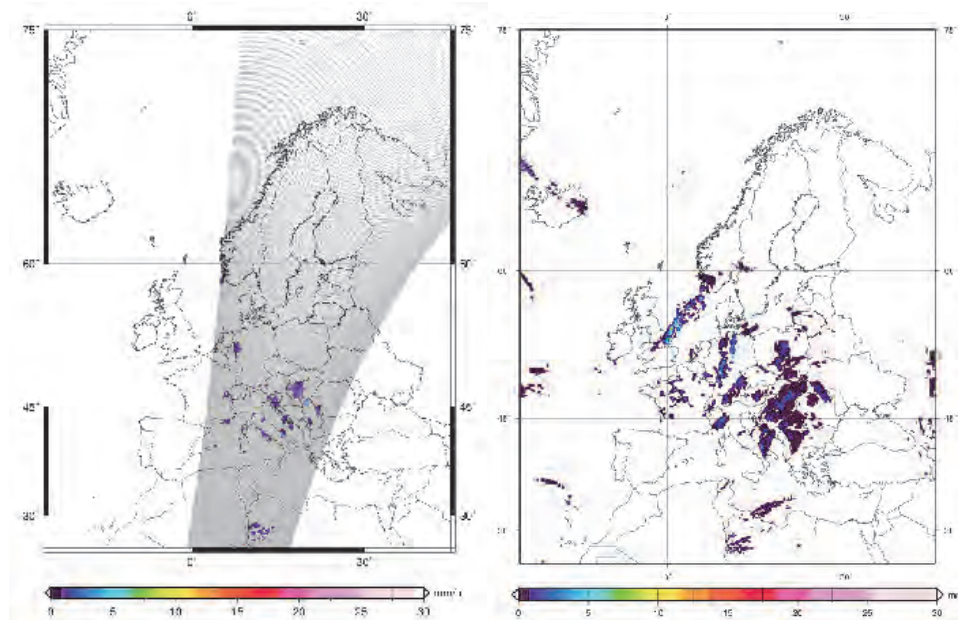


*Fig. 1.* Instantaneous precipitation rain rate from microwave (MW) observation (H01) on the left side, and from MSG IR measurement (H03) on the right side.

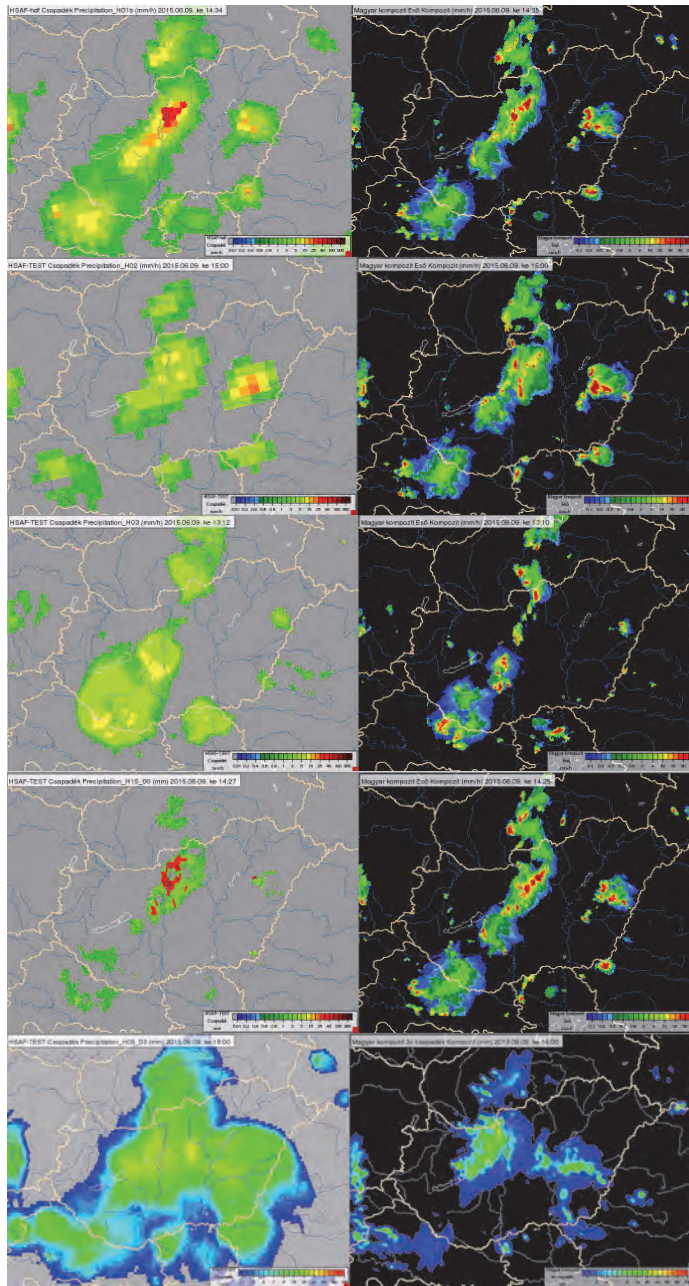


*Fig. 2.* On the left side, the different precipitation products (H01, H02, H03, H15, H05) can be seen, on the right side, the actual radar composite images are presented at different times (H01-14:34 UTC, H02-15:00 UTC, H03-13:12 UTC, H15-14:27 UTC, H05-18:00 UTC) but on the same day, June 9, 2015.

The H02 precipitation product is determined from the MW measurements of the AMSU-A and AMSU-B instruments onboard NOAA satellites (NOAA-18, NOAA-19), and AMSU-A instruments onboard MetOp satellites (MetOp-A, MetOp-B). The precipitation rate is calculated by applying artificial neural network technique. This product consists of the surface precipitation rate and indication of the phase of the precipitation.

The H03 gives instantaneous precipitation intensity in every 15 minutes using IR and MW data. The blended algorithm is based on a real-time collection of IR brightness temperature from MSG satellites and rain intensity estimation from MW measurement (H02) matching in time and space.

The H05 product is an accumulated precipitation product generated from H03 products. The product is derived in every 3 hours, and provides the accumulated precipitation over 3, 6, 12, and 24 hours. It is generated from the H03 data using time integration, but other information such as rain-gauge measurements and very short forecasts from numerical weather prediction model are also used.

H15 product provides instantaneous precipitation intensity in every 15 minutes, which is based on H03 product and DYNAMIC NEFOanalysis (NEFODINA) techniques (*Puca et al., 2005; Melfi et al., 2012*). The NEFODINA is applied for the determination of a convection mask and for redistributing the precipitation value from H01 and H02, based on the characteristics of the convective cells.

### **3. Snow products**

Monitoring the snow parameters – e.g., snow covered area, snow water equivalent (*Fig. 3*) – is not easy because of its natural physical properties. The determination of snow products over mountainous regions is much more complicated. Therefore, different methods were developed for flat land and for mountainous area (*Surer et al., 2012*).

The snow cover map (H10) is derived based on visible and infrared images from both polar and geostationary satellites. Spectral threshold methods are applied. The different spectral characteristics of cloud, snow, and land determine the structure of the algorithm, and these characteristics are obtained from subjective classification of known snow cover features in the images.

The snow status (H11) product gives information whether it is wet or dry and in time series thawing or freezing. At the calculation MW measurements are used, considering that the snow emissivity is different for dry and wet snow. The emissivity increases when snow is wet.

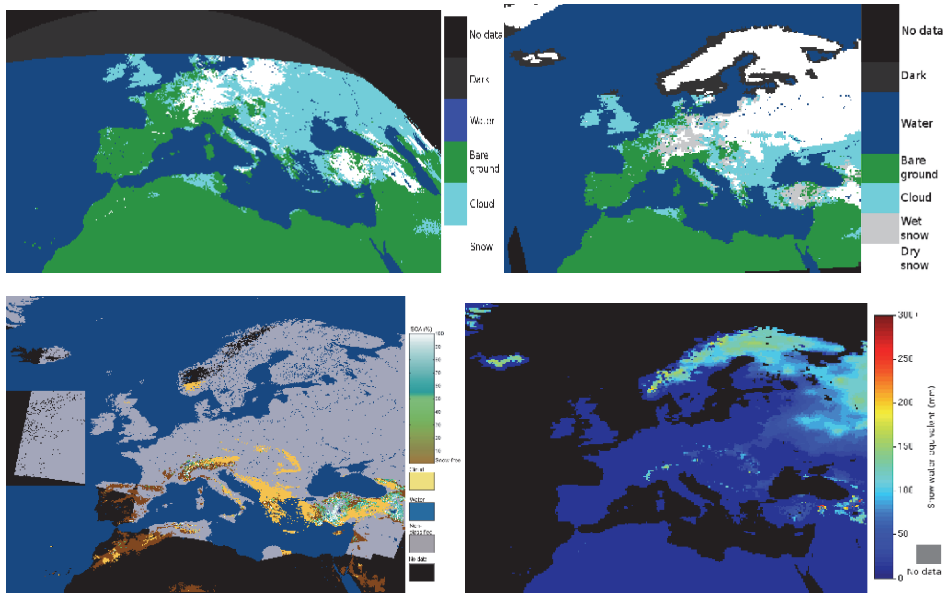


Fig. 3. Top left is the snow cover, top right is the snow status, bottom left is the effective snow cover, bottom right is the snow water equivalent image on January 6, 2017.

The effective snow cover (H12) algorithm is based on a sub-pixel reflectance model applied on METOP-AVHRR data. The product describes the percentage of Snow Covered Area (SCA) within product pixels (0–100%). Knowing the effects of topography on satellite-measured radiances in rough terrain, the sun zenith and azimuth angles, as well as direction of observation relative to these are taken into account in estimating the target reflectances from the satellite images.

The snow water equivalent product (H13) is derived using MW measurements considering that the MWs are sensitive to snow thickness and density. Depending on the snow being dry or wet, the penetration changes (dry snow is more transparent). For mountainous areas, H13 is derived using radiometer data only, while for flat areas, H13 is an assimilation of ground based snow depth observations and satellite data.

#### 4. Soil moisture products

Compared to other components of the hydrologic cycle, the volume of soil moisture is small, nonetheless, it has fundamental importance in many hydrological, biological, and biogeochemical processes, it is a key parameter for flood forecast and numerical weather prediction systems.

The large scale surface soil moisture for the 0.5–2 cm surface layer (H07) is derived using ASCAT scatterometer (Cenci *et al.*, 2016). Based on ERS-1/2

and MetOp scatterometers, there is possibility to measure soil moisture because of the high sensitivity of microwaves to the water content in the soil surface layer due to the pronounced increase in the soil dielectric constant with increasing water content. We have to mention that the scattering depends on vegetation and surface roughness.

The small scale surface soil moisture (H08) is derived from the global product (H07) limited to the H-SAF area. It is generated by disaggregating the global-scale product (25 km resolution) to 1 km sampling. The disaggregation process is performed with a fine-mesh layer.

The profile index in the roots region (H14) is derived by ASCAT scatterometer data assimilation in the ECMWF Land Data Assimilation System. It is derived for 4 layers (thicknesses 0.07, 0.21, 0.72, and 1.89 m). The ECMWF model generates soil moisture profile information according to the Hydrology Tiled ECMWF Scheme for Surface Exchanges over Land (HTESSEL).

*Fig. 4* shows examples for these soil moisture parameters.

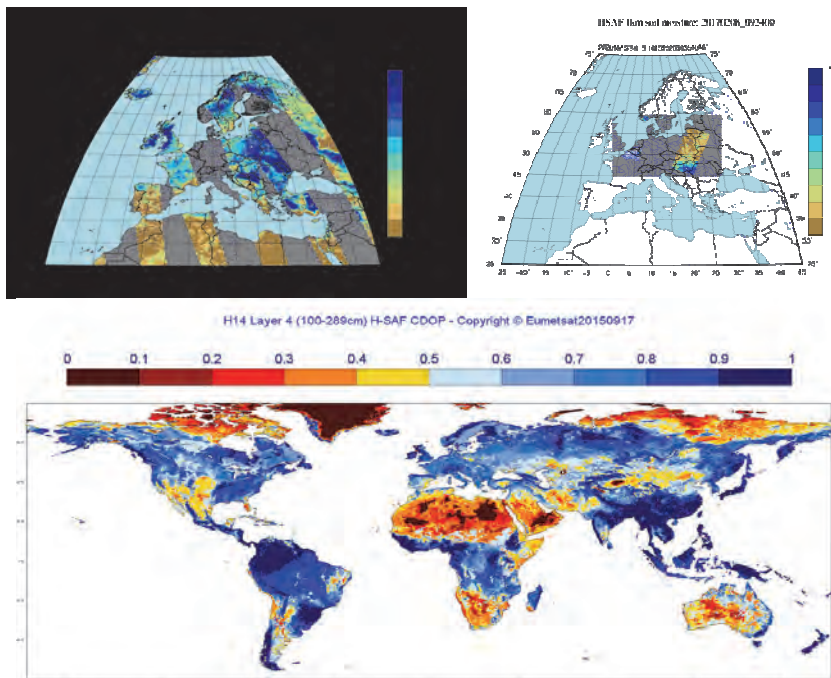


*Fig. 4.* The top left image shows an example for the large scale surface soil moisture. The top right image presents the small scale surface soil moisture. The bottom image is an example of the profile index in the roots region.

## 5. Precipitation validation at the Hungarian Meteorological Service

In the H-SAF project, an independent working group was established to validate the products (*Puca et al.*, 2014). The Hungarian Meteorological Service takes part in the precipitation validation (PV) work. The main activity of the PV is:

- to calculate statistical scores using ground measurements (radar and rain-gauge measurements),
- to perform case study analyses.

For the validation the Hungarian Meteorological Service uses both radar and rain-gauge datasets. The radar network consists of four C-band Doppler radars, the data are available in every 5 minutes. 269 automatic rain-gauge measurements are also used in the validation. From the instantaneous rain-gauge precipitation intensity, at first one hour precipitation intensity is derived, after that the Random Generator of Space Interpolations from Uncertain Observation (GRISO) method (*Pignone et al.*, 2010) is applied to create a precipitation field. *Fig. 5* shows an example for the GRISO precipitation field compared to radar measurements. The interpolated field and the radar measurements show good accordance both in precipitation area and precipitation intensity, mainly at high intensity precipitation.

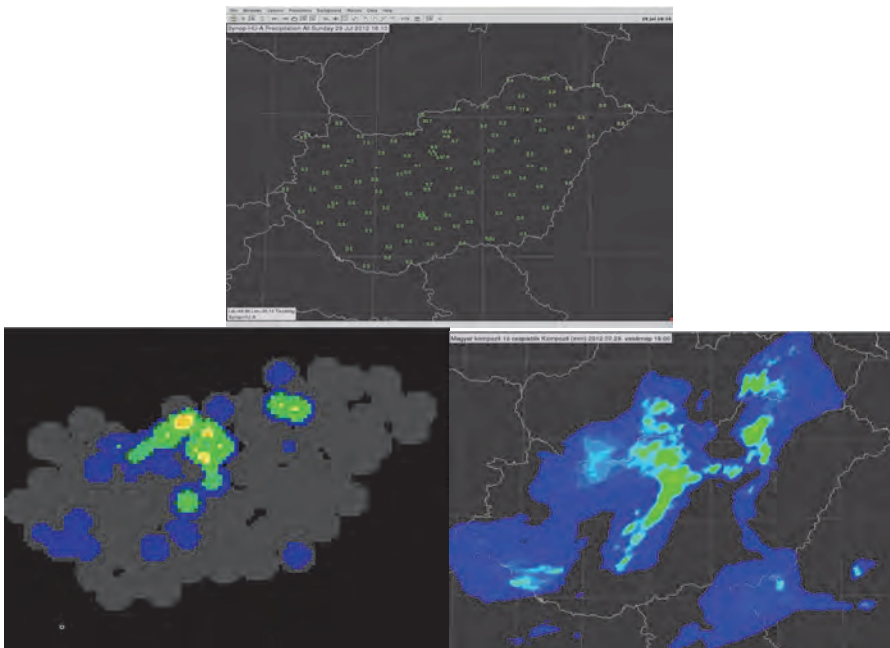


*Fig. 5.* The top image shows the precipitation measurements based on rain-gauge network. The bottom left image presents the interpolated precipitation field based on GRISO method. The bottom right image is the radar measurements.

Statistical scores (mean error, standard deviation, root mean square error, correlation coefficient) for a monthly dataset are calculated. Multicategory scores (probability of detection (POD), false alarm rate (FAR), critical success index (CSI)) are also derived.

Hereinafter we would like to show an example from the multicategory results. *Fig. 6* shows the scores for H03 product for the June 2012 – May 2013 period. The statistical calculation is performed for different precipitation categories. This figure shows the multicategory scores when the precipitation intensity is larger than 0.25 mm/h (index is 0), and at >1 mm/h (index is 1). As we can see they have an annual trend. During the summer period, POD values are much higher than during winter time. During summer time, when convective precipitation is much more frequent and the intensity is higher, the determination of the precipitation intensity values is much easier.

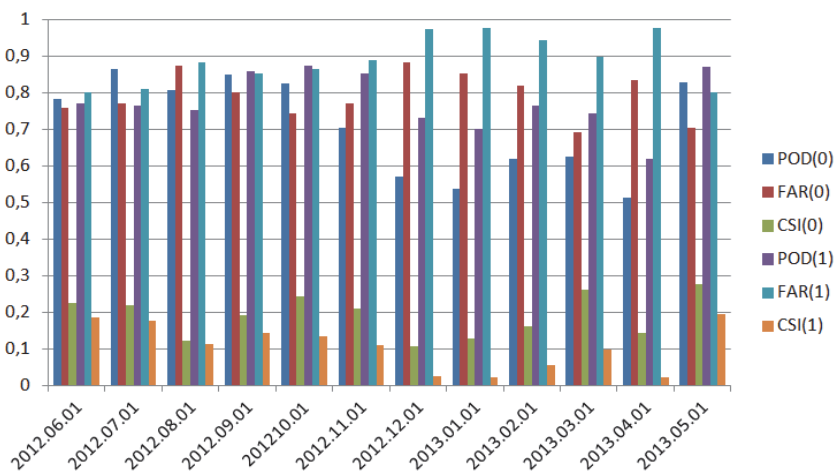


*Fig. 6.* Multicategory scores for the H03 product for the June 2012 – May 2013 period for two different datasets: precipitation intensity is larger than 0.25 mm/h (index is 0), and at >1 mm/h (index is 1).

### 6. Hydrological validation

The main purpose of the hydrological validation program is products' quality assessment and their continuous monitoring by product validation, evaluation, and interfacing with hydrological models, performed both through near real-time and off-line impact studies. The test sites for hydrological validation are located in different parts of the HSAF area. 8 countries (Belgium, Bulgaria, Finland, Germany, Italy, Poland, Slovakia, and Turkey) participate in the validation (*Fig. 7*).

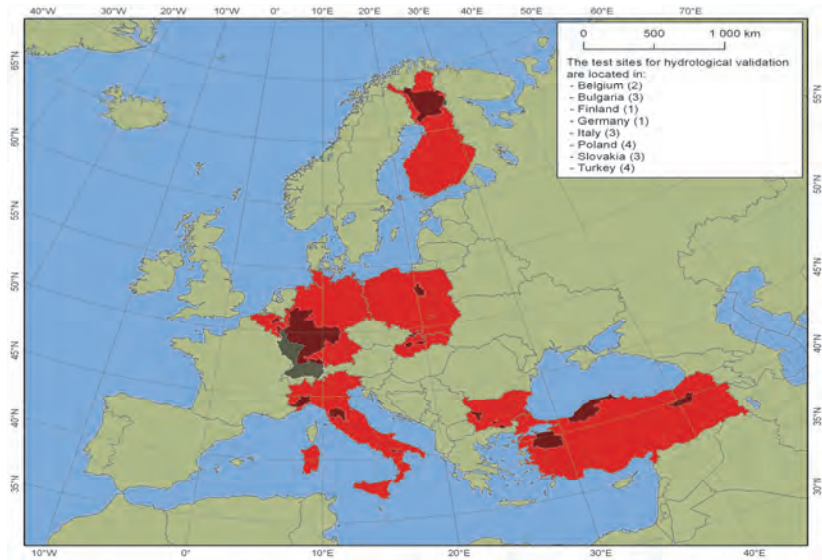


Fig. 7. The test sites of the hydrological validation program.

Different runoff models are applied by the countries to calculate the discharge. Using the runoff model, they calculate the discharge for the catchment area using H-SAF, or ground precipitation products. These calculations are compared with ground truth measurements. Fig. 8 shows the scheme of this proceeding. At the simulation the H03 and H05 products are used, considering the time resolution.

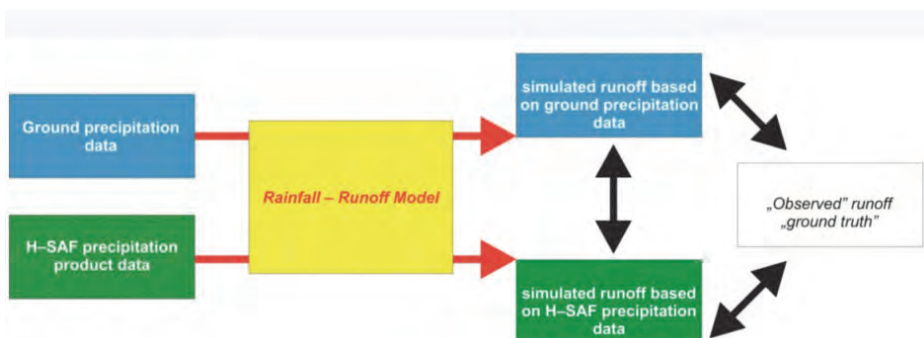
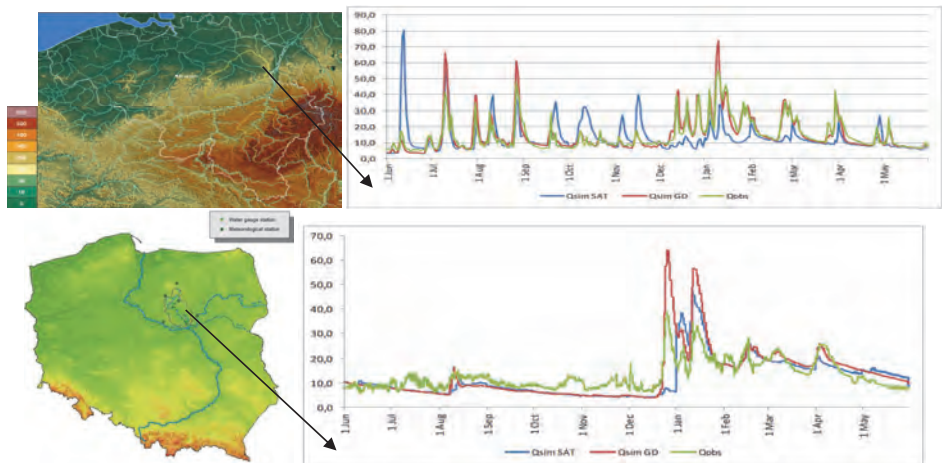


Fig. 8. The scheme of the hydrological validation using runoff model based on two different datasets (H-SAF product, ground precipitation product) and ground truth measurement.

In the next part, 2 different results will be shown, one is calculated for the Demer catchment area in Belgium, the other is for Wkra catchment area in Poland during the June 2012 – May 2013 period (*Fig. 9*).

Red lines show the results simulated by ground measurements, blue lines represent the calculation using the H-SAF product, finally, green lines indicate the ground observations. If we look at the result at Demer catchment, we can see better agreement during the summer period than in winter, due to the fact that the determination of the precipitation area / intensity is much more easier at convective cases. If we look at the other catchment area, during the first half of the period when the discharges were low, the two simulated data show very good agreement, while the measured data were higher. In the second half, for example in January, the two simulated data overestimated the discharge, while since February, the three dataset show similar trends.



*Fig. 9.* The top images show the catchment area in Belgium, and the results of the hydrological validation, the bottom images show the same in Poland

In Hungary, no company takes part in the Hydrology Validation group. Nevertheless, recently the General Directorate of Water Management in Hungary has chance within a framework of a Visiting Scientific Program (2017) to make similar calculation for the Rába catchment area to investigate the H-SAF precipitation products. The first preliminary results are shown in *Fig. 10*.

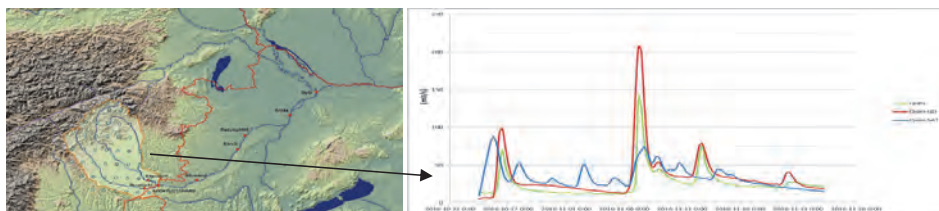


*Fig. 10.* The images show the catchment area in Hungary, and the results of the hydrological validation for the period October 22–November 26, 2016.

In October 2016, large flood caused problem at the Rába River. Based on the 3-hour H05 precipitation product, the discharge was calculated for this period. At the beginning of the period, a time shift can be seen at the simulated discharge derived from H-SAF data. To derive the reason of this, further investigation is needed. In some days, when the discharge was low, the H-SAF product overestimated it, while other cases were underestimated. Only at the last 10 days we can see good agreement between the three datasets.

## 7. Summary

In this paper we gave a short description about the Hydrology SAF work. The webpage of the H-SAF project, where all information can be reached is <http://hsaf.meteoam.it/>.

All H-SAF products are available for all users free of charge. At the moment, there are two ways to get the H-SAF product: download the data from H-SAF server, the near real-time data are available via EUMETCast (EUMETSAT's primary dissemination mechanism). The number of the users reached 1000 by the end of 2015. The main users are: state institutions (51%), universities (20%), private companies (18%), and private users (11 %).

In this paper we presented the products developed until the end of the CDOP-2 period. The following period started in March 2017. The EUMETSAT in this 5-year period plans to launch the Meteosat Third Generation (MTG) satellite, which will give much more information: better time and spatial resolution, more channels. For example, the benefits of the Lightning Imager are detecting, monitoring, tracking, and extrapolating, in space as development of active convective areas and storm lifecycles in time. The application of this information will improve the accuracy of the precipitation area derived by H-SAF.

**Acknowledgements:** The H-SAF project is funded by EUMETSAT. I am grateful for the cooperation of all members of the project, but first of all *Silvia Puca* (Italian Civil Protection Department, Italy) who is the coordinator of the Product Validation Group. I would like to say thanks to *Michal Kasina* (Institute of Meteorology and Water Management, Poland) and *Pierre Baguis* (Royal Meteorological Institute of Belgium) who gave images about the results for their catchment area, and also to *Boglárka Gnandt* (General Directorate of Water Management, Hungary) for providing her preliminary results of the hydrological validation.

## References

- Cenci, L., Laiolo, P., Gabellani, S., Campo, L., Silvestro, F., Delogu, F., Boni, G., and Rudari, R., 2016: Assimilation of H-SAF Soil Moisture Products for Flash Flood Early Warning Systems. Case Study: Mediterranean Catchments. *IEEE J. Select. Topics Appl. Earth Observ. Remote Sens.* 9(12) Part 2.
- Melfi, D., Zauli, F., Biron, D., Vocino, A., and Sist, M., 2012: The impact of NEFODINA convective cloud identification in the rain rate retrieval of H-SAF. Proceedings of the 2012 EUMETSAT Meteorological Satellite Conference, Sopot, Poland, 3-7 September 2012, EUMETSAT P61.
- Mugnai, A., Casella, D., Cattani, E., Dietrich, S., Laviola, S., Levizzani, V., Panegrossi, G., Petracca, M., Sano, P., Di Paola, F., Biron, D., De Leonibus, L., Melfi, D., Rosci, P., Vocino, A., Zauli, F., Pagliara, P., Puca, S., Rinollo, A., Milani, L., Porcu, F., and Gattari, F., 2013: Precipitation products from the hydrology SAF. *Nat. Hazards Earth Syst. Sci.* 13, 1959–1981.  
<https://doi.org/10.5194/nhess-13-1959-2013>
- Pignone, F., Rebora, N., Silvestro, F., and Castelli, F., 2010: GRISO – Rain, CIMA R Research Foundation, Savona, Italy. Operational Agreement 778/2009 DPC-CIMA, Year-1 Activity Report 272/2010. (in Italian)
- Puca, S., De Leonibus L., Zauli, F., Rosei, P., and Biron, D., 2005: Improvements on numerical “object” detection and nowcasting of convective cell with the use of SEVIRI data (IR and WV channels and neural techniques, The World Weather Research Programme’s Symposium on Nowcasting and very Short range Forecasting, Toulouse, France, 5-9 September 2005.
- Puca, S., Porcu, F., Rinollo, A., Vulpiani, G., Baguis, P., Campione, E., Ertürk, A., Gabellani, S., Iwanski, R., Jurasek, M., Kanak, J., Kerényi, J., Koshinchanov, G., Kozinarova, G., Krahe, P., Lapeta, B., Lábó, E., Milani, L., Okon, L., Öztopal, A., Pagliara, P., Pignone, F., Rachimow, C., Rebora, N., Roulin, E., Sönmez, I., Toniazzo, A., Biron, D., Casella, D., Cattani, E., Dietrich, S., Laviola, S., Levizzani, V., Melfi, D., Mugnai, A., Panegrossi, G., Metracca, M., Pano, P., Zauli, F., Rosei, P., De Leonibus, L., Agosta, A., and Gattari, F., 2014: The validation service of the hydrological SAF geostationary and polar satellite precipitation products. *Nat. Hazards Earth Syst. Sci.* 14, 871–889.  
<https://doi.org/10.5194/nhess-14-871-2014>
- Surer, S. and Akyurek, Z., 2012: Evaluating the utility of the EUMETSAT HSAF snow recognition product over mountainous areas of eastern Turkey. *Hydrol.Sci. J.* 57, 1684–1894.  
<https://doi.org/10.1080/02626667.2012.729132>



# IDŐJÁRÁS

*Quarterly Journal of the Hungarian Meteorological Service  
Vol. 122, No. 1, January – March, 2018, pp. 15–30*

## **Validation of diurnal soil moisture dynamic-based evapotranspiration estimation methods**

**Zoltán Gribovszki**

*Institute of Geomatics and Civil Engineering, University of Sopron  
Sopron, Bajcsy-zs. u. 4. H-9400, Hungary*

*Author E-mail: gribovszki.zoltan@uni-sopron.hu*

*(Manuscript received in final form September 8, 2017)*

**Abstract**—Evapotranspiration (*ET*) is one of the most important elements of water balance. Despite its importance, exact determination for a mosaic surface cover is very limited; therefore, there is a demand for relatively simple and cheap methods of determination that work on a small spatial scale.

Water uptake of forest vegetation in groundwater discharge areas generally has a strong influence on the water resources induced diurnal signal in soil moisture, and in the water table. Diurnal methods in a shallow groundwater environment are widely used nowadays for *ET* estimation.

By modifying the well-known *White* (1932) method and adapting to soil moisture data, a new technique was developed to calculate *ET* from soil moisture readings, eliminating the need of specific yield (a weakest point of the groundwater signal based methods). The new method was validated using hydro-meteorological data of the Hidegvíz Valley experimental catchment located in the Sopron Hills at the western border of Hungary.

The 30-min *ET* rates of the proposed method lag 30-60 minutes behind those of the reference Penman–Monteith method, but otherwise the two estimates compare favorably.

On a daily basis, the newly derived *ET* rates are very close to PM estimates, but on average, they are 38% higher than the ones obtainable with the original *White* method. Comparing the *ET* rates of the proposed method with traditional *ET* estimates from soil moisture, a significant difference can be ascertained.

The proposed method has potential benefits in groundwater discharge areas, especially in light of the changing climate with its warmer and drier growing seasons, that will likely result in limited water resources.

*Key-words:* evapotranspiration, soil moisture, diurnal signal, discharge areas, forest

## 1. Introduction

After precipitation, evapotranspiration (*ET*) is the second largest element of the water balance globally. In Hungary (on the border of the sub-humid and semi-arid climate conditions), *ET* makes up about 90% of the precipitation on the catchments scale in long-term average. Despite the importance of *ET*, it is determined mostly as a lumped residual flux from a long-term water balance equation of a catchment. This method has some drawbacks. It cannot give spatially distributed information within a catchment and is limited in terms of time resolution, because it only considers long-term average values. Using data of a local weather station for *ET* calculation, we can acquire more detailed time information, but the space domain limits of the approach remain. Nowadays, the scintillometer technique and remote sensing based information has started to resolve the problem of spatial distribution at a larger scale, but the application of these methods are still limited with highly heterogeneous, mosaic surface cover within a small spatial scale (*Nachabe et al.*, 2005).

Moreover, in some forest covered shallow groundwater areas of the Hungarian Great Plain, *ET* was determined to be larger than precipitation using remote sensing based *ET* estimation techniques (*Szilágyi et al.*, 2012). The deep root system of forests can often tap the shallow groundwater level (if it exists), thus leading to high *ET* that frequently exceeds precipitation. In these groundwater discharge areas, the average annual *ET* was about 70–80 mm more than the mean annual precipitation rate of the region. This negative water balance can be maintained if forests create a local depression in the water table so as to induce groundwater flow directed toward them. Otherwise, forest growing in these groundwater discharge areas possess very good biological productivity, enabling forest management companies to secure a reliable income. As the previous example showed, exact estimation of *ET* in shallow groundwater areas are important not only from a water resources viewpoint, but also from an ecological and economic viewpoint as well.

In areas with a high aridity index ( $ETP/P > 1$ ) and a shallow water table, groundwater supplies most of the plant transpiration requirements (*Luo and Sophocleous*, 2010; *Loheide et al.*, 2005; *Gribovszki et al.*, 2008; *Nachabe et al.*, 2005).

In these shallow water table environments, transpiration of plants induces a diurnal signal not only in the water table, but in soil moisture as well. *Haise and Kelley* (1950) first described a diurnal signal of the soil moisture profile in their tensiometer experiments. These fluctuations can be observed mostly in groundwater discharge areas (*Gribovszki et al.*, 2010; *Móricz et al.*, 2012).

The direct driving force of the signal in the growing season is evapotranspiration (during rainless periods the latter is dominated by transpiration), and the signal is regulated by relative humidity and radiation. The evapotranspiration-induced diurnal signal (in soil moisture and groundwater) has

an early morning maximum and a late afternoon minimum (Fig. 1). *Gribovszki et al.* (2010) prepared an elaborate review about this signal and the characteristics of it.

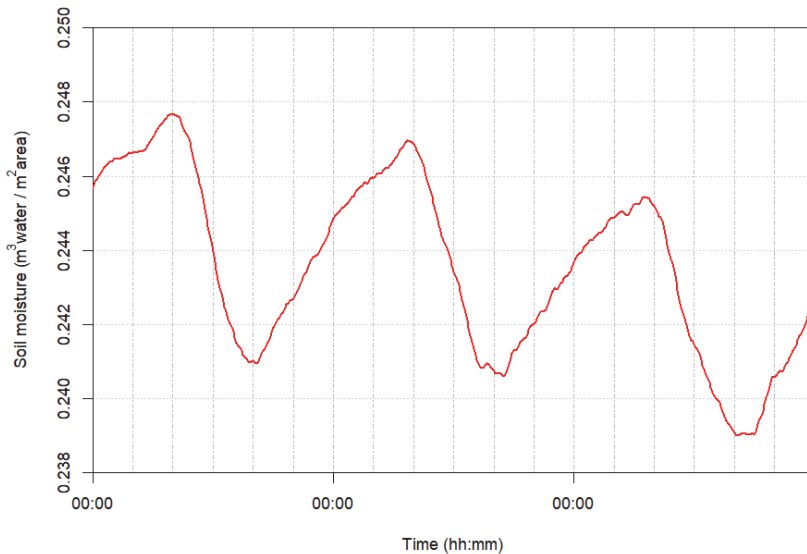


Fig. 1. Typical diurnal pattern in soil moisture induced by evapotranspiration.

*White* (1932) developed a method that uses observations of the groundwater diurnal signal to calculate plant groundwater uptake. Use of this technique and its modifications is frequent for *ET* estimation (*Bauer et al.*, 2004; *Dolan et al.*, 1984; *Engel et al.*, 2005; *Gribovszki et al.*, 2008; *Loheide*, 2008; *Mould et al.*, 2010; *Reigner*, 1966; *Schilling*, 2007, *Soylu et al.*, 2012, *Gribovszki et al.*, 2010); nevertheless, specific yield estimation remained a weak point of the groundwater signal based methods.

*Nachabe et al.* (2005) used the *White* (1932) approach for high frequency soil moisture profile data, thereby eliminating the application of the specific yield. *Gribovszki* (2014) modified the *Nachabe et al.* (2005) technique by adapting the empirical version of *Gribovszki et al.* (2008) method, taking into account the diurnally changing replenishment rate from the water table to the vadose zone. The main objective of this paper is to validate the new diurnal soil moisture based technique (which calculates diurnally changing replenishment rate (*Gribovszki*,

2014) using reference *ET* estimations and compare this new method with the White approach (which calculates constant replenishment rate all along the day (Nachabe *et al.*, 2005)) and traditional technique (which does not calculate any replenishment rate (Dingman, 2002)).

## 2. Material and methods

The dataset used for *ET* estimation originated from a valley location (47°40'20"N, 16°27'42"E) of the Hidegvíz Valley experimental catchment in western Hungary (Fig. 2).

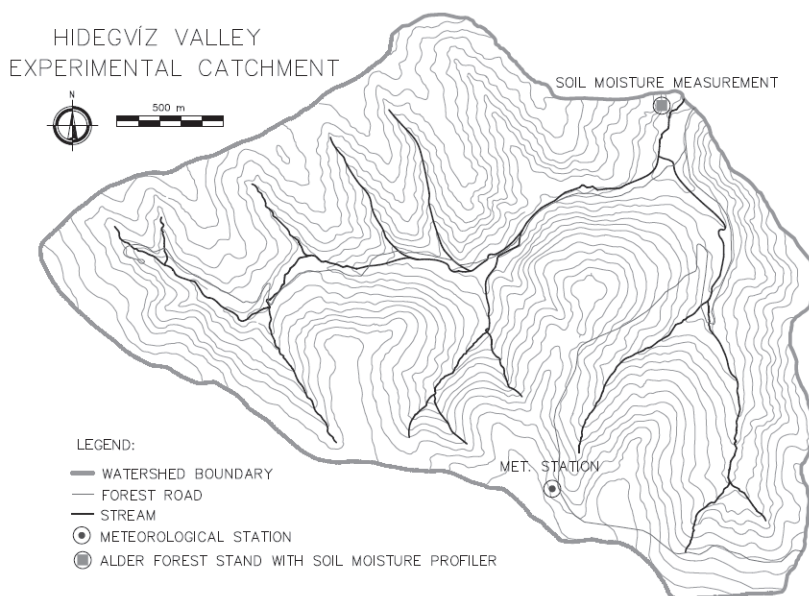


Fig. 2. Location of the study site at the outlet point of the experimental catchment.

There are fluvial sediments deposited on the crystalline bedrock in the research area. Over the slopes and hilltops, an unclassified formation in a 10–50-m-thick layer exists. A finer-grained sandy layer, which is a good aquifer, appears in the valleys (Kisházi and Ivancsics, 1985).

The experimental plot is in a valley bottom, and the soil type there (groundwater discharge area) is loamy sand. The average physical properties of the soil profile are the following: saturated hydraulic conductivity  $k=0.18$  m/d; saturated moisture content  $\theta_{sat}=0.51$ ; field capacity at 0.33bar  $\theta_{fc}=0.28$ .

The vegetation of the experimental plot is a typical phreatophyte azonal ecosystem dominated by alder (*Alnus glutinosa* (L.) Gaertn.). The mean height of the middle-aged riparian forest stand is about 15 m with a mean trunk diameter of 13 cm (at a height of 1.3 m). The leaf area index (*LAI*) of this forest stand in the growing season was approximately 7.

The area enjoys a sub-alpine climate, with daily mean temperatures of 17 °C in the summer, and with an annual precipitation of 750 mm (*Marosi and Somogyi, 1990*). A more detailed description of the area can be found in *Gribovszki et al. (2006)*.

### 2.1. Soil moisture and groundwater data sampling

Six soil moisture capacitive sensors were implemented at 10, 20, 30, 40, 60, and 100 cm below the ground surface in a riparian alder forest (*Fig. 2*). Sensors provide volumetric water content ranging from oven dryness to saturation with accuracy of  $\pm 0.06$  m<sup>3</sup>/m<sup>3</sup>. Soil moisture values were collected every 10 minutes. These data were used for estimation of total soil moisture of the unsaturated soil profile using the following equation:

$$\theta_T = \int_0^{z_0} \theta dz, \quad (1)$$

where  $\theta_T$  is the total soil moisture (m),  $z$  is the depth (m) below the ground surface, and  $\theta$  is the water content (m<sup>3</sup> water in m<sup>3</sup> soil). For  $z_0$  we used 1.2 m as an arbitrary depth regarding *Fig. 3*, because it is always below the water table even during the growing season.

A groundwater well dataset showed that the groundwater depth in the riparian zone varied between 0.8 to 1.1 m during typical drought periods (*Fig. 3*). Consequently, the tree root system is in direct contact with the saturated zone or, at the very least, with the capillary fringe throughout the year in this shallow water table environment (*Shah et al., 2007*).

For the analysis, we used the rainless periods in the summer of 2013 (altogether 89 days). 30-minute estimates were compared in selected completely rainless periods. For daily comparison, we selected days with less than 3 mm of precipitation. Rain events below this threshold did not present significant disturbance in the soil moisture diurnal signal; therefore, they did not cause problems for *ET* calculation. The canopy catches the precipitation from these light rain events completely.

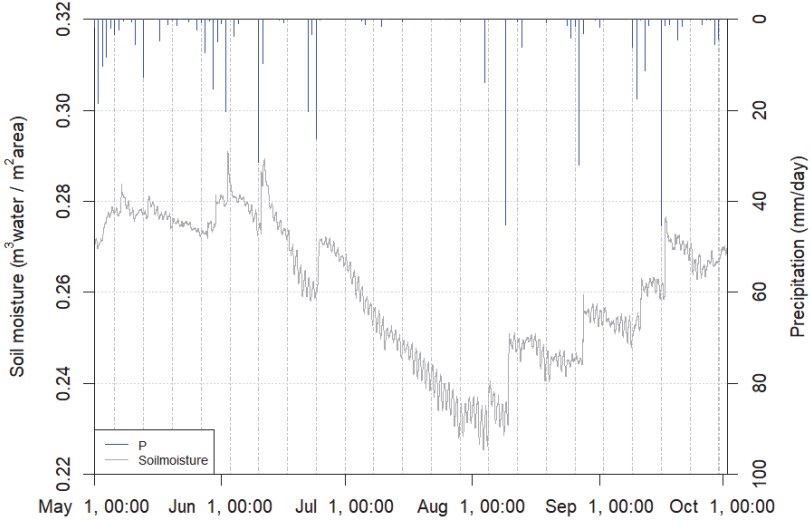


Fig. 3. Soil moisture and precipitation time series for the 2013 growing season.

For  $ET$  estimation, very accurate soil moisture measurements with relatively high frequency are crucial. Whenever the original measurements are inaccurate, differentiation of the soil moisture record may invoke large errors in the estimations. The application of a low-pass filter (smoother) is recommended to reduce uncertainty. Care must be taken not to “over-filter” the time series, because this can lead to the loss of important details about the process of the diurnal fluctuations. We used 30-min data for the analysis, and the sampling interval was 10 min.

## 2.2. Theoretical basis of $ET$ estimation

The basic expression of  $ET$  estimation is the water balance equation for the soil moisture profile:

$$\frac{dS_{sm}}{dt} = \frac{d\theta_T}{dt} = Q_i - Q_o - ET = Q_{net\_sm} - ET, \quad (2)$$

where  $S_{sm}$  ( $\text{m}^3/\text{m}^2$ ) is the stored volume of water in the soil moisture profile in a unit area, which is the same as  $\theta_T$  is the total soil moisture in soil profile ( $\text{m}^3/\text{m}^2$ ),  $Q_i$  is the incoming and  $Q_o$  is the outgoing water flux ( $\text{m}^3/\text{s}/\text{m}^2$ ) to and from the soil column,  $Q_{net\_sm} = Q_i - Q_o$  is the net flux/replenishment rate ( $\text{m}^3/\text{s}/\text{m}^2$ ), and  $ET$  is the evapotranspiration ( $\text{m}^3/\text{s}/\text{m}^2$ ).

The soil moisture of the riparian zone, which is directly connected to the water table in discharge zones of shallow groundwater environments, generally meets the transpiration demand of vegetation. In drought periods, groundwater typically replenishes the soil moisture used by evapotranspiration. Around the timing of the soil moisture extrema, when  $dS_{sm}/dt = 0$ , the net flux,  $Q_{net\_sm}$  and the  $ET$  demand, are in an equilibrium in Eq. (2).  $dS_{sm}/dt > 0$  and  $Q_{net\_sm} > ET$  on the rising limb and  $dS_{sm}/dt < 0$  and  $Q_{net\_sm} < ET$  are on the falling limb of the soil moisture hydrograph. The  $ET$  rate is largest during the day when the soil moisture curve is approximately the steepest on the falling limb, which is typically close to the radiation maxima. The smallest  $ET$  rate, however, does not necessarily take place when the rising limb of the groundwater level signal is the steepest, but rather just prior to dawn when vapor pressure deficit is at its diurnal minimum. The minima in the soil moisture is accompanied by the steepest hydraulic gradients, so when  $ET$  starts to decrease, the steep hydraulic gradient can deliver water to the vadose zone very efficiently, replenishing it fastest right after the occurrence of the soil moisture minimum.

### 2.3. Traditional method

Traditionally, soil moisture data on a daily time step can be used for  $ET$  ( $ET_{trad}$ ) calculation (Dingman, 2002). The calculation process follows the rearranged Eq. (2) neglecting the net flux rate in a daily time step:

$$ET_{trad} = \frac{d\theta_T}{dt_{daily}} = \theta_{T(j)} - \theta_{T(j-1)}, \quad (3)$$

where  $\theta_{T(j)}$  is the total soil moisture of the  $j$ th day,  $\theta_{T(j-1)}$  is the total soil moisture of the  $(j-1)$ th day. Eq. (3) neglects the replenishment rate from below. This is true only in circumstances where the water table is deep enough to prevent root contact.

### 2.4. Traditional diurnal method (White approach)

White (1932) worked out a method of estimating  $ET$  rates on a daily time step based on diurnal fluctuations of the water table. Nachabe (2005) adapted this method for total soil moisture of the vadose zone, thereby eliminating the difficulty of estimating the specific yield, which was the limitation of the original White approach and all other groundwater fluctuation based methods.

Using the original White (1932) approach, Nachabe (2005) assumed that during the predawn/dawn hours, when  $ET$  is negligible, the rate of the observed total soil moisture increase is directly proportional to the net flux rate (it represents the rate of water supply to a unit area). The slope of the tangential line ( $Q_{netmin\_sm}$  ( $m^3/s/m^2$ )) drawn to the total soil moisture level curve in these sections was determined. By extending the tangential line over a 24-hour period and taking the

difference in total soil moisture, one would obtain an estimate of the total water supply to the unit area over a day. The daily rate of water supply obtained thus (replenishment rate) must typically be modified by  $d\theta_T/dt_{daily}$  ( $m^3/s/m^2$ ), the difference in the observed soil moisture over the 24-hour period, since it is rare for soil moisture to return to the same elevation it had the day before. Otherwise, the  $d\theta_T/dt_{daily}$  value is the same as the evapotranspiration from traditional estimates ( $ET_{trad}$ ) regarding Eq. (3).

In this way, the daily  $ET$  rate is obtained by

$$ET_{white\_sm} = 24 \cdot Q_{netmin\_sm} + \frac{d\theta_T}{dt}_{daily} \cdot \quad (4)$$

It is worth noting that the White approach assumes a constant net supply rate throughout the day. This flux is estimated in the predawn/dawn hours when  $ET$  is close to zero and the supply rate is the smallest for the day.

### 2.5. New diurnal method (diurnally changing replenishment rate)

The water table diurnal signal was used for  $ET_{gw}$  (evapotranspiration from groundwater) estimation by *Gribovszki et al.* (2008). This approach takes into account a diurnally changing replenishment rate, not a constant one as *White* (1932) had supposed earlier. The theory of the groundwater diurnal signal based method *Gribovszki* (2014) applied for  $ET$  calculation used soil moisture data.

The steps of the new  $ET$  estimation approach are the following. First, the total soil moisture is differenced in time (half-hourly or hourly time steps are convenient) to obtain  $d\theta_T/dt$ . The new time series (*Fig. 4*) symbolizes the difference between water supply ( $Q_{net\_sm}$ ) and demand ( $ET$ ) over the soil profile. At night when  $ET$  is almost zero,  $Q_{net\_sm}$  can be calculated using the simplified water balance:

$$\frac{d\theta_T}{dt} = Q_{net\_sm} \cdot \quad (5)$$

To get a continuous time series of the net flux ( $Q_{net\_sm}$ ) through the course of the whole day, a so-called empirical sub-method theory developed for the groundwater diurnal signal (*Gribovszki et al.*, 2008) was adapted for soil moisture data (*Gribovszki*, 2014).

The maximum of  $Q_{net\_sm}$  for each day was calculated by selecting the largest positive value from differential total soil moisture ( $Q_{netmax\_sm} = \max(d\theta_T/dt)$ ), while the minimum was obtained by calculating the mean value from  $d\theta_T/dt$  taken in the predawn/dawn hours ( $Q_{netmin\_sm} = \text{mean}(\theta_{Tpredawn}/dt)$ ). Averaging is necessary to minimize the relatively large role of measurement error may play at dawn when the changes of soil moisture are small. The obtained values of the  $Q_{net\_sm}$  then were assigned to those temporal locations where the soil moisture

extrema took place ( $Q_{netmax\_sm}$  to the time of soil moisture minima and  $Q_{netmin\_sm}$  to the time of soil moisture maxima). This was followed by a spline (or when the data are very noisy a linear) interpolation of the  $Q_{net\_sm}$  values to derive intermediate values between the specified characteristic points (Fig. 4).

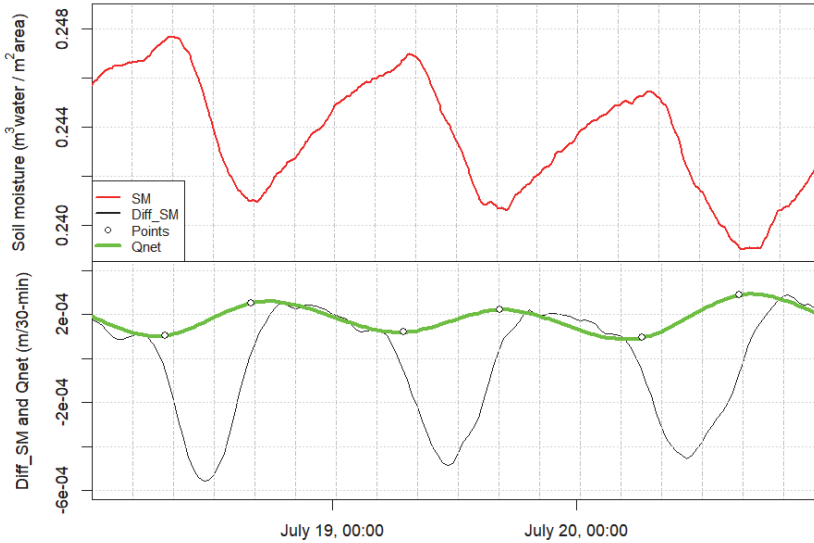


Fig. 4 The principle of the proposed method (SM: soil moisture, Points: characteristic points,  $Q_{net}$ : replenishment, Diff\_SM: differential soil moisture) for some selected days.

$ET$  rates from soil moisture signal considering a diurnally changing replenishment rate can be obtained by rearranging the former water balance equation (Eq. (2)) as

$$ET = Q_{net\_sm} - \frac{d\theta_T}{dt}. \quad (6)$$

## 2.6. Reference $ET$ calculation

Different  $ET$  estimations were compared to reference  $ET$  determined by the Penman-Monteith ( $PM\_ET$ ) method (Allen et al., 1998). This method is one of

the most reliable methods in estimating evapotranspiration from densely vegetated surfaces as

$$PM\_ET = \frac{\Delta(R_0 - S) + \rho c_p VPD r_a^{-1}}{L_v[\Delta + \gamma \cdot (1 + r_c r_a^{-1})]}, \quad (7)$$

where  $PM\_ET$  is the Penman–Monteith  $ET$  (mm time<sub>step</sub><sup>-1</sup>),  $L_v$  is the latent heat of vaporization (MJ kg<sup>-1</sup>),  $\Delta$  is the slope of the saturation vapor pressure curve (kPa °C<sup>-1</sup>),  $\gamma$  is the psychrometric constant (kPa °C<sup>-1</sup>),  $R_0$  is the net radiation (MJ m<sup>-2</sup> time<sub>step</sub><sup>-1</sup>),  $VPD$  is the vapor pressure deficit (kPa),  $S$  is the soil heat flux and temporary storage of energy into the tree itself (MJ m<sup>-2</sup> time<sub>step</sub><sup>-1</sup>),  $\rho$  is the air density (kg m<sup>-3</sup>),  $c_p$  is the specific heat of moist air (kJ kg<sup>-1</sup> °C<sup>-1</sup>),  $r_a$  is the aerodynamic resistance (s m<sup>-1</sup>), and  $r_c$  is the bulk canopy resistance (s m<sup>-1</sup>).

The meteorological data for  $PM\_ET$  calculation originated from climate station sensors located 2 m above the forest canopy, 1.6 km away from the soil moisture measurement site.

The tree canopy is 10–15 m above the soil surface at the study site, so soil heat flux contributions to the available energy for the canopy were considered very small. Temporary energy storage in tree stems and twigs was estimated at 5% of the solar radiation (Goodrich *et al.*, 2000). Goodrich *et al.* (2000) also offered a high  $r_c$  value (i.e., 5000 s m<sup>-1</sup>) for the night in order to cease  $ET$  at night. This high resistance value is not always realistic, because nocturnal sap flow can be as high as 10–25% of the daily  $ET$  in some situations (Gazal *et al.*, 2006). Therefore, positive  $ET$  at night, as our estimates in some cases suggest (Fig. 5), can be realistic. Seasonal changes of the  $r_c$  value were estimated using  $LAI$  measurements ( $r_c = 200/LAI$  (Allen *et al.*, 1998)) during the summer. In our case, Penman–Monteith estimates represent “real world”  $ET$  of well-watered forest vegetation that can be used as a benchmark to compare with the proposed methods.  $ET$  values produced by the new method were compared with those of the Penman–Monteith method at a 30-min resolution, of the traditional, and of the White approach-based methods on a daily basis.

For comparison of different  $ET$  estimations, the Tukey HSD (honestly significant difference) post hoc test and correlation test were used in an R software environment (R Core Team, 2012).

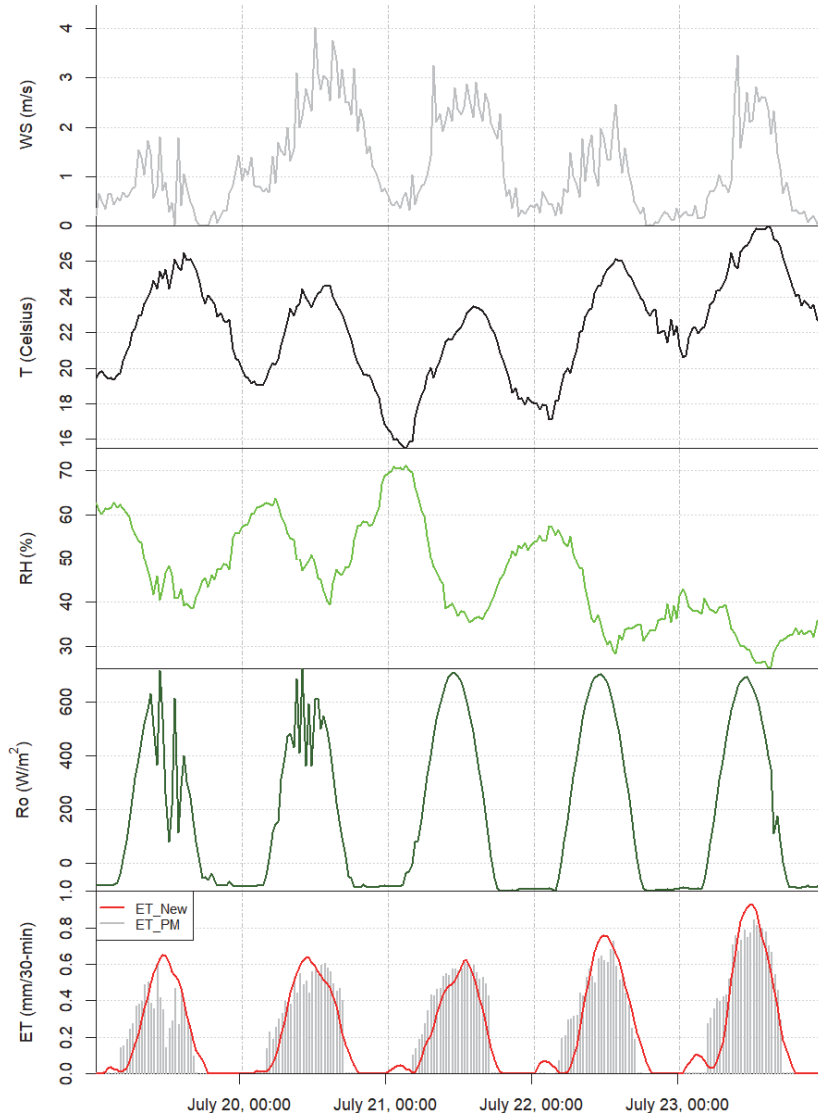


Fig. 5 Half hourly evapotranspiration estimates of new soil moisture based [ $ET\_New$ ] and PM [ $ET\_PM$ ] methods plotted together with meteorological parameters [ $WS$ : wind speed,  $T$ : temperature,  $RH$ : relative humidity,  $R_o$ : net radiation] for some selected days

### 3. Results and discussion

Half-hourly  $ET$  estimates of the new method are compared with the  $PM\_ET$  values in three selected rainless periods (June 3–9, 2013, July 16 – August 5, 2013,

September 1–8, 2013). *Fig. 5* illustrates *ET* values for some selected days at the end of July together with meteorological parameters.

Cross-correlation analysis of the half-hourly *ET* values (between the Penman–Monteith and the new method) show a peak ( $r = 0.854\text{--}0.914$ ) generally at a separation distance of 30–60 min with the new method’s values lagging behind those of the Penman–Monteith approach. Larger lag time is more typical closer to the start (at the beginning of June) and at the end (in September) of the growing season. The lag can be the consequence of the delayed transport mechanism in the xylem from the roots to the leaves. The travel time of the water particle allows some difference between the time of the transpiration and absorption of water from the soil.

*Fig. 6* displays the estimated *ET* rates on a daily basis, obtained by daily calculation (White and traditional estimates) and by summing the 30-min values over the days (PM and proposed diurnal method estimates). By using new diurnal method for *ET* estimation, a better correlation (0.85) can be found with *PM\_ET* values than when White approach (0.76) and traditional estimates (0.38) were applied. Not only the correlation was better, but the absolute values for *ET* (*ET\_New*) are also much closer to *PM\_ET* as *Table 1* shows.

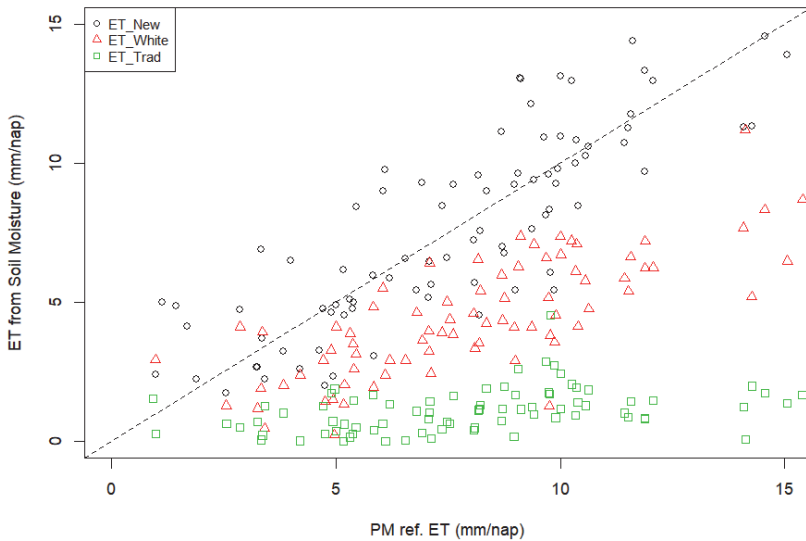


*Fig. 6.* *ET* values of different soil moisture-based methods versus *PM\_ET* values as a reference method (*ET\_New*: diurnal proposed method – black circles, *ET\_White*: White approach – red triangle, *ET\_Trad*: traditional method – green squares).

Table 1. *ET* values from different methods ( $n=89$ )

Method	Mean (sd) (mm d <sup>-1</sup> )	Diff from <i>ET</i> <sub>PM</sub> (mm d <sup>-1</sup> )	Tukey HSD test p-value*	correlation with <i>ET</i> <sub>PM</sub>
<i>ET</i> <sub>PM</sub>	7.21 (3.73)	–	–	–
<i>ET</i> <sub>New</sub>	7.84 (3.66)	0.63	0.4341	0.846
<i>ET</i> <sub>White</sub>	4.43 (2.11)	2.78	0.0000	0.762
<i>ET</i> <sub>Trad</sub>	1.11 (0.79)	6.10	0.0000	0.379

sd: standard deviation, p-value\*: Tukey HSD test significance compared with *ET*<sub>PM</sub>.

The Tukey HSD test result shows (Table 1) that only the proposed, new method does not differ significantly from *PM*<sub>*ET*</sub>. The White approach underestimates reference *PM*<sub>*ET*</sub> by 38%, while traditional calculation gives only 1/6–1/7 of the Penman-Monteith values.

The explanation of the deviations between the different assumptions is the following:

The original White approach assumes a constant replenishment rate to the vadose zone throughout the day. The replenishment is estimated when *ET* is close to zero in the late night hours, when the net flux is reduced due to a diminished hydraulic gradient. Contrasting the new method accounts for this diurnal change of the replenishment rate, which has a maximum when *ET* is most intensive and a minimum in the morning hours.

The traditional method does not take into account any replenishment from below; thus, the estimated *ET* values of that approach are very low. The relative importance of the net flux can be up to 90% of the *ET* rates (Gribovszki, 2014); therefore, neglecting this rate from below very significantly distorts the estimated *ET*.

Comparing *ET* from the new method (7.8 mm d<sup>-1</sup>) with results of other studies, it can be stated that these values typically represent the high-end of those estimates. It is worth noting that only dry and hot periods of the vegetation season were used for estimations of *ET*. Nachabe *et al.* (2005) calculated monthly average total *ET* rates of 1.5–6.3 mm d<sup>-1</sup> for a forest with the help of continuous soil moisture profile measurements in Florida using the White approach. Gazal *et al.* (2006) found *ET* as 2–7 mm d<sup>-1</sup> for a cottonwood forest in semiarid region of Australia. Goodrich *et al.* (2000) obtained 4–8 mm d<sup>-1</sup> *ET* values for mixed vegetation, while Hughes *et al.* (2001) found 2–6 mm d<sup>-1</sup> *ET* rates for a temperate salt marsh in Australia. In the cases of the last three research studies, sap flow measurements and micrometeorological methods were employed for calculating total *ET*. Important vegetation parameters (such as *LAI*) cannot always be deduced from these previous studies; therefore, comparison is not straightforward with

present estimates. Notwithstanding, the new *ET* estimation seems to yield realistic values. Especially when one considers the ready access of vegetation to vadose zone soil moisture directly connected with the shallow water table, the abundance of available energy in the growing season considered, as well as a large value of *LAI*, all combined with a favorable match with the Penman–Monteith *ET* values as a control. *ET* estimates of the new method seem also to be acceptable if the oasis effect (Morton, 1983) is taken into account in a well-watered valley situation, in a period when a hot and dry environment can add a significant amount of heat enhancing *ET*.

#### 4. Conclusions

The current *ET* estimation method is an enhanced version of the original White (1932) method adapted to soil moisture diurnal signal measured with high frequency.

The new method has been successfully validated using a well-known Penman-Monteith approach. Penman-Monteith *ET* values show a good correlation with present estimates; deviations between the reference and proposed method are small, not only on daily, but also on half-hourly scale. The estimated relatively high evapotranspiration values seem to be acceptable if the oasis effect is taken into account. Compared to traditional approaches and the White approach based diurnal techniques for soil moisture data, this new method gives significantly higher *ET* rates by taking into account continuous, diurnally changing soil moisture replenishment from shallow groundwater to the vadose zone.

The advantage of this new soil moisture-based diurnal technique over the groundwater signal based estimates is that only a soil moisture profile dataset is needed for the calculation of *ET*, and there is no need for specific yield (the most problematic parameter of groundwater diurnal signal based methods) values of a given soil profile.

The proposed method has potential benefits for determining *ET* rates in a changing climate with warmer and drier growing seasons. The *ET* of well-watered vegetation in groundwater discharge areas in hot and dry environments will probably increase in the future. The used water amount has a strong connection to biological productivity, and precise determination of *ET* from those areas is important from a water resources protection point of view as well.

**Acknowledgements:** This research has been supported by “Agrárklíma.2” (VKSZ\_12-1-2013-0034) project. The research of Zoltán Gribovszki was supported by the European Union and the State of Hungary, co-financed by the European Social Fund in the framework of TÁMOP 4.2.4. A/2-11-1-2012-0001 'National Excellence Program'. The author is grateful to the Institute of Environmental and Earth Sciences for supplying 30-min meteorological data applied in the analysis, and to the anonymous reviewer whose comments and suggestions improved this study.

## References

- Allen, R.G., Pereira, L.S., Raes, D., and Smith, M., 1998: Crop evapotranspiration – Guidelines for computing crop water requirements. *FAO Irrigation and Drainage* 56. <http://www.fao.org/docrep/X0490E/x0490e06.htm>
- Dingman, S.L., 2002: Physical Hydrology, Prentice Hall, Upper Saddle River, New Jersey.
- Bauer, P., Thabeng, G., Stauffer, F., and Kinzelbach, W., 2004: Estimation of the evapotranspiration rate from diurnal groundwater level fluctuations in the Okavango Delta, Botswana. *J. Hydrology* 288, 344–355. <https://doi.org/10.1016/j.jhydrol.2003.10.011>
- Dolan, T.J., Hermann, A.J., Bayley, S.E., and Zoltek, J., 1984: Evapotranspiration of a Florida, USA, fresh-water wetland. *J. Hydrology* 74, 355–371. [https://doi.org/10.1016/0022-1694\(84\)90024-6](https://doi.org/10.1016/0022-1694(84)90024-6)
- Engel, V., Jobbágy, E.G., Stieglitz, M., Williams, M., and Jackson, R.B., 2005: The hydrological consequences of Eucalyptus afforestation in the Argentine Pampas. *Water Resour. Res.* 41, W10409. <https://doi.org/10.1029/2004WR003761>
- Gazal, R.M., Scott, R.L., Goodrich, D.C., and Williams, D.G., 2006: Controls on transpiration in a semiarid riparian cottonwood forest. *Agric. Forest Meteorol.* 137 56–67. <https://doi.org/10.1016/j.agrformet.2006.03.002>
- Gribovszki, Z., Kalicz, P., and Kucsara, M., 2006: Streamflow Characteristics of Two Forested Catchments in Sopron Hills. *Acta Silv Lign Hung* 2, 81–92.
- Gribovszki, Z., Kalicz, P., Szilágyi, J., and Kucsara, M., 2008: Riparian zone evapotranspiration estimation from diurnal groundwater level fluctuations. *J. Hydrology* 349, 6–17. <https://doi.org/10.1016/j.jhydrol.2007.10.049>
- Gribovszki, Z., Szilágyi, J., and Kalicz, P., 2010: Diurnal fluctuations in shallow groundwater levels and in streamflow rates and their interpretation - a review. *J. Hydrology* 385, 371–383. <https://doi.org/10.1016/j.jhydrol.2010.02.001>
- Gribovszki, Z., 2014: Diurnal Method for Evapotranspiration Estimation from Soil Moisture Profile. *Acta Silv Lign Hung* 10, 67–75. <https://doi.org/10.2478/aslh-2014-0005>
- Goodrich, D.C., Scott, R., Qi, J., Goff, B., Unkrich, C.L., Moran, M.S., Williams, D., Schaeffer, S., Snyder, K., MacNish, R., Maddock, T., Poole, D., Chehbounif, A., Cooper, D.I., Eichinger, W.E., Shuttleworth, W.J., Kerri, Y., Marsetta, R., and Ni, W., 2000: Seasonal estimates of riparian evapotranspiration using remote and in situ measurements. *Agric. Forest Meteorol.* 105, 281–309. [https://doi.org/10.1016/S0168-1923\(00\)00197-0](https://doi.org/10.1016/S0168-1923(00)00197-0)
- Haise, H.R. and Kelley, O.J., 1950: Causes of diurnal fluctuations of tensiometers. *Soil Science* 70, 301–313. <https://doi.org/10.1097/00010694-195010000-00006>
- Hughes C.E., Kalma J.D., Binning, P., Willgoose, G.R., Vertzonis, M., 2001: Estimating evapotranspiration for a temperate salt marsh, Newcastle, Australia. *Hydrol. Process.* 15, 957–975. <https://doi.org/10.1002/hyp.189>
- Kishazi, P. and Ivancsics, J., 1985: Sopron környéki üledékek összefoglaló földtani értékelése. Kezirat, Sopron, 48 p. (in Hungarian).
- Loheide, II., S.P., Butler, Jr. J.J., and Gorelick, S.M., 2005: Estimation of groundwater consumption by phreatophytes using diurnal water table fluctuations: A saturated-unsaturated flow assessment. *Water Resour. Res.* 41, W07030. <https://doi.org/10.1029/2005WR003942>
- Loheide, II., S.P., 2008: A method for estimating subdaily evapotranspiration of shallow groundwater using diurnal water table fluctuations. *Ecohydrology* 1, 59–66. <https://doi.org/10.1002/eco.7>
- Luo, Y. and Sophocleous, M., 2010: Seasonal groundwater contribution to crop-water use assessed with lysimeter observations and model simulations. *J. Hydrology* 389, 325–335. <https://doi.org/10.1016/j.jhydrol.2010.06.011>
- Marosi, S., and Somogyi, S., (eds.) 1990: Magyarország kistájainak katasztere I. [MTA Földrajztudományi Kutató Intézet, Budapest, 479 p. (in Hungarian).
- Móricz, N., Mátyás, C., Berki, I., Rasztovíts, E., Vekerdy, Z., and Gribovszki, Z., 2012: Comparative water balance study of forest and fallow plots. *iForest* 5, 188–196.
- Morton, F.I., 1983: Operational estimates of areal evapotranspiration and their significance to the science and practice of hydrology. *J. Hydrology* 66, 1–76. [https://doi.org/10.1016/0022-1694\(83\)90177-4](https://doi.org/10.1016/0022-1694(83)90177-4)

- Mould, D.J.E., Frahm, T. Salzmann, K. Miegel, and M.C. Acreman, 2010: Evaluating the use of diurnal groundwater fluctuations for estimating evapotranspiration in wetland environments: case studies in southeast England and northeast Germany. *Ecohydrology* 762, 294–305  
<https://doi.org/10.1002/ecco.108>
- Nachabe, M., Shah, N., Ross, M., and Womacka, J., 2005: Evapotranspiration of two vegetation covers in a shallow water table environment. *Soil Science Society of America Journal* 69, 492–499.  
<https://doi.org/10.2136/sssaj2005.0492>
- R Core Team, 2012: R: A language and environment for statistical computing. R Foundation for Statistical Computing, Vienna, Austria. <https://www.r-project.org/>
- Reigner, I.C., 1966: A method for estimating streamflow loss by evapotranspiration from the riparian zone. *Forest Science* 12, 130–139.
- Schilling, K.E., 2007: Water table fluctuations under three riparian land covers, Iowa (USA). *Hydrologic. Proc.* 21, 2415–2424. doi: 10.1002/hyp.6393.
- Shah, N., Nachabe, M., and Ross, M., 2007: Extinction depth and evapotranspiration from ground water under selected land covers. *Ground Water* 45, 329–338.  
<https://doi.org/10.1111/j.1745-6584.2007.00302.x>
- Soylu, M.E., Lenters, J.D., Istanbuluoglu, E., and Loheide, II., S.P., 2012: On evapotranspiration and shallow groundwater fluctuations: A fourier-based improvement to the white method. *Water Resour. Res.* 48, W06506. <https://doi.org/10.1029/2011WR010964>
- Szilágyi, J., Kovács, A., Józsa, J., 2012: Remote sensing based groundwater recharge estimates in the Danube-Tisza Sand Plateau region of Hungary. *J. Hydrol. Hydromech.* 60, 64-72,  
<https://doi.org/10.2478/v10098-012-0006-3>
- White, W.N., 1932: Method of Estimating Groundwater Supplies Based on Discharge by Plants and Evaporation from Soil – Results of Investigation in Escalante Valley. Tech. Rep., Utah – US Geological Survey. *Water Supply Paper* 659-A.

# IDŐJÁRÁS

*Quarterly Journal of the Hungarian Meteorological Service*  
*Vol. 122, No. 1, January – March, 2018, pp. 31–40*

## **Impact of precipitation and temperature on the grain and protein yield of wheat (*Triticum aestivum* L) varieties**

**Márton Jolánkai\*, Katalin Kassai M., Ákos Tarnawa,  
Barnabás Pósa, and Márta Birkás**

*Szent István University Crop Production Institute,  
Páter Károly utca 1., 2100 Gödöllő, Hungary*

*\*Corresponding author E-mail: jolankai.marton@mkk.szie.hu*

*(Manuscript received in final form April 11, 2017)*

**Abstract**—Impacts of agronomic applications were studied in a field experiment to determine water availability, grain yield, and protein formation interrelations. Three winter wheat varieties and six nitrogen application levels were applied in two consecutive crop years representing different precipitation and temperature patterns to evaluate yield, yield components, and quality manifestation. The research results suggest that precipitation patterns in relation with the wheat development phenophases had profound influence on the grain yield and protein formation of wheat crop. Varietal differences were determined regarding yield and protein values in relation with plant nutrition and crop year impacts. There were no, or minor differences only between varieties, however plant nutrition treatments induced significant differences in both crop years.

*Key-words:* crop year weather, nitrogen supply, wheat, grain yield, protein yield

### **1. Introduction**

The amount and quality of grain yield of winter wheat *Triticum aestivum* L. is highly influenced by the meteorological conditions of the given crop year, especially the amount and distribution of precipitation and the actual temperature (Grimwade et al., 1996; Győri, 2008; Pepó, 2010). Temperature

patterns have been changed and are associated with warming. The growing season has been modified during the past decades in the Carpathian Region (Lakatos *et al.*, 2016). Weather conditions are evaluated and labeled favorable or non-favorable in relation with the optimum requirements of the crops' phenophases (Lásztity, 1999; Ványiné and Nagy, 2012). In case of precipitation, the most vulnerable periods during growth and development of winter wheat are the phenophases of heading and flowering (stage 10–10.5 on the Feekes scale; stage 51–70 on the Zadoks scale). In relation with temperature, two critical periods can be detected. One is the vernalization, and the other is the ripening stage (Feekes 1–3 and 11; Zadoks 10–13 and 71–99) (Pollhamer, 1981; Kismányoky and Ragasits, 2003).

Crop yield and grain quality can also be influenced by agronomic applications. Plant nutrition in general and N topdressing in particular should be considered as the most effective treatments within the technologies of winter wheat production. The amount of nitrogen and the timing and distribution of the application have an impact on wheat quality, especially on the protein production of the crop (Győri, 2006; Pepó, 2010; Vida *et al.*, 1996).

## 2. Materials and methods

High milling and baking quality winter wheat *Triticum aestivum* L. varieties were examined under identical agronomic conditions in a long term field trial. The small plot trials were run at the Nagygyombos experimental field of the Szent István University, Crop Production Institute, Hungary (N 47°40'58" – E 19°40'11"). Soil type of the experimental field is chernozem (calciustoll).

Annual precipitation of the experimental site belongs to the 550–600 mm belt of the northern edges of the Hungarian Great Plain. Experiments were conducted in a split-plot design with four replications. The size of each plot was 10 m<sup>2</sup>. Plots were sown and harvested by plot machines (standard Wintersteiger cereal specific experimental plot machinery series). Various identical agronomic treatments were applied to plots. Plant nutrition applications were done in single and combined treatments. Nitrogen topdressing variants were representing 6 levels: 0, 80, 80+40, 120, 120+40 and 160 kg/ha, nitrogen in single and split applications. All plots were sown with identical series of wheat varieties for studying their performance related to agronomic impacts. The recent study presents the performance and evaluations of three winter wheat varieties (Alföld-90, Mv Karéj, and Mv Toborzó) of 2014–2015 and the 2015–2016 crop years. Wheat grain quality parameters: protein and wet gluten contents were determined from grain samples, as well as quality characteristics at the Research Laboratory of the Crop Production Institute of the Szent István University and the laboratories of the Regional Knowledge Center according to Hungarian and EU standards (MSZ 1998; EK 2000). The

protein figures correlated with the treatments applied, and analyses were done by Microsoft Office 2003 statistical programmes (Horváth, 2014). Fig. 1 demonstrates the phenophases of winter wheat by the grading of two internationally used systems. Phenological phases have been evaluated in accordance with the monthly precipitation and temperature figures of the respective crop years by the methods of Pollhamer (1981) and Kismányoky and Ragasits (2003).

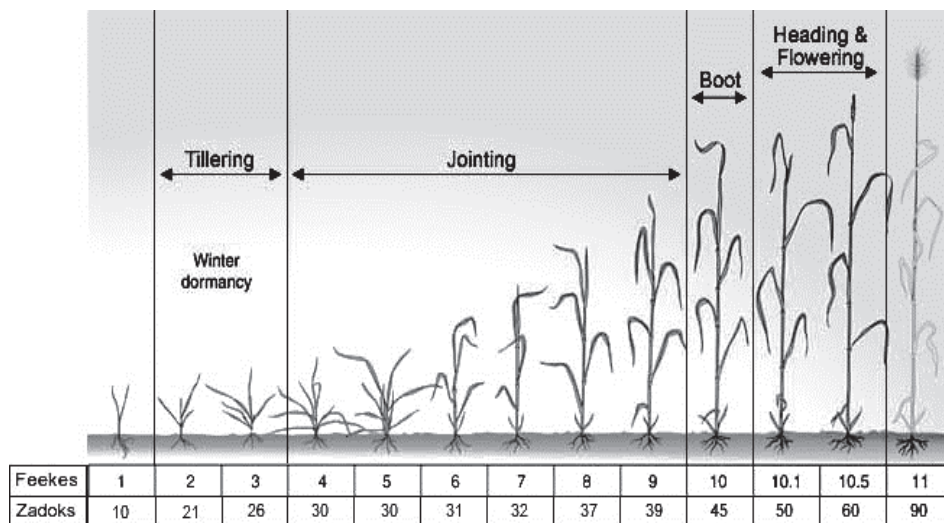


Fig. 1. Growth stages of winter wheat - Feekes and Zadoks values. (Source: Kismányoky and Ragasits, 2003).

Crop year conditions were evaluated in accordance with the monthly values of temperature and precipitation in non-favorable (2014–2015) and favorable (2015–2016) crop years during the vegetation period.

The monthly periods are considered in accordance with the magnitude of deviation in relation with the long-term mean temperature and precipitation values. A plus or minus 20% of precipitation and 1 °C of temperature were applied as threshold values as it is indicated in Table 1.

*Table 1.* Precipitation and temperature patterns of experimental site during the respective crop years. Nagygyombos 2014–2015; 2015–2016. Source: KDVVIZIG (2016)

Period	Precipitation (mm)	Long-term mean (mm)	D	Temperature (°C)	Long-term (°C)	D
2014–2015 (non-favorable crop year)						
September	100	43	57	16.4	15.5	0.9
October	57	45	12	11.6	10.1	1.5
November	25	54	-29	6.9	4.0	2.9
December	48	45	3	2.7	0.3	2.4
January	60	35	25	1.5	-1.2	2.7
February	17	33	-16	1.7	0.7	1.0
March	21	33	-12	6.2	5.1	1.1
April	6	44	-38	10.4	10.1	0.3
May	65	62	3	15.6	15.5	0.1
June	26	73	-47	19.6	18.5	1.1
July	38	59	-21	22.9	20.3	2.6
August	76	54	22	22.8	19.9	2.9
2015–2016 (favorable crop year)						
September	80	43	37	17.0	15.5	1.5
October	95	45	50	9.5	10.1	-0.6
November	27	54	-27	6.2	4.0	2.2
December	4	45	-41	2.4	0.3	2.1
January	54	35	19	-1.7	-1.2	-0.5
February	106	33	73	5.2	0.7	4.5
March	30	33	-3	6.5	5.1	1.4
April	18	44	-26	12.0	10.1	1.9
May	76	62	14	15.6	15.5	0.1
June	52	73	-21	20.3	18.5	1.8
July	130	59	71	21.5	20.3	1.2
August	54	54	0	19.7	19.9	-0.2

long-term data: 1971–2000

### 3. Results and discussion

The two consecutive crop years represented different meteorological conditions regarding wheat cropping. The 2014–2015 crop year in general was slightly dryer in comparison with the long-term average of precipitation of the experimental site (539 versus 580 mm). The actual annual precipitation

deficiency was  $-7.1\%$ , however, the distribution of that was much more diverse. The magnitude of water deficiency with an exception of one spring month ranged from  $-12$  to  $-47\%$  during the critical phenophases from tillering to flowering. At the same time, the temperature values proved to be  $1.6\text{ }^{\circ}\text{C}$  higher than the long term average. Especially, the warm and frost free winter period may have influenced the vernalisation processes of the crop.

The 2015–2016 crop year provided the wheat crop with more favorable conditions. The amount of precipitation was  $25.1\%$  higher, and the distribution of that was better concerning the phenophases. The temperature patterns were closer to that of the long-term values, however, this crop year was also  $1.3\text{ }^{\circ}\text{C}$  warmer than the average.

Yield results of the trial are summarized in *Figs. 2* and *3*. The total amount of grain yield (t/ha) is indicated for the two respective crop years for all the wheat varieties examined.

The results suggest, that the two crop years examined had different levels of grain yield of certain varieties. In 2015 grain yield amounts ranged from 1,9 to 3.1 t/ha with definite differences between N applications, while in 2016 this turned to be 5.1 to 8.6 showing less variations between plant nutrition treatments. In both crop years only minor varietal differences were detected.

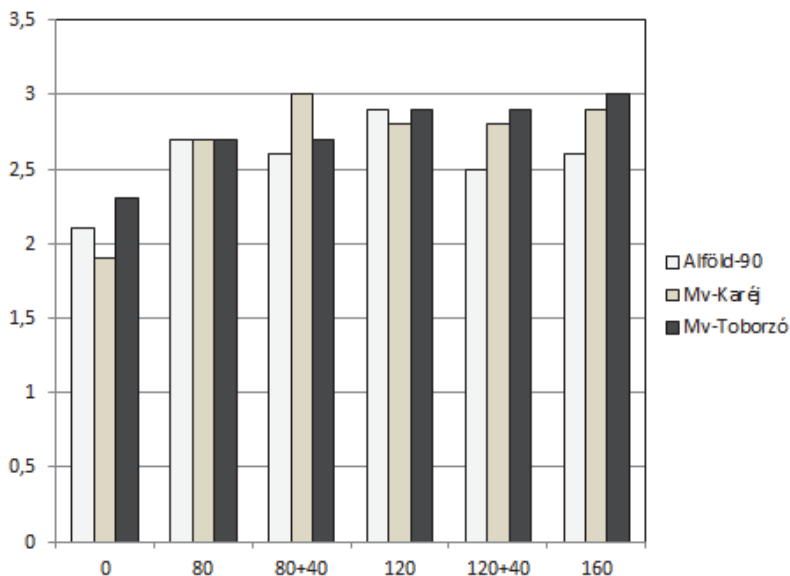


*Fig. 2.* Total grain yields in the non-favorable crop year. Nagygyombos, 2015.

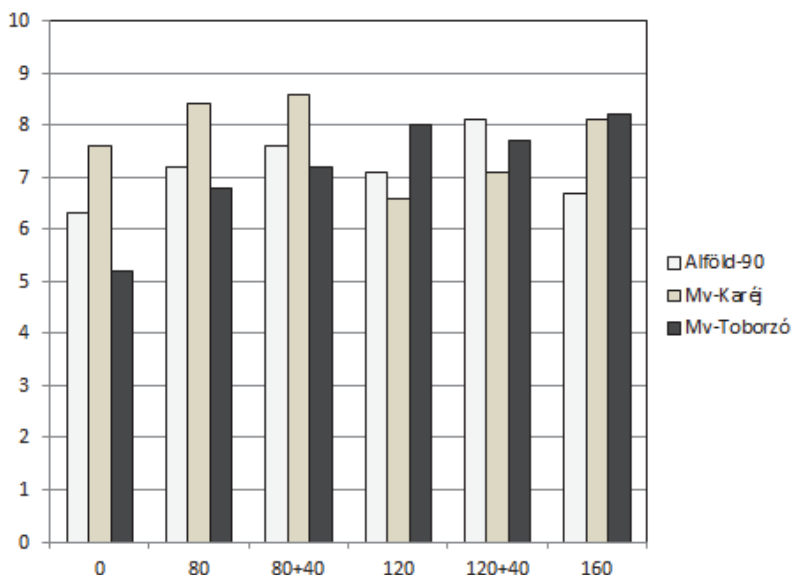


Fig. 3. Total grain yields in favorable crop year. Nagygyombos, 2016.

Quality information is provided by *Figs. 4* and *5*. The total amount of protein yield (t/ha) is indicated for the two respective crops years by all the wheat varieties examined. The results obtained highlight three factors. The first is the difference between the amounts of protein yield. In the arid year 2015, the range of total amount of protein was between 224 and 609 kg/ha. 2016, a favorable crop year resulted in 692 and 1247 kg/ha protein yield values.

The second is the consequent differences between the impacts of nitrogen application levels. These differences were significantly bigger in the favorable crop year in comparison with those of the non-favorable vintage. The reason of such deviation was due to the amount of precipitation during the phenophases of flowering and grain filling of the respective crop years.

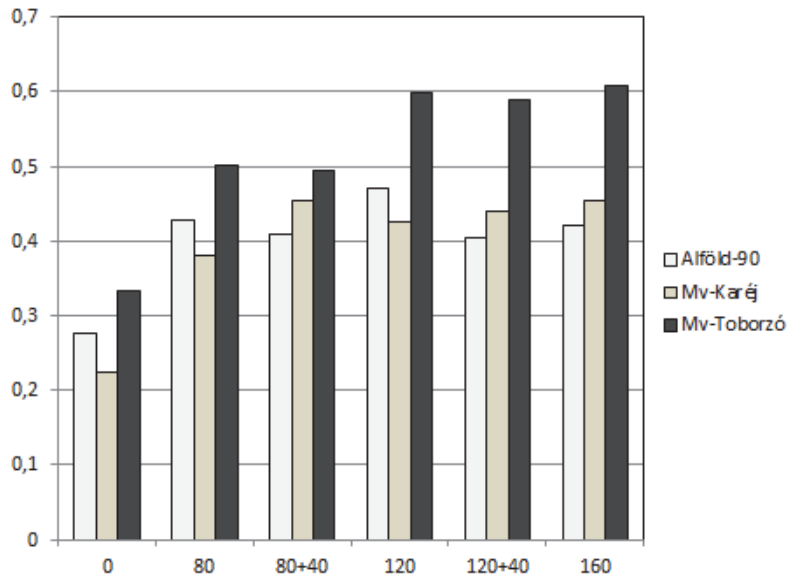


Fig. 4. Total protein yields in non-favorable crop year. Nagygyombos, 2016.

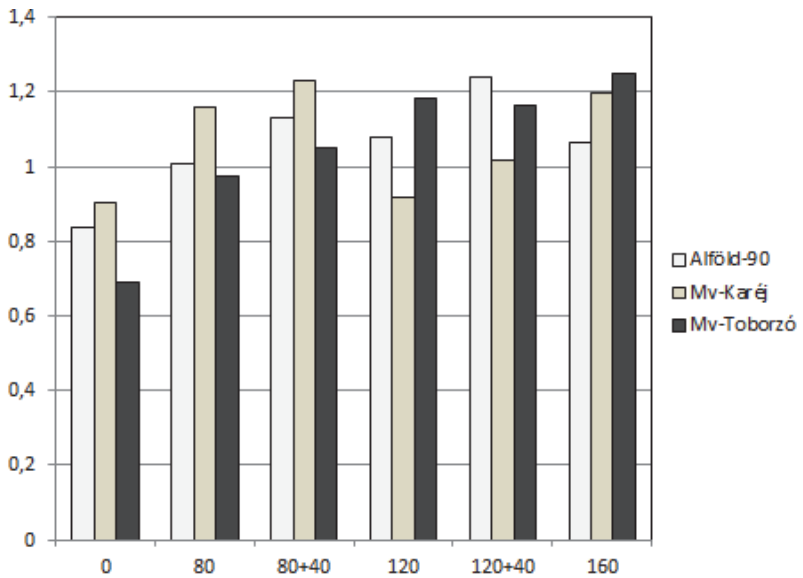


Fig. 5. Total protein yields in the favorable crop year. Nagygyombos, 2016.

The third factor detected was the performance of varieties. From among the three varieties examined, two cultivars – Mv Karéj and Mv Toborzó proved to be the most efficient regarding the amount of total protein yield production. The highest protein yields were obtained by Mv Toborzó in both years.

Table 2 presents correlation figures of experimental variants for both crop years. For better understanding, the tables show data on further interrelations not discussed in this paper, but which may provide information on the protein formation performance, like the pattern of monthly temperature, or the protein content of grain yield samples.

The experimental results suggest that the strongest correlation was detected between the total amount of protein and the experimental treatments, with no impact of crop years' weather in accordance with the findings of Gyóri (2008) and Pepó (2010).

Table 2. Correlation between precipitation, temperature, plant nutrition (control versus treatments), grain yield, and protein yield of wheat varieties. Nagyombos, 2015, 2016.

Correlation r value	Precipitation	Temperature	N supply	Crop variety	Grain yield	Protein content	Protein yield
Precipitation	1						
Temperature	0.156	1					
N supply	0.378	-0.023	1				
Crop variety	0.453	0.234	0.571	1			
Grain yield	0.784	-0.214	0.873		1		
Protein content	0.512	0.103	0.776	0.613	-0.216	1	
Protein yield	0.886	-0.317	0.912	0.566	0.879	0.762	1

Yield figures of the cultivars were in close correlation with plant nutrition with a few exceptions only. However, this correlation proved to be stronger and at the same time more balanced in the favorable crop year.

The correlations of crop yield components were much weaker in both crop years in comparison with those of yield and protein values. The most vulnerable phenological periods of winter wheat were the stages of heading and flowering related to precipitation, and vernalization and ripening concerning temperature performance in accordance with the results of Pollhamer (1981) and that of Kismányoky and Ragasits (2003).

#### 4. Conclusions

Precipitation and temperature patterns were studied in a long-term field experiment to determine water availability and plant nutrition impacts on yield quantity and quality. The aim of the study was to evaluate favorable and non-favorable crop year conditions for winter wheat *Triticum aestivum* L. Three winter wheat varieties and six nitrogen topdressing application levels were applied in two consecutive crop years representing different precipitation and temperature patterns to evaluate yield, yield components, and quality manifestation. The results of the experiment suggest that precipitation patterns related to the wheat development phenophases had profound influence on the yield and the protein formation of the crop. From among phenophases, flowering and grain filling periods proved to be the most influential stages. The two crop years resulted in different amounts of protein yield. The favorable one significantly increased the total amount of protein in comparison with that of the non-favorable vintage. There were detectable differences in the protein yield of the wheat varieties studied; however, the efficiency of the respective varieties also differed in the two crop years. Strong correlation was detected between the total amount of protein and the experimental treatments in both years. Yield figures of the wheat varieties were in close correlation with plant nutrition in general. Correlations of crop yield components were lower in both crop years in comparison with those of yield and protein values.

**Acknowledgements:** This paper presents research results gained from a long-term trial supported by VKSZ and NVKP funds of the Government of Hungary.

#### References

- Grimwade B, Tatham AS, Freedman RB, Shewry PR, and Napier JA. 1996: Comparison of the expression patterns of wheat gluten proteins and proteins involved in the secretory pathway in developing caryopses of wheat. *Plant Mol. Biol.* 30, 1067–1073.  
<https://doi.org/10.1007/BF00020817>
- Győri, Z., 2006: A trágyázás hatása az őszi búza minőségére. *Agrofórum* 17(9), 14–16.
- Győri, Z. 2008: Complex evaluation of the quality of winter wheat varieties. *Cereal Res. Commun.* 36, 1907–1910. <https://doi.org/10.1556/CRC.36.2008.Suppl.1>
- Horváth Cs., 2014: Storage proteins in wheat (*Triticum aestivum* L.) and the ecological impacts affecting their quality and quantity, with a focus on nitrogen supply. *Columella* 1(2), 57–75.  
<https://doi.org/10.18380/SZIE.COLUM.2014.1.2.57>
- KDVVIZIG, 2016: Monthly precipitation and temperature. Hydrometeorological databank.  
<http://www.kdvvizig.hu/index.php/vizrajz/havi-hidromet-tajekoztato/>
- Kismányoky, T. and Ragasits, I., 2003: Effects of organic and inorganic fertilization on wheat quality. *Acta Agronomica Hungarica*, 51, 47–52. <https://doi.org/10.1556/AAGR.51.2003.1.6>
- Lakatos M., Bihari Z., Szentimrey T., Spinoni J., and Szalai, S., 2016: Analyses of temperature extremes in the Carpathian region in the period 1961–2010. *Időjárás* 120, 41–51.
- Lásztity, R., 1999: Cereal Chemistry. Akadémiai Kiadó: Budapest.

MSZ 6383:1998, 824/2000/EK Wheat quality standards.

Pepó, P., 2010: Adaptive capacity of wheat (*Triticum aestivum* L.) and maize (*Zea mays* L.) crop models to ecological conditions. *Növénytermelés* 59, Suppl. 325–328.

<https://doi.org/10.1556/Novenyterm.59.2010.Suppl.3>

Pollhamer, E. 1981: A búza és a liszt minősége. Mezőgazdasági Kiadó, Budapest.(in Hungarian)

Ványiné, Sz. A., Nagy, J., 2012: Effect of nutrition and water supply on the yield and grain protein content of maize hybrids. *Australian J. Crop Sci.* 6. 381–388.

<https://doi.org/10.21475/ajcs.2016.10.06>

Vida, Gy., Bedő, Z., and Jolánkai, M., 1996: Agronómiai kezeléskombinációk őszi búzafajták sütőipari minőségére gyakorolt hatásának elemzése főkomponens-analízissel. *Növénytermelés* 45. 453–462. (in Hungarian)

# IDŐJÁRÁS

*Quarterly Journal of the Hungarian Meteorological Service*  
Vol. 122, No. 1, January – March, 2018, pp. 41–58

## Estimation of natural water body's evaporation based on Class A pan measurements in comparison to reference evapotranspiration

Angéla Anda\*, Brigitta Simon, Gábor Soós, and Tamás Kucserka

*Department of Meteorology and Water Management,  
Georgikon Faculty, University of Pannonia,  
Festetics Str. 7. Keszthely, H-8360, Hungary*

*\*Corresponding author E-mail: anda-a@georgikon.hu*

*(Manuscript received in final form March 21, 2017)*

**Abstract**—A Class A pan (C) evaporation ( $E_p$ ) study was conducted at the Agrometeorological Research Station of Keszthely, in the growing season of 2016. Some of the evaporation pans were implemented with freshwater aquatic macrophytes (*Myriophyllum* sp., *Potamogeton* sp., and *Najas* sp.) ( $P_s$ ) and sediment covered bottom (S). The applied macrophytes were the predominant species of Keszthely Bay (Balaton Lake). Reference ( $E_o$ ) after Shuttleworth and reference evapotranspiration ( $ET_o$ ) after Penman-Monteith (FAO-56 formula) were also included for the  $E$  study. Of pre-selected four investigated variables, air temperature and air humidity impacted  $E_p$  of treated Class A pans the most. Cumulative  $E_p$  values for 2016 were 363.1, 427.7, and 461.5 mm in C, S, and  $P_s$ , respectively. There was no difference in measured cumulative  $E_p$  of  $P_s$  (461.5 mm) and computed  $ET_o$  (472.1 mm) during the studied season.

On the basis of a simplified water budget,  $E$  rate of Keszthely Bay increased with 16.9%, when macrophytes and sediment cover were accounted. It is equivalent to 264,000,000 m<sup>3</sup> water in Keszthely Bay's  $E$  estimation. Simple  $E$  approach - when lake's components, such as submerged macrophytes and sediment cover were also accounted - could extend the accuracy of natural lake's  $E$  estimation in a broader circle than earlier.

*Key-words:* Class A pan evaporation, aquatic macrophytes, Keszthely Bay (Balaton Lake)

## 1. Introduction

Evaporation ( $E$ ) is the process of conversion of liquid water to water vapor, widely measured by standard dish filled with water. Evaporation pans provide a measurement of the integrated influence of temperature, humidity, wind speed, and solar radiation on  $E$  (Majidi et al., 2015; Kim et al., 2013). In the last century, due to its cost-effectiveness and easy-applicability, pan evaporation ( $E_p$ ) measuring network has been established worldwide (Stanhill, 2002). The physical basis of Class A pan's  $E_p$  was investigated among others by Roderick et al. (2007) and Jacobs et al. (1998).  $E_p$  has also been applied as an index of lake and reservoir  $E$  (Wang et al., 2017; Kim et al., 2015; Allen et al., 1998) beyond traditional  $E_p$  uses in water budget estimation, plant-weather interactions, etc. Spatial and temporal limitations of pan application due to instrumental and practical issues were also integrated (Marti et al., 2015; Shiri et al., 2011). Several empirical methods based on local variables, in many cases various meteorological drivers, have been developed to estimate  $E_p$  in different climate conditions. Weaknesses in use of empirical or half-empirical equations may be the limited data availability and completeness (Majidi et al., 2015). The other option in  $E$  estimation is the modeling approach, the Penman-Monteith reference evapotranspiration ( $ET_0$ ) model (Allen et al. 1998, 2005; FAO-56 equation) is probably the most widely employed method among  $E$  approximations.

Linacre (1994) issued that  $E_p$  does not correspond well to open-water  $E$  due to modified intercepted radiation and enhanced heat exchange of the pan wall. To manage issues of A pan's heat transfer modifications, a pan coefficient (below unity) is in use to get near-natural  $E$  values (Allen et al. 1998; Linacre, 1994). In addition to radiation and heat transfer variations, Rotstayn et al. (2006) identified aerodynamic deviations in pan's physical behavior. Recognizing fragility of our knowledge in physical properties of pans, Yang and Yang (2012) found that  $E$  pans are not desirable in open-water  $E$  estimations. Lim et al. (2012) collected the most frequent sources of errors when Class A pan is used: the upper thin layer's surface temperature declines due to evaporation, unknown water mixing inside the dish, experimental shortcomings of some researchers, etc. (Anda et al., 2016).

The term macrophyte comprises plants which are at least with their roots under water (Barrat-Segretain, 1996). One of the three sub-groups of macrophytes (emergent, floating leaved, and submerged) is the submerged one, which keep their leaves permanently under water. Brothers et al. (2013) found that submerged macrophytes are the key factors in aquatic ecosystems as they strongly impact lake productivity. Another important role of submerged macrophytes is their contribution to clear-water conditions of shallow lakes and rivers (Hilt et al., 2011). Three predominant submerged macrophyte species are present at Keszthely Bay (Balaton Lake): *Myriophyllum* sp., *Potamogeton* sp., and *Najas* sp. (Vári, 2012).

There are not any studies in the literature that account impact of sediments and submerged macrophytes in estimating lake's  $E$ . Information deficit related to living water  $E$  approach, when class A pan is in use, might impede for the present measurement of a more accurate  $E$  estimation.

## 2. Materials and methods

### 2.1. Study site and pan treatments with $E$ estimations

Class A pan's  $E_p$  observations were carried out at the Keszthely Agrometeorological Research Station (latitude:  $46^{\circ} 44' N$ , longitude:  $17^{\circ} 14' E$ , elevation: 124 m above sea level) in the growing season of 2016 (Fig. 1). Three different pan treatments were set in the study:

- Class A pan as control pan (C),
- Class A pan implemented with submerged macrophytes ( $P_s$ ),
- Class A pan with sediment covered bottom (S).

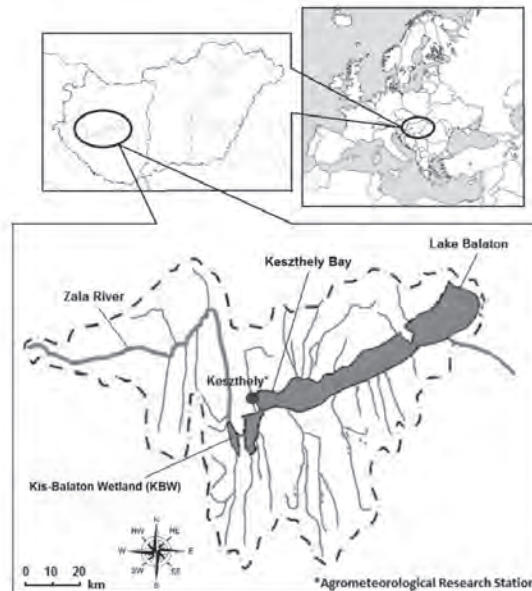


Fig. 1. Watershed of the Balaton Lake with the site of the observation. Meteorological observations with pan evaporation measurements were done at the Agrometeorological Research Station.

Operation of Class A pan, placed on a 0.15 m high wooden platform, was performed following a standard procedure given by the Hungarian Meteorological Service. After daily water height observations carried out at 7.00 am, water replenishing was executed with tap water. Water temperature,  $T_w$  at a depth of 0.02 m was measured with thermocouples at 10 min intervals.  $E_p$  observations were only carried out during the growing season.

Predominant submerged freshwater macrophytes (*Myriophyllum* sp., *Potamogeton* sp., *Najas* sp.) were implemented into the Class A pan on June 6, 2016, at the same time when the species emerged in the Balaton Lake (Keszthely Bay). The amount and species distribution of plant samples were consistent with plant density of the Keszthely Bay. Fresh weight of samples was determined at the pan's seeding time (spring) and in the end of  $E$  measurements, on September 30, 2016. Thickness of sediment on the bottom of Class A pan was 0.02 m. Sediment was obtained from the Balaton Lake. The layout of the pan treatments and instruments of the meteorological station included in the study are presented in Fig. 2.

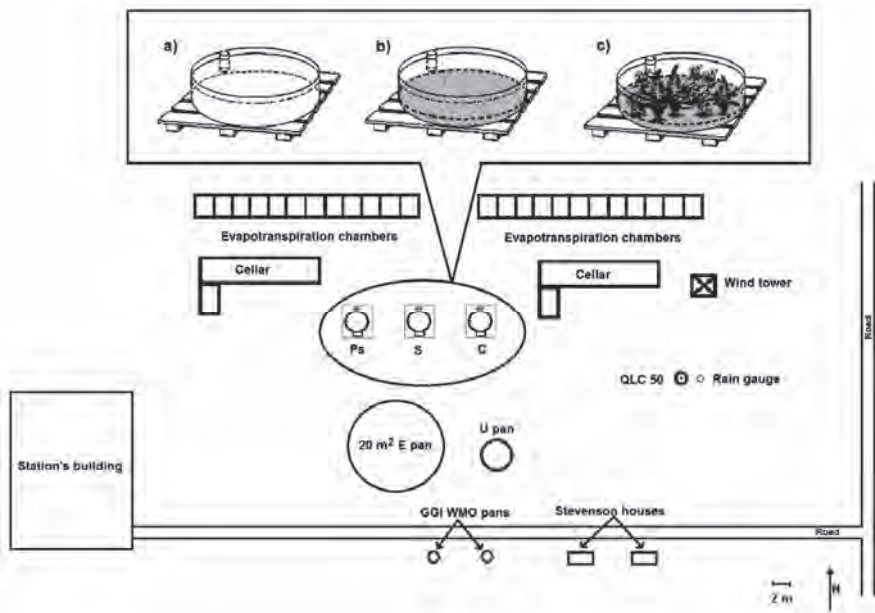


Fig. 2. Layout of the evaporation pans with the sketch of instrumentation of the Agrometeorological Research Station at Keszthely.

Daily  $E_o$  rate [mm day<sup>-1</sup>] of water bodies was computed by the Shuttleworth formula (Shuttleworth, 1993), which was adapted from the original Penman equation (Penman, 1948):

$$E_o = \frac{mR_n + \gamma * 6.43 (1 + 0.536 * u_2) \delta_e}{\lambda_v (m + \gamma)}, \quad (1)$$

where  $R_n$  is net radiation [MJ m<sup>-2</sup> day<sup>-1</sup>],  $m$  is the slope of the saturation vapor pressure curve [kPa K<sup>-1</sup>],  $u_2$  is wind speed [m s<sup>-1</sup>] at 2 m height,  $\delta_e$  is the vapor pressure deficit [kPa],  $\lambda_v$  is the latent heat of vaporization [MJ kg<sup>-1</sup>], and  $\gamma$  is a psychrometric constant [kPa °C<sup>-1</sup>].

Daily plant  $ET_o$  rate [mm day<sup>-1</sup>] was computed by the widely spread FAO-56 Penman-Monteith equation (Monteith, 1965; Penman, 1948):

$$ET_o = \frac{0.408 \Delta (R_n - G) + \gamma \frac{900}{T + 273} u_2 (e_s - e_a)}{\Delta + \gamma \Delta (1 + 0.34 u_2)}, \quad (2)$$

where  $G$  is the soil heat flux density [MJ m<sup>-2</sup> day<sup>-1</sup>],  $T_a$  is the mean daily air temperature at 2 m height [°C],  $e_s$  is the saturation vapor pressure [kPa],  $e_a$  is the actual vapor pressure [kPa],  $\Delta$  is the slope of the vapor pressure curve [kPa °C<sup>-1</sup>] and 0.408 is the a conversion factor from MJ m<sup>-2</sup> day<sup>-1</sup> to equivalent evaporation in mm day<sup>-1</sup>.  $R_n$  was the estimated using the sediment covered bottom treatment (S), from daily mean  $T_a$ , mean daily  $e_a$ , the site latitude and elevation after Allen et al. (2005). A fixed value of 0.23 was applied for albedo.  $R_n$  was also computed after Allen et al. (2005). Detailed description of the way of  $R_n$  computation can be read in Soos and Anda (2014) as follows:

$R_n$  is the difference between the incoming net shortwave ( $R_{ns}$ ) and the outgoing net longwave radiation ( $R_{nl}$ ):

$$R_n = R_{ns} - R_{nl}. \quad (3)$$

The net solar or shortwave radiation,  $R_{ns}$  [MJ m<sup>-2</sup> day<sup>-1</sup>] is given by:

$$R_{ns} = (1 - \alpha) R_s, \quad (4)$$

where  $\alpha$  is the albedo for the reference crop. The incoming solar radiation,  $R_s$  [MJ m<sup>-2</sup> day<sup>-1</sup>] was measured locally by a CM-3 pyranometer.

Net longwave (outgoing) radiation,  $R_{nl}$  [MJ m<sup>-2</sup> day<sup>-1</sup>] was calculated as follows:

$$R_{nl} = \sigma \left[ T_{mean,K}^4 \right] (0.34 - 0.14 \sqrt{e_a}) (1.35 \frac{R_s}{R_{SO}} - 0.35), \quad (5)$$

where  $\sigma$  is the Stefan-Boltzmann constant [  $4.903 \cdot 10^{-9} \text{ MJ K}^{-4} \text{ m}^{-2} \text{ day}^{-1}$  ],  $T_{mean,K}$  is the mean temperature during the 24-hour period [K],  $R_s/R_{so}$  is the relative shortwave radiation (limited to  $\leq 1.0$ ),  $R_s$  is the measured solar radiation [ $\text{MJ m}^{-2} \text{ day}^{-1}$ ],  $R_{so}$  is the calculated clear-sky radiation [ $\text{MJ m}^{-2} \text{ day}^{-1}$ ].

To get clear-sky solar radiation  $R_{so}$  [ $\text{MJ m}^{-2} \text{ day}^{-1}$ ], the station elevation is required:

$$R_{SO} = (0.75 + 2 * 10^{-5}Z)R_a , \quad (6)$$

where  $R_a$  is the extraterrestrial radiation [ $\text{MJ m}^{-2} \text{ day}^{-1}$ ].

$R_a$ , [ $\text{MJ m}^{-2} \text{ day}^{-1}$ ] is calculated by:

$$R_a = \frac{24(60)}{\pi} G_{SC} d_r [\omega_s \sin(\varphi) \sin(\delta) + \cos(\varphi) \cos(\delta) \sin(\omega_s)] , \quad (7)$$

where  $G_{sc}$  is the solar constant =  $0.0820 \text{ MJ m}^{-2} \text{ min}^{-1}$ ,  $d_r$  is the inverse relative distance between the Earth and Sun,  $\delta$  is the solar declination [rad],  $\omega_s$  is the sunset hour angle [rad],  $\varphi$  is the latitude [rad] at Keszthely.

The lacking parametrs are calculated as follows:

$$d_r = 1 + 0.033 \cos\left(\frac{2\pi}{365} J\right) . \quad (8)$$

$$\delta = 0.409 \sin\left(\frac{2\pi}{365} J - 1.39\right) , \quad (9)$$

where  $J$  is the number of the day in the year between 1 (January 1) and 365 or 366 (December 31).

The sunset hour angle,  $\omega_s$ , is given by:

$$\omega_s = \arccos[-\tan(\varphi) \tan(\delta)] . \quad (10)$$

As the magnitude of the day or ten-day soil heat flux beneath the grass reference surface is relatively small, it may be ignored, and thus (Allen et al., 2005):

$$G_{day} \approx 0 . \quad (11)$$

Class A pan's coefficients ( $K$ ) were derived from the measured  $E_p$  of S ( $K_s$ ) and P<sub>s</sub> ( $K_p$ ), and the control Class A pan  $E_p$ :

$$K_s = \frac{E_p \text{ of } S}{E_p} , \quad (12)$$

$$K_p = \frac{E_p \text{ of } P_s}{E_p} . \quad (13)$$

### *Weather conditions*

Weather variables were recorded by a QLC-50 climate station (Vaisala, Helsinki, Finland) equipped with a CM-3 pyranometer (Kipp & Zonen Corp., Delft, the Netherlands). The combined  $T_a$  and humidity sensors were placed at a standard height (2 m above the soil surface). Signals from meteorological elements were collected every 2 second, and 10 minute means were logged by the station. The height of the anemometer was 10.5 m.

The wind speed was adjusted to standard height,  $u_2$ , [ $\text{m s}^{-1}$ ] of 2 m:

$$u_2 = u_z \frac{4.87}{\ln(67.8z_m - 5.42)}, \quad (14)$$

where  $u_z$  is the measured wind speed at 10.5 m above the ground surface [ $\text{m s}^{-1}$ ],  $z_m$  is the height of measurement above the ground surface (10.5 m).

The weather conditions of the studied months were specified by the monthly Thornthwaite index,  $TI$  of the World Meteorological Organisation (WMO, 1975):

$$TI = 1.65(P/T_a + 12.2)^{10/9} \quad (15)$$

where  $P$  and  $T_a$  are the monthly sum of precipitation and the monthly mean air temperature, respectively.

In classifying the weather conditions in each season's months, a 20% deviation was assumed from the climate normals (1971–2000), above and below the  $TI_{norm}$  for both included meteorological variables ( $P$  and  $T_a$ ), allowing the following weather classes to be distinguished (Anda *et al.*, 2014):

- warm-dry month ( $h$ ):  $TI_{month} > TI_{norm} \times 0.8$ ;
- cool-wet month ( $c$ ):  $TI_{month} > TI_{norm} \times 1.2$ ;
- month with normal weather ( $n$ ):  $TI_{norm} \times 0.8 \leq TI_{month} \leq TI_{norm} \times 1.2$ .

By counting the highest number of months within each of these three groups, the season was considered to be either normal, cool(wet), or warm(dry).

### *2.2. Statistical analysis*

In the analysis of  $E_p$  variations with normal distribution [ $\text{mm season}^{-1}$ ] two-tailed  $t$ -test was applied. Normality was checked by the Shapiro-Wilks test. When non-normal distribution was observed, a non-parametric statistical hypothesis test, the Wilcoxon signed-rank test was used. To get the influence of meteorological variables (Class A pan,  $R_n$ ,  $T_a$ ,  $T_w$ ,  $RH$ ,  $u_z$ ,  $P$ ) on  $E_p$  rates, Pearson's correlation analysis was applied. Analyzing the combined effect of different meteorological variables on  $E_p$  rates, multiple stepwise regression analysis was carried out. All tests were carried out with SPSS Statistics version 17.0 software (IBM Corp., New York, USA).

### 3. Results and discussion

#### 3.1. Weather conditions and dry matter accumulation in the season of 2016

On a seasonal average basis, the mean  $T_a$  of Keszthely (16.8 °C) was almost the same as the climate normal (16.9 °C) during the season of 2016. Seasons between 1971 and 2000 are included in the long-term average. Long-term seasonal mean  $P$  sum from March through October was 384.4 mm at Keszthely. Conditions in 2016 were much wetter than the long-term average with 525.4 mm  $P$  total. Season of 2016 received about one third more rainfall than that of the long-term  $P$  sum of the studied region. After all, wet characteristic of our season was also confirmed by the Thornthwaite index classification (Table 1).

Table 1. Weather conditions of the studied growing season using the Thornthwaite index,  $TI$

	April	May	June	July	August	September	i-season
2016	dry	wet	normal	wet	wet	dry	wet

Macrophyte implementation into Class A pan happened with 2.832 kg (fresh weight) of plant mass, on June 6, 2016. Plant material was collected from the lakeshore of Balaton (at Keszthely Bay). Similarly to natural conditions of Keszthely Bay, equal weight of all the three dominant macrophyte species were implemented into Class A pan (*Myriophyllum* sp., *Potamogeton* sp., *Najas* sp.). In the end of the season (September 30, 2016), the harvested fresh weight of submerged aquatic macrophytes was almost twice as much as the initial weight (4.763 kg).

#### 3.2. $E_p$ , $E_o$ , and $ET_o$ variations during 2016

$E_p$  of C ranged from 0.7 to 5.8 mm day<sup>-1</sup> on July 12 with a seasonal average of 3.03±1.23 (Fig. 3).  $E_p$  of S ranged from 0.7 to 6.9 mm day<sup>-1</sup> on July 5 with a seasonal average of 3.65±1.51. In the pan with macrophytes,  $E_p$  ranged from 1 to 7.3 mm day<sup>-1</sup> on August 6 with a seasonal average of 3.84±1.57. Reference  $E_o$  and  $ET_o$  values exceeded the measured  $E_p$  ones. Daily mean  $E_o$  and  $ET_o$  were 4.65±1.43 and 3.93±1.25, respectively. The maximum  $E_o$  and  $ET_o$  values occurred on June 25 and 28 as 7.2 mm day<sup>-1</sup> and 6.1 mm day<sup>-1</sup>, respectively. The probably reason of low pan  $E_p$  might have been the special geographical position of

Keszthely meteorological station. The meteorological station is placed at about 200 m from Keszthely Bay (Balaton Lake), that is sheltered by surrounded mountains causing lower wind speeds (Anda *et al.*, 2016). In accordance with the studies of McVicar *et al.* (2012), there has also been a decline in near surface  $u$ , contributing to a reduced rate of evaporative demand.

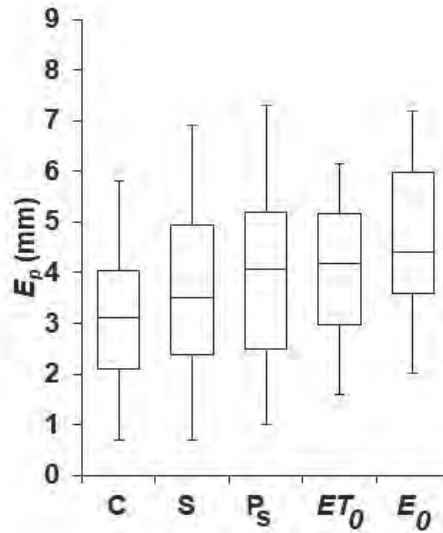


Fig. 3. Statistical analysis for daily Class A pan evaporation,  $E_p$  during the 2016 growing season. The bottom and top of boxes are the 25th and 75th percentiles (the lower and upper quartiles), respectively, and the band near the middle of the boxes is the median (50th percentile). Vertical lines that end in a horizontal stroke above and below each box are drawn from the upper and lower hinges to the upper and lower adjacent values. C, S, and P<sub>s</sub> denote Class A pan, Class A pan with sediment-covered bottom, and Class A pan implemented with macrophytes, respectively.

Both sediment cover and macrophytes placed Class A pan increased daily  $E_p$  rates significantly. Increments in seasonal mean daily  $E_p$  rates were 16.3% ( $p \leq 0.0001$ ) and 23.8% ( $p \leq 0.0001$ ) in S and P<sub>s</sub>, respectively. Difference in measured daily mean  $E_p$  and computed  $E_o$  was even greater (42.3%;  $p \leq 0.0001$ ). No deviation between  $ET_o$  and  $E_p$  of P<sub>s</sub> ( $p \leq 0.2838$ ) was observed, confirming that Class A pan  $E_p$  implemented with submerged macrophytes is closer to the computed reference  $ET_o$  than that of the empty Class A pan. Surprising result emerged when  $E_o$  and  $ET_o$  were compared; a 16.6% ( $P \leq 0.0001$ ) overestimation was found with  $E_o$  in comparison to  $ET_o$ .

According to daily mean  $E_p$  rates, the cumulative  $E_p$  values were 363.1, 427.7, and 461.5 mm in C, S, and Ps, respectively (Fig. 4). At the same time, higher reference  $E$  values were computed ( $E_o$ : 551.9 mm;  $ET_o$ : 472.1 mm). The impact of pan implementation for total  $E_p$  was always highly significant ( $p \leq 0.0001$ ). There was no difference in the measured cumulative  $E_p$  of Ps (461.5 mm) and computed Penman-Monteith  $ET_o$  (472.1 mm) during the season of 2016 ( $p \leq 0.2400$ ).

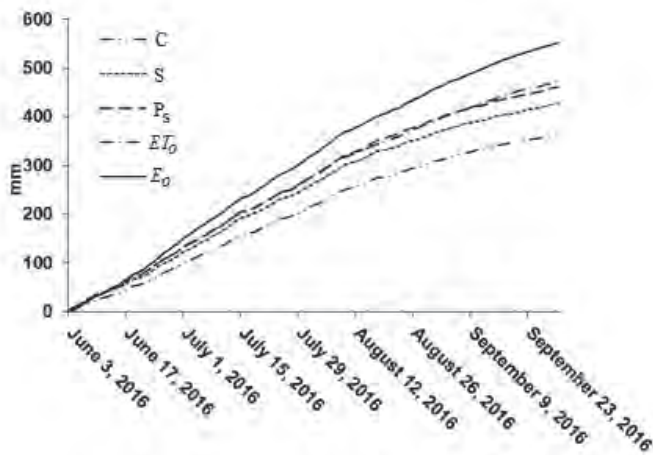


Fig. 4. Cumulative evaporations [mm] of Class A pan, implemented pan with macrophytes ( $P_s$ ), and implemented pan with sediment cover (S), and the reference evaporation,  $E_o$ .  $ET_o$  denotes the Penman-Monteith reference evapotranspiration total.

Irrespective of pan treatments, there was a large scatter in the data of daily measured  $E_p$  rates and computed reference  $E_o$  values (Fig. 5).

The slopes of linear regression between measured and computed  $E$  rates ranged from 0.68 to 0.92 (RMSE: 0.0679 – 0.7007 mm day<sup>-1</sup>). Better fit was observed between  $E_o$  and  $E_p$  with implemented macrophytes (slope: 0.92). Irrespective of pan treatments, computed  $E_o$  rates overestimated the measured  $E_p$  values during the 2016 growing season.

The relationship between the measured  $E_p$  of implemented Class A pan and reference  $ET_o$  (using Suttleworth formula) is improved in comparison to the relation between  $E_p$  and  $E_o$  (Fig. 6).

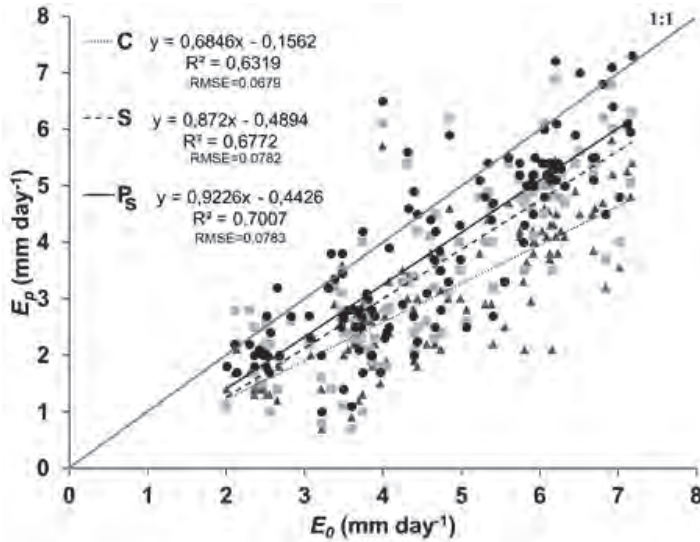


Fig. 5. Relationship between the daily measured Class A pan evaporations ( $E_p$ ) and daily reference evaporations ( $E_o$ ) computed by the Suttleworth formula. C, S, and  $P_s$  denotes empty, sediment covered, and macrophyte implemented Class A pans, respectively.

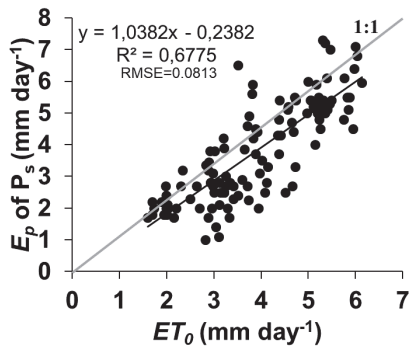


Fig. 6. Relationship between the daily measured pan evaporation ( $E_p$ ) of Class A pan implemented with macrophytes and daily reference evapotranspiration ( $ET_o$ ) computed by Penman-Monteith (FAO-56) formula.

The slope of linear regression was close to 1 (1.03; RMSE: 0.0813 mm day<sup>-1</sup>) implying that Penman-Monteith approximation (reference  $ET_o$ ) seems to be useful in estimation of the vaporation of the lake that contains submerged aquatic macrophytes.

### 3.3. Pan coefficient, $K$ , for implemented Class A pans

The ratio between the implemented Class A pan's  $E_p$  and empty pan's  $E_p$  provided a pan coefficient for those pan containing sediments ( $K_s$ ) and/or macrophytes ( $K_p$ ). The way of obtaining these coefficients was similar to computing the widely applied crop coefficients ( $K_c$ ) in evapotranspiration estimation. In accordance to increased daily and total  $E_p$  values for implemented Class A pans, the monthly average  $K$  values permanently exceeded 1 (Table 2). The seasonal mean  $K_s$  and  $K_p$  values were 1.18 (range: 1.13–1.27) and 1.30 (range: 1.24–1.37) in S and Ps, respectively. The highest increments in  $K$  values were observed during June, due to warmer weather conditions.

These  $K$  values may be useful in improving the Class A pan based  $E$  estimation of lakes or reservoirs which contain sediment covered bottom and/or submerged macrophytes.

Table 2. Monthly average pan coefficients for Class A pan with sediment-covered bottom ( $K_s$ ) and containing macrophytes ( $K_p$ ) in the growing season of 2016

	2016				
	June	July	August	September	Mean
$K_s$	1.27±0.24	1.19±0.15	1.14±0.15	1.13±0.3	<b>1.18±0.22</b>
$K_p$	1.37±0.29	1.24±0.23	1.33±0.41	1.26±0.15	<b>1.30±0.29</b>

### 3.4. Impact of weather on $E_p$ of implemented Class A pans

Correlation analysis to study the influence of weather variables (daily mean of  $T_a$ ; daily means of water temperature,  $T_w$ ; net radiation,  $R_n$ ; relative humidity,  $RH$ ; wind speed  $u$ ; precipitation  $P$ ) on daily measured  $E_p$  rate of Class A pan with macrophytes and/or sediment cover was carried out (Table 3).

Table 3. Correlation coefficients ( $r$ ) for daily measured evaporation rate ( $E_p$ ) for Class A pans with macrophytes and/or sediment cover. The following daily weather variables were accounted: daily mean of air temperatures,  $T_a$ ; daily means of water temperature,  $T_w$ ; net radiation,  $R_n$ ; relative humidity,  $RH$ ; wind speed,  $u_z$ ; and precipitation,  $P$

	Class A pan [mm]	$R_n$ [MJm <sup>-2</sup> ]	$T_a$ [°C]	$T_w$ [°C]	$RH$ [%]	$u_z$ [ms <sup>-1</sup> ]	$P$ [mm]
S	0.941**	0.789***	0.560***	0.577***	-0.571***	0.075	0.144
Ps	0.913***	0.795***	0.590***	0.642***	-0.577***	0.076	0.126

\* Marginally significant correlation  $|r|>0.1$ ,  $p<0.01$

\*\* Marginally significant correlation  $|r|>0.1$ ,  $p<0.001$

\*\*\* Significant correlation  $|r|>0.4$ ,  $p<0.0001$

The closest relationship between the  $E_p$  of Class A pan and  $E_p$  of S ( $r=0.941$ ) and Ps ( $r=0.913$ ) was not unexpected. Meteorological variables related to available energy ( $R_n$ ,  $T_a$ ,  $T_w$ ) have also high positive correlation coefficients in both implemented pan treatments (S and Ps).  $R_n$  had governmental role in  $E_p$  regulation on the basis of its correlation coefficient size among energy related variables ( $r=0.789$  and  $r=0.795$  in S and Ps). Somewhat lower correlation coefficients of  $T_a$  and  $T_w$  ranged from  $r=0.56$  (S) to  $r=0.642$  (Ps). *Martinez et al.* (2006) and *McVicar et al.* (2007) communicated the decisive effect of  $T_w$  on the rate of Class A pan  $E_p$ . *Gundalia and Mrugen* (2013) and *Xiaomang et al.* (2011) also found high positive correlation between  $T_a$  and  $E_p$ . In our study, a negative correlation of  $r=-0.57$  was noticed with  $RH$  (both  $E_p$  of S and Ps), in accordance with earlier observations of *Singh et al.*, (1992).

A weak positive correlation coefficient for  $u$  has not confirmed the earlier result of *McVicar et al.* (2012) for  $E_p$ . The probably reason of very loose relation between  $u$  and  $E_p$  may be the geographical position of Keszthely Bay, that is sheltered by Keszthely Mountains from the side of prevailing northern wind direction. Weak correlation of  $P$  with  $E_p$  came as no surprise, due to the water replacement practice of pan operation.

$E_p$  rate is defined as the difference in vapor pressure between the pan's surface and surrounding atmosphere, providing a simple integrated measurement of complex meteorological interaction between  $R_n$ ,  $T_a$ ,  $RH$ ,  $u_z$ , and  $E_p$  (*Roderick et al.*, 2009). Due to strong variability in the magnitude of the above specified meteorological elements, measured  $E_p$  rates can strongly differ from place to place (*Yang and Yang*, 2012). These qualifying differences in spatial  $E_p$  might also be displayed in variation of correlation coefficients existing between meteorological variables and  $E_p$  rates.

Only easily accessible meteorological variables are included in the multiple stepwise regression analysis ( $T_a$ ,  $RH$ ,  $u_z$ ,  $P$ ). Class A pan,  $R_n$  and  $T_w$  were excluded

from the investigation. In the course, three meteorological variables remained in the regression equations ( $T_a$ ,  $u_z$ , and  $RH$ ). These meteorological variables are available even in such places where meteorological stations are missing (research stations, universities, etc.). Our analysis showed that two meteorological variables ( $T_a$  and  $RH$ ) impacted the  $E_p$  of P<sub>s</sub> and S the most (Table 4). The first two equations of Table 4 present the possibility of computing  $E$  of a lake/reservoir with macrophytes and/or sediments, when the only available meteorological variable is the  $T_a$  (in P<sub>s</sub>) or  $RH$  (in S). The second two equations of  $E$ , estimation when macrophytes and sediment cover are accounted, contain two meteorological variables,  $T_a$  and  $RH$ . Observation of  $T_a$  or  $RH$  might not cause difficulties in the present time.

Table 4. Multiple stepwise regression analysis between meteorological elements (air temperature,  $T_a$ , relative humidity,  $RH$ ; wind speed  $u_z$ , precipitation,  $P$ ) and measured Class A pan evaporation ( $E_p$ ) with macrophytes (P<sub>s</sub>) and sediment covered bottom (S) in the season of 2016.  $r$ : coefficient of multiple correlation.

	Adjusted $r^2$	$F$	$F$ sig.	$SE$ of coefficient	Regression equation
1. $E_p$ of S	0.321	57.227	0.000	Const.= 1.385	$E_p = -0.139RH + 14.003$
				$RH = 0.018$	
2. $E_p$ of S	0.497	59.776	0.000	Const.= 1.540	$E_p = -0.111 RH + 0.212T_a + 7.660$
				$RH = 0.016$	
				$T_a = 0.033$	
1. $E_p$ of P <sub>s</sub>	0.343	63.059	0.000	Const.= 0.752	$E_p = 0.297T_a - 2.051$
				$T_a = 0.037$	
2. $E_p$ of P <sub>s</sub>	0.530	68.201	0.000	Const.= 1.548	$E_p = 0.237T_a - 0.114RH + 7.740$
				$T_a = 0.033$	
				$RH = 0.016$	

### 3.5. Simple water budget terms on Balaton Lake (Keszthely Bay) during the growing season of 2016

There are two important terms describing the simplified water budget of a lake: the precipitation  $P$  as an input and the evaporation  $E$  as the output of water. Specification of exact water balance of studied site was excluded from our investigation. Our purpose was a simple comparison of the two most important simplified water balance members at Keszthely Bay. The area of Keszthely Bay is 39 km<sup>2</sup>, less than 10% of the whole area of Balaton Lake. Based on local observations, the submerged macrophytes occupies 5–10% of the whole bay (Anda et al., 2016). The remaining part of the bay accounted for as covered bottom with sediments.

Despite wet conditions of the growing season, computed  $E$  of Keszthely Bay surpassed seasonal amount of  $P$  in 2016 (Table 5). Slightly more than 90% of  $E$  derived from  $P$  in the 2016 growing season. On daily mean basis, the  $E$  rate of Keszthely Bay increased with 16.9% when macrophytes and sediment cover were accounted. Increment in seasonal total  $E$  for the whole bay resulted 264,000,000 m<sup>3</sup> water, when macrophytes and sediment cover were included in Keszthely Bay's  $E$  estimation. During arid seasons, this  $E$  rate may increase substantially strengthening the importance of  $E$  related investigations of natural lakes.

Table 5. Seasonal sums of precipitation ( $P$ ) and evaporation ( $E$ ) [mm] of Keszthely Bay including daily  $E$  rates [mm day<sup>-1</sup>]. The  $E$  estimates of the lake were based on weighting averages of a) using pan coefficients with sediment-covered bottom ( $K_s$ ), and macrophytes ( $K_p$ ) and b) simple Class A pan measurements.

**a) Simple water budget terms of Keszthely Bay (macrophytes and sediment cover included)**

Seasonal sums [mm]		Daily rates [mm day <sup>-1</sup> ]		Water total [10 <sup>6</sup> m <sup>3</sup> ]		
$P$	$E$	$\Delta$	$E$	$P$	$E$	$\Delta$
328.5	430.69	-102.19	3.59	12.81	16.8	-3.99

**b) Simple water budget computed by Class A pan data only**

Seasonal sums [mm]		Daily rates [mm day <sup>-1</sup> ]		Water total [10 <sup>6</sup> m <sup>3</sup> ]		
$P$	$E_p$	$\Delta$	$E_p$	$P$	$E_p$	$\Delta$
328.5	363.15	-34.65	3.03	12.81	14.16	-1.35

#### 4. Conclusions

A simple approach was presented to evaluate the  $E$  of a natural fresh water lake in Hungary. To achieve this goal, Class A pans were implemented with aquatic submerged macrophytes and/or their bottom was covered by sediment.  $E_p$  rate of treated Class A pans increased significantly. The impact of macrophytes and sediment cover on the  $E$  of the lake can be computed directly through using pan's coefficients.

In our study, we received a Class A pan coefficient of above 1 ( $K_{as}$ :1.18;  $K_{ap}$ :1.3) in comparison to the calculated potential evapotranspiration, which is in contrast to the most reported cases in the literature, where values of well below 1 (around 0.75) were received. Similarly to our outstanding results in 2016, annual

mean value of 0.99 for one separate warm and arid year was published by *Sabziparvar et al.* (2009). *Allen et al.* (1998) have also imparted that Class A pan coefficient may vary highly depending on the geographical site and the actual weather conditions.

The reason of  $K_c$  deviation could lie in biased wind profile – i.e., biased measurement of wind speed and/or its correction to 2 m height. Moreover, the special hill-surrounded (shadowed) location of Keszthely Agrometeorological Research Station may also reduce the impact of wind on evaporation. *Roderick et al.* (2007) revealed differences among 41 investigated sites between 1977 and 2004, where decreasing wind speed was found to be the main reason for changing Class A pan evaporation. Other possible reason of altered  $K_c$  may be the estimation of net radiation instead of measurement together with neglected factors influencing pan energy balance. Therefore, our Class A pan coefficient should be used with attention to local environmental conditions, and should be re-calibrated before application, if possible.

Growing season of investigation has the characteristic of a wet weather. Even in the course of the wet season, the increment in  $E$  of Keszthely Bay (Balaton Lake) reached 16.9% (264,000,000 m<sup>3</sup>), when macrophytes and sediments were also accounted. This simple approach using pan coefficients may extend the accuracy of the  $E$  estimation of natural lakes, based on Class A pan in a broader circle than earlier.

**Acknowledgement:** We acknowledge the financial support of Széchenyi 2020 under the EFOP-3.6.1-16-2016-00015. The project is co-financed by Széchenyi 2020.

## References

- Allen, R.G., Clemmens, A.J., Burt, C.M., Solomon, K., and O'Halloran, T.*, 2005: Prediction accuracy for projectwide evapotranspiration using crop coefficients and reference evapotranspiration. *J. Irrig. Drain. Eng. ASCE*, 131, 24–36. [https://doi.org/10.1061/\(ASCE\)0733-9437\(2005\)131:1\(24\)](https://doi.org/10.1061/(ASCE)0733-9437(2005)131:1(24))
- Allen, R.G., Pereira, L.S., Raes, D., and Smith, M.*, 1998: Crop evapotranspiration – guidelines for computing crop water requirements. FAO Irrigation and Drainage Paper 56, Rome, Italy.
- Anda, A., Simon, B., Soos, G., Teixeira da Silva, J.A., and Kucserka, T.*, 2016: Effect of submerged, freshwater aquatic macrophytes and littoral sediments on pan evaporation in the Lake Balaton region, Hungary. *J. Hydrol.* 542, 615–626. <https://doi.org/10.1016/j.jhydrol.2016.09.034>
- Anda, A., Teixeira da Silva, J.A., and Soos, G.*, 2014: Evapotranspiration and crop coefficient of the common reed at the surroundings of Lake Balaton, Hungary. *Aquatic Bot.* 116, 53–59. <https://doi.org/10.1016/j.aquabot.2014.01.008>
- Barrat-Segretain, H.M.*, 1996: Strategies of reproduction, dispersion, and competition in river plants: A review. *Vegetatio* 123, 13–37. <https://doi.org/10.1007/BF00044885>

- Brothers, S., Hilt, S., Meyer, S., and Köhler, J., 2013: Plant community structure determines primary productivity in shallow, eutrophic lakes. *Freshw. Biol.* 58, 2264–2276. <https://doi.org/10.1111/fwb.12207>
- Gundalia, M.J., and Mugen D.B., 2013: Modelling pan evaporation using mean air temperature and mean pan evaporation relationship in middle south Saurashtra Region. A review. *Int. J. Water Res. Environ. Engin.* 5, 622–629.
- Hilt, S., Adrian, R., Köhler, J., Monaghan, M.T., and Sayer, C., 2013: Clear, crashing, turbid and back e long-term macrophyte changes in a shallow lake. *Freshw. Biol.* 58, 2027–2036. <https://doi.org/10.1111/fwb.12188>
- Jacobs, A.F.G., Heusinkveld, B.G., and Lucassen, D.C., 1998. Temperature variation in a class A evaporation pan. *J. Hydrol.* 206, 75–83. [https://doi.org/10.1016/S0022-1694\(98\)00087-0](https://doi.org/10.1016/S0022-1694(98)00087-0)
- Kim, S., Shiri, J., Singh, V.P., Kisi, O., and Landaras, G., 2015: Predicting daily pan evaporation by soft computing models with limited climatic data. *Hydrol. Sci. J.* 60, 1120–1136. <https://doi.org/10.1080/02626667.2014.945937>
- Lim, W.H., Roderick, M.L., Hobbins, M.T., Wong, S.C., and Farquhar, G.D., 2013: The energy balance of a US Class A evaporation pan. *Agric. Forest Meteorol.* 182–183, 314–331. <https://doi.org/10.1016/j.agrformet.2013.07.001>
- Linacre, E.T., 1994: Estimating United States Class-A pan evaporation from few climate data. *Water Int.* 19, 5–14. <https://doi.org/10.1080/02508069408686189>
- Majidi, M., Alizadeh, A., Farid, A., and Vazifedoust, M., 2015: Estimating evaporation from lakes and reservoirs under limited data condition in a semi-arid region. *Water Res. Manage.* 29, 3711–3733. <https://doi.org/10.1007/s11269-015-1025-8>
- Martí, P., González-Altozano, P., López-Urrea, R., Mancha, L.A., and Shiri, J., 2015: Modeling reference evapotranspiration with calculated targets. Assessment and implications. *Agric. Water Manage.* 149, 81–90. <https://doi.org/10.1016/j.agwat.2014.10.028>
- Martinez, J.M.M., Alvarez, V.M., Gonzalez-Real, M.M., and Baille, A., 2006: A simulation model for predicting hourly pan evaporation from meteorological data. *J. Hydrol.* 318, 250–261. <https://doi.org/10.1016/j.jhydrol.2005.06.016>
- McVicar, T.R., Roderick, M.L., Donohue, R.J., Li, L.T., Van Niel, T.G., Thomas, A., Grieser, J., Jhajharia, D., Himri, Y., Mahowald, N.M., Mescherskaya, A.V., Kruger, A.C., Rehman, S., and Dinpashoh, Y., 2012: Global review and synthesis of trends in observed terrestrial near-surface wind speeds: implications for evaporation. *J. Hydrol.* 416–417, 182–205. <https://doi.org/10.1016/j.jhydrol.2011.10.024>
- McVicar, T.R., Van Niel, T.G., Li, L.T., Hutchinson, M.F., Mu, X.M., and Liu, Z.H., 2007: Spatially distributing monthly reference evapotranspiration and panevaporation considering topographic influences. *J. Hydrol.* 338, 196–220. <https://doi.org/10.1016/j.jhydrol.2007.02.018>
- Monteith, J.L., 1965: Evaporation and environment. In (Ed.: Fogg, G.E.) *The State and Movement of Water in Living Organism*. Proc. XIX. Symp. Soc. Exp. Biol. Cambridge University Press, Cambridge. 205–234.
- Penman, H.L., 1948: Natural evaporation from open water, bare soil and grass. *Proc. Royal Soc. London. Ser. A, Mathematical Phys. Sci.* 193 (1032), 120–145. <https://doi.org/10.1098/rspa.1948.0037>
- Roderick, M.L., Rotstayn, L.D., Farquhar, G.D., and Hobbins, M.T., 2007: On the attribution of changing pan evaporation. *Geophys. Res. Lett.* 34, L17403. <https://doi.org/10.1029/2007GL031166>
- Rotstayn, L.D., Roderick, M.L., and Farquhar, G.D., 2006. A simple pan-evaporation model for analysis of climate simulations: evaluation over Australia. *Geophys. Res. Lett.* 33, L17715. <https://doi.org/10.1029/2006GL027114>

- Sabziparvar, A.A., Tabari, H., Aeni, A., and Ghafouri, M., 2010: Evaluation of Class A Pan Coefficient Models for Estimation of Reference Crop Evapotranspiration in Cold Semi-Arid and Warm Arid Climates. *Water Res. Manage* 24, 909–920. <https://doi.org/10.1007/s11269-009-9478-2>
- Shiri, J., Dierickx, W., Baba, A.P.A., Neamati, S., and Ghorbani, M.A., 2011: Estimating daily pan evaporation from climatic data of the State of Illinois, USA using adaptive neuro-fuzzy inference system (ANFIS) and artificial neural network (ANN). *Hydrol. Res.* 42, 491–502. <https://doi.org/10.2166/nh.2011.020>
- Shuttleworth, W.J., 1993. Evaporation. In (ed.: Maidment, D.R.) *Handbook of Hydrology*. McGraw and Hill, New York.
- Singh, R., Bishnoi, O.P., and Ram, N., 1992: Relationship between evaporation from class 'A' open pan evaporimeter and meteorological parameters at Hisar. *Haryana Agri. Univ. J. Res.* 22, 97–98.
- Soos, G. and Anda, A., 2014: A methodological study on local application of the FAO-56 Penman-Monteith reference evapotranspiration equation. *Georgikon for Agric.* 18, 71–85.
- SPSS Statistics version 17.0 software. IBM Corp., New York, USA.
- Vári, Á., 2012. Propagation and growth of submerged Macrophytes in Lake Balaton. PhD Dissertation.
- Wang, L., Kisi, O., and Zounemat-Kermani, Li, H., 2017: Pan evaporation modeling using six different heuristic computing methods in different climates of China. *J Hydrol.* 544, 407–427. <https://doi.org/10.1016/j.jhydrol.2016.11.059>
- WMO Report, 1975. Drought and Agriculture. WMO Techn. Note No. 138.
- Xiaomang, L., Yuzhou, L., Dan, Z., Minghua, Z., and Changming, L., 2011. Recent changes in pan-evaporation dynamics in China. *Geophys. Res. Lett.* 38, 13–19.

# IDŐJÁRÁS

*Quarterly Journal of the Hungarian Meteorological Service  
Vol. 122, No. 1, January – March, 2018, pp. 59–79*

## **Application of European numerical weather prediction models for hydrological purposes**

**István Ihász<sup>1\*</sup>, Amarilla Mátrai<sup>2</sup>, Balázs Szintai<sup>1</sup>, Mihály Szűcs<sup>1</sup>,  
and Imre Bonta<sup>1</sup>**

<sup>1</sup>*Hungarian Meteorological Service,  
P.O. Box 38, H-1525 Budapest, Hungary*

<sup>2</sup>*General Directorate of Water Management  
P. O. Box 32, H-1518 Budapest, Hungary  
E-mail: matrai.amarilla@ovf.hu*

*\*Corresponding author E-mail: [ihasz.i@met.hu](mailto:ihasz.i@met.hu)*

*(Manuscript received in final form August 22, 2017)*

**Abstract**—Nowadays, hydrological forecasts are based on wide range of meteorological inputs, including observations and forecasts. In this paper four main areas are covered. First of all, milestones covering last four decades from usage of a simple statistical method to regional limited area modeling are summarized. Then an overview of the main activities of the European Flood Awareness System (EFAS) is given. Usage of ensemble forecasts for providing uncertainty is getting larger and larger attention for hydrological applications too. Benefits of a locally developed new tool, the ensemble calibration method based on reforecast model climate is given in the third part. Finally, local developments on regional hydrostatic and non-hydrostatic models are shown. It is shown that a high resolution limited area non-hydrostatic model can predict summer heavy precipitation more accurately.

*Key-words:* ensemble forecasts, case studies, flood, EFAS, precipitation, probability, calibration, numerical weather prediction models, ECMWF, ALADIN, AROME

### ***1. Introduction***

Necessity of the study of meteorological and hydrological circumstances of floods on two main rivers (Danube and Tisza) got a special emphasize after a severe flood event on Tisza, which caused extreme damages in spring 1970 (Bonta and Újváry, 2011). In the middle of the 1970s, several projects were

realized to study the weather scenarios causing heavy floods (*Bodolainé*, 1976). As model forecasts from large European meteorological services were available only in the beginning of the 1980s, a statistical method was constructed to estimate the precipitation amount. The Precipitation Synoptic Division was established headed by *Bodolainé*, forecasts were made daily for 20 water basins of rivers Danube and Tisza. It was a pioneering activity (both in Hungary and Europe in general) in studying the relation between weather conditions causing heavy floods (*Bodolainé*, 1983). A comprehensive study was made on the heavy floods of the '80s and '90s by *Szépszó* (2003).

Since the 1970s, global models have been operationally running at the largest meteorological services, and relatively few countries were able to run regional models providing downscaled weather forecasts. In the '80s, due to rapid development of limited area regional models, significant benefits could be provided, especially in surface weather parameters, like precipitation, 10m wind, and 2m temperature compared to global forecasts. Consequently, the Hungarian Meteorological Service (OMSZ) considered to implement a state-of-the-art model in the second part of the 1980s. Three main conditions had to be available to fulfil this plan. First of all, a powerful computer had to be installed, a BASF 7/61 type computer was purchased in 1986. The Swedish grid point limited area model was one of the best in his field, it was bought by OMSZ in 1988. A small new team focusing on this activity was headed by *Dezső Dévényi*. After having solved several problems in July 1991, the adapted model having 0.9\*0.9 degrees horizontal resolution and 12 levels in the vertical became operational covering Europe (*Ihász*, 1992, 2014). After having signed a cooperation agreement between the European Centre for Medium-Range Weather Forecasts (ECMWF) and Hungary in the spring of 1995, lateral boundary conditions had been operationally used for the model, and this development provided improved precipitation forecast for the rest of the model life, until 1998.

In 1991, Météo France invited several central European countries to take part in developments for creating the ALADIN hydrostatic spectral limited area model from the global ARPEGE model (*Horányi et al.*, 1996). This model became operational in May 1994 in Toulouse, and it started to provide precipitation forecasts via Météo-France's satellite broadcasting system for meteorological data & product (RETIM).

After installing a new high performance computing facility, the ALADIN/HU model became operational at OMSZ in 1998 (*Horányi et al.*, 2006). The model was coupled to the global ARPEGE model in the first 10 years of operational usage, and after several pioneering activities, the model was coupled to the ECMWF deterministic global model, providing significant improvement in quality of the forecasts (*Bölöni et al.*, 2009). In the first decade of the 21st century, a non-hydrostatic model was developed in the framework of an international cooperation. The AROME model became operational at OMSZ

in 2010 (Horányi *et al.*, 2011). This non-hydrostatic model could provide very useful information, especially in summer extreme precipitation events.

After signing a cooperation agreement between Hungary and ECMWF in July 1994, deterministic and ensemble forecasts became available for forecasters in January 1995. In the last two decades, a lot of local developments were done for providing support in decision making of the forecasters.

There were many pioneering activities in use of ensemble forecasts at OMSZ. Since 2003 ensemble clustering focusing on Central European meteorological patterns has been operationally done (Ihász, 2004). Ensemble representative member and ensemble mean for each clusters are available for the General Directorate of Water Managements, too. Quality of the ensemble forecasts could be significantly improved by ensemble calibration for weather elements, as 2m temperature, 10m wind speed, and precipitation (Ihász *et al.*, 2010; Mátrai, 2015; Mátrai and Ihász, 2017). Since 2011 ensemble vertical profile as newly developed product could support to make decision on both precipitation type in winter and intensity of convective events in summer (Ihász and Tajti, 2011). Usage of ensemble forecasts for prediction of the upper level lows causing heavy precipitation is especially useful (Gaál and Ihász, 2015). Benefits of the complex usage of the ensemble forecasts were proved in heavy convective events (Lázár and Ihász, 2016).

## ***2. The European Flood Awareness System (EFAS)***

In 2002, a devastating flood went down on Elba and Danube rivers, causing large damages. In response to this event, the EFAS was created within a co-financing framework at the European Commission Joint Research Centre, in close cooperation with the European national hydrological and meteorological services, the ECMWF, and the Monitoring and Information Centre (MIC). The aim of EFAS is to increase defence capabilities against natural disasters and floods. In recent years, EFAS transformed to an advanced flood forecasting system, with number of state-of-the-art products, like probability flood forecasting. The EFAS system has been working operationally since 2012.

The EFAS basically ordered the hydrological events to the quantitative indicators of the meteorological events in the past.

The hydrological model (LISHFLOOD) of EFAS provides early flood warning twice a day with 6-hour and daily intervals. The EFAS results are based on multiple weather forecasts with different spatial and temporal resolutions. The meteorological data originate from different weather services, high resolution (deterministic) and ensemble forecasts, and provide short and medium range products (European Centre for Medium Range Weather Forecasts – ECMWF, Deutscher Wetterdienst – DWD, and Consortium for Small-scale Modeling – COSMO).

From Hungary, the only EFAS partner is the General Directorate of Water Management. However, EFAS partner could be any national or regional or local authority, which provides flood forecast services or has a role in flood risk management in their own country.

Different maps and graphic products were made based on the incoming data from the EFAS members. These EFAS products are available on the official website: [www.efas.eu](http://www.efas.eu). For example, we can find information about the national flood monitoring gauges and management of these. Several meteorological and hydrological layers can be reached for the European region.

If the risk of flood or flash flood is high on the catchment of the member country, then EFAS send flood or flash flood notifications to the members. The disclosure of the information is based on exceeding a critical threshold, not on quantity water discharge forecast. The notification includes the river name, catchment, date of the forecast, date of predicted start of the event, date of earliest predicted peak, and the probability of the return period magnitude.

For more detailed information about the structure, operation, and products of the EFAS, refer to the official ECMWF Technical Memorandum (*Smith et al.*, 2016).

### ***3. Ensemble calibration***

With the unification of the ECMWF medium-range ensemble prediction system (ENS) and monthly forecasting system (MFS) on March 11, 2008 (*Hagedorn*, 2008), a new reforecast dataset has become available for a variety of applications. A reforecast dataset is a collection of forecasts with start and prediction dates from the past, usually going back for a considerable number of years. In order to ensure consistency between reforecasts and actual forecasts, reforecasts are produced specifically with the same model system that is used to produce the actual forecasts. Before the unification of the medium-range and monthly forecast systems, reforecasts were only produced – and thus applicable – for the monthly forecast system. However, through the unification of both systems, it is now possible to use the reforecasts produced with the unified system for both the ensemble and monthly forecasts.

Originally, the reforecasts of the monthly forecast system were mainly used to determine the model climate and forecast anomalies with respect to this model climate. Now, with the reforecasts also being applicable to the medium-range ensemble forecasts, new applications are possible. One of these new applications is the calibration of the medium-range ENS forecasts. Testing various calibration methods has shown that the forecasts can be significantly improved through calibration, in particular for near-surface weather parameters (*Gneiting*, 2014; *Richardson et al.*, 2014).

Nowadays, 11 reforecast ensemble members for 45 days ahead are operationally generated for the last 20 years every Monday and Tuesday. In our period of investigation (2008–2013), reforecasts were available for 5 members once a week (on Thursdays).

### 3.1. Comparison of reforecast and observation climates

Ensemble calibration can provide valuable improvement if there is a significant difference between the distribution of modeled and observed climates. Significance was investigated with two sample Kolmogorov-Smirnov tests. Stable model climate can be produced by using reforecasts from 5 consecutive weeks centered on the current date. Model climate was generated for each week and every year in this selected period (2008–2013).

The influence of model developments can easily be studied by comparison of ensemble reforecast climates, too. The horizontal resolution was 50 km between 2006 and 2010 and 32 km between 2011 and 2015. The vertical resolution covered 62 levels between 2006 and 2013 and it has been 91 since 2013. Comparative study was made between the observed climates and the consecutive model climates for 20 individual catchments of Danube and Tisza rivers (*Fig. 1*). Common characteristics were tried to find for the following three catchment types: flat, mountainous, and mixed areas. It was supposed that the influence of the model evolution can be seen on the model climates too.

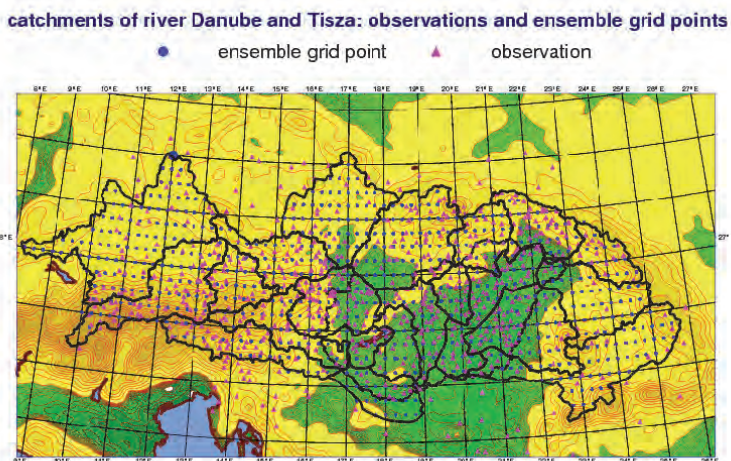


*Fig. 1.* 21 catchments of rivers Danube and Tisza (border of catchments (black), ensemble grid points (blue), and observations (magenta)).

In the mountainous type differences between model climates for the same catchments were generally larger than in the flat or mixed types. These features are demonstrated for the Upper-Tisza catchment in *Fig. 2*. The Kolmogorov-Smirnov test also proved this statement.

As a summary of this investigation, a common conclusion can be made for all catchments as:

- There are usually quite large differences among the model climates for the same catchment.
- Model climates of 2011 and 2008 are closer to each other than in case of 2014 and 2011.
- Due to smaller differences between modeled and observed climates for small or moderate precipitation amounts in flat regions, the calibration is generally not a necessity. It is especially true for the 2014 model climate.
- In case of large or extreme precipitation, the differences are remarkable, so calibration is beneficial.
- The minimum difference between the model climate and the observed climate occurred in 2014.

Seasonal and annual similarities and differences were also examined. Similar investigation was applied for observed and modeled climates for 2014 to see the weaknesses and strengths of the model and to support the best decision making in flood situations. It can be concluded that larger differences usually appear in summer due to more intensive convection. In any seasons, developments of the model can be seen in the distributions of the model climates, too. The largest positive changes between model climates (2008 and 2014) were found in summer, and it underlines the positive impact of model developments on convective precipitation forecasts. Even the largest differences between the modeled and observed climates for 2014 appeared in spring and summer, so some further improvements on the model are still needed. There was no common typical characteristic for three predefined catchment types (flat, mountainous, and mixture), which statement supports the necessity of calibration separately for each catchment.

As a conclusion, it can be noted that even if there is continuous development on the ensemble system resulting in more precise precipitation forecast, calibration is needed for all catchments and all seasons.

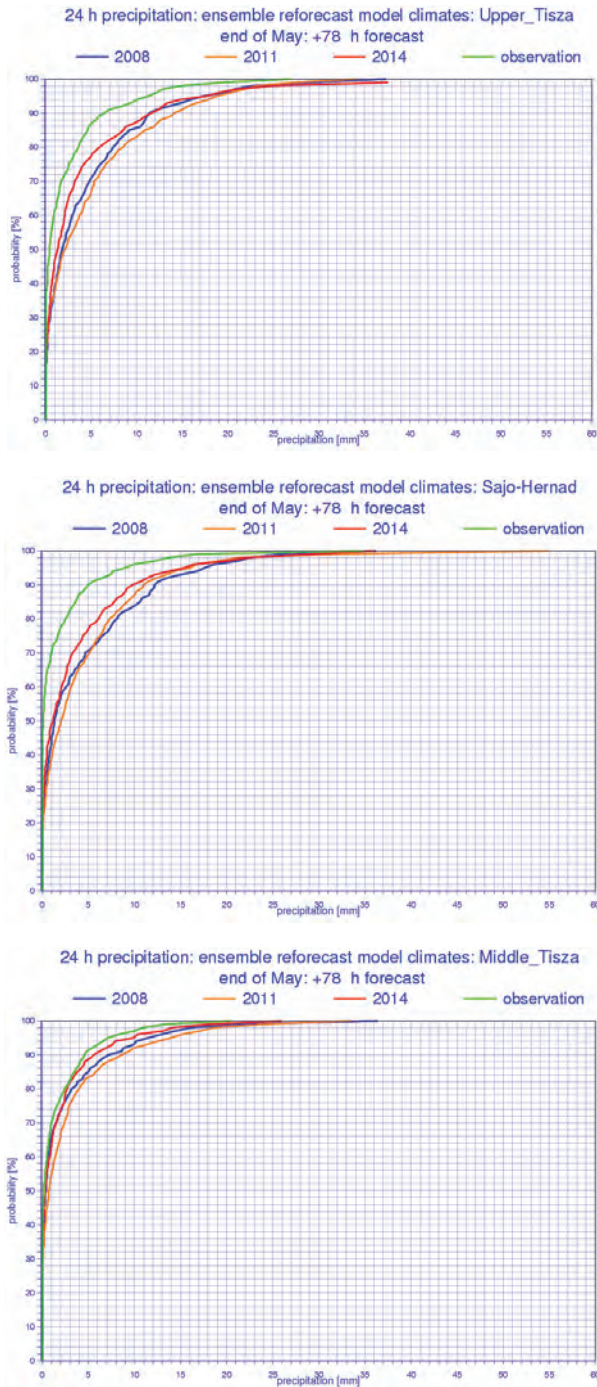


Fig. 2. Comparison of reforecast climates (2008, 2011, 2014) and observed climate for the mountainous (Upper-Tisza), mixed (Sajó-Hernád), and flat (Middle-Tisza) catchments

### 3.2. Calibration method

Calibration is a statistical adjustment of the forecast. To make calibration, following data were needed (on spatial mean of a catchment):

- reforecast climate: model climate distribution function made from the reforecasts,
- observed climate: distribution function of observed data, and
- ensemble forecast: distribution function of the current ENS forecast.

During the calibration, the adjustment of ensemble forecast was made by the difference of the observed climate and reforecast climate. More difference between the climates made more correction on the calibrated ensemble forecast. If the observed climate and reforecast climate were close together, then less correction in the calibration was applied (Mátrai and Ihász, 2017).

To understand our calibration method itself, the procedure is illustrated in *Fig. 3*. Suppose that one of our ensemble members predicts a precipitation amount of 6 mm. First, we have to find the frequency in the model climate that belongs to the value of 6 mm. Then, this frequency (87%) must be projected onto the observed climate. And finally, we get a value belonging to this frequency which is the new value of our ensemble member (8.5 mm). As a matter of fact, we assume that the distribution of observed values describes weather conditions more accurately in a given place than the distribution of values forecasted by a numerical model. Thus, instead of a simple shifting of the curve of distribution functions, like in case of bias correction, we look for the frequency of each ensemble value both in the modeled and observed climates.

Importantly, all of the distribution functions should be made for the same time period. If the studied period is too short, it may occur that the period does not include an extreme event. The result of the calibration method is an adjusted distribution function, which can be easily compared with the raw one and can help the forecasters to decide, whether to correct the precipitation forecast or not.

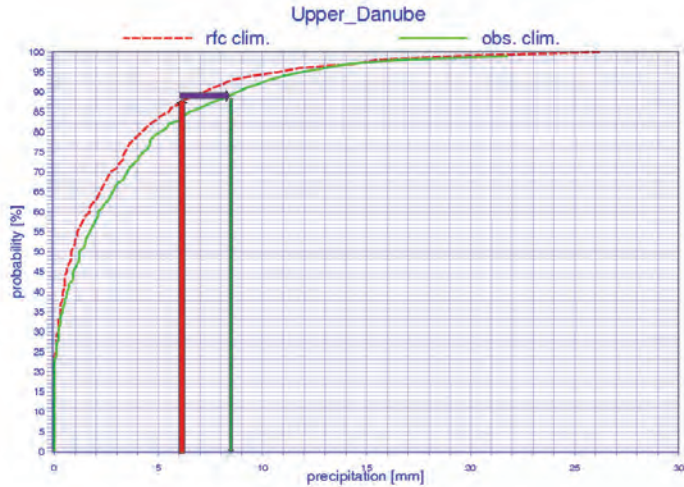


Fig. 3. Example of the calibration method.

### 3.3. Extreme flood on the Danube, May-June 2013

In late May and early June, a heavy flood event caused extreme damages in upper Danube due to intensive cyclone activity, which existed a few days around the Alps. In Hungary, the water level exceeded the former records registered in 2002, along the whole river, until the Hungarian-Serbian border. This extreme flood was caused by extreme precipitation fallen in 4 days in the three upper catchments of Danube. The largest amount of daily precipitation was recorded on June 2, 2013: Upper Danube - 35 mm/24h, Inn - 48 mm/24h, Traun-Enns - 53 mm/24h.

Fig. 4 shows the forecasts of high resolution (HRES) and ensemble (ENS) models mean. It can be seen that the area of intensive precipitation was well-defined, however, the HRES model overpredicted, the ENS mean underpredicted the daily precipitation amount by 10–20 mm during the whole period. It is important to note that the position and intensity of the extreme event were predicted by both models several days ahead.

Fig. 5 shows the plume diagram based on the May 29, 2013, 12 UTC model runs. Both high resolution and ensemble models predicted the large amount of the precipitation, while the ensemble system had a quite large spread.

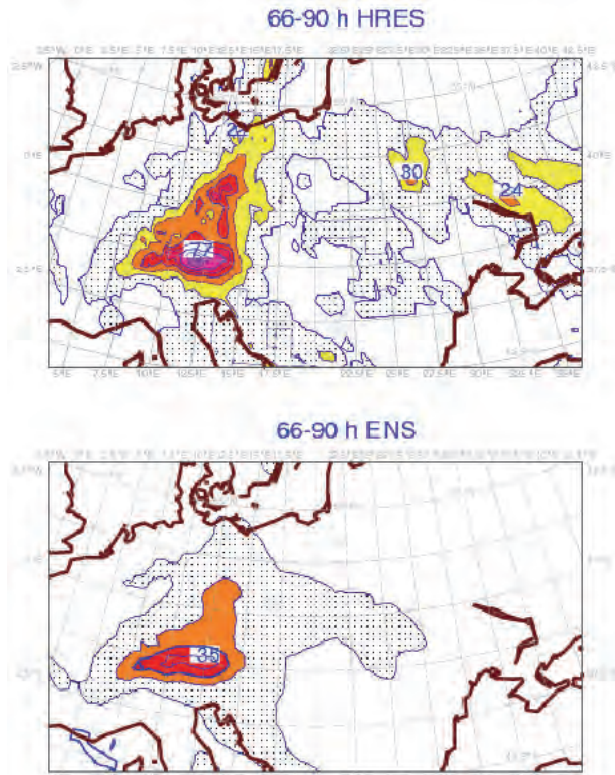


Fig. 4. Precipitation forecasts starting at 12 UTC on May 30, 2013 showing (a) the HRES 24-hour precipitation forecast 66 to 90 hours ahead and (b) the ENS mean 24-hour precipitation forecast 66 to 90 hours ahead.

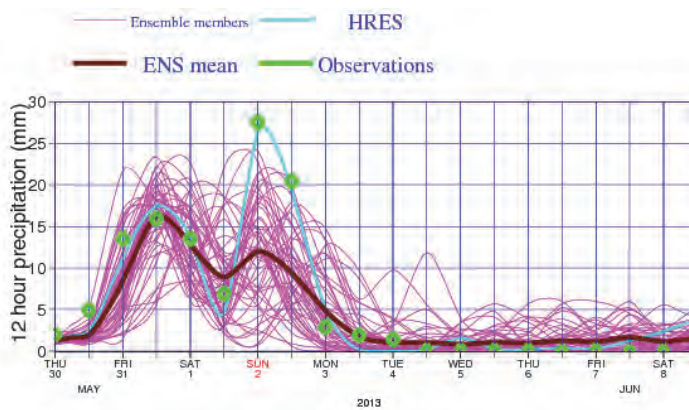


Fig. 5. ENS 12-hour precipitation plume and HRES forecast for the upper Danube area starting at 12 UTC on May 29, 2013.

It can be seen that the ensemble forecasts were still not accurate enough, so the calibration method was expedient to use. The next few figures show the result of the calibration for the upper Danube catchments.

Fig. 6 presents the impact of calibration on the precipitation probability for two catchments in the Alpine region, based on the May 28, 2013, 00 UTC model run and the 30–54h forecasts. In both forecasts, the observed climate and the reforecast climate remain close together, bigger differences occurred between 8–16 mm and in case of only few mm precipitations. Hence, the calibration method will make the biggest adjustment in these ranges (Fig. 7).

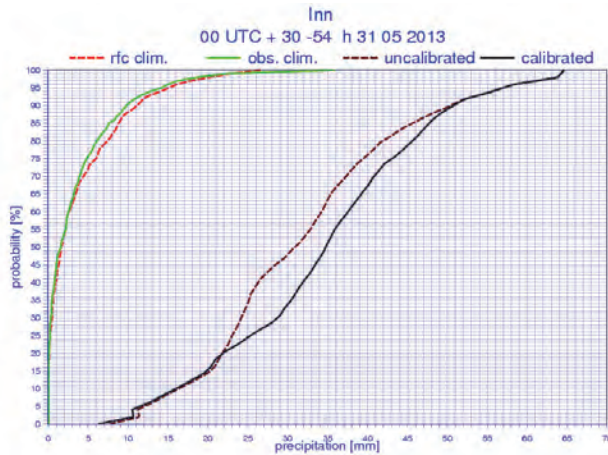


Fig. 6. Calibrated and uncalibrated distributions of precipitation probability for the Inn

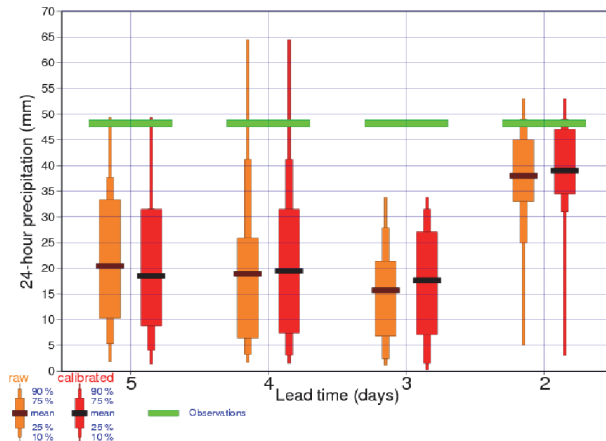


Fig. 7. Calibrated and uncalibrated 24-hour precipitation forecasts valid for 06 UTC, June 1, 2013 – 06 UTC, June 2, 2013 for the Inn catchment area, initialised on four consecutive days starting from 06 UTC May 27. The horizontal green line shows the observed value.

This study shows that the calibration can improve the accuracy of the forecast, however, one must take into account the differences from the topography. The results of the calibration might be giving more information to the forecasters, in such a way that the relationship of observed and reforecast climates can give information about distribution of the precipitation during the past few years on catchments. Comparing the raw and the calibrated forecasts, the experts can decide whether to modify the forecasted precipitation amount.

### 3.4. Verification

The comparative verification test was made from the uncalibrated and calibrated ensemble forecasts based on about 100 extreme precipitation cases in the 2008–2013 intervals. Fig. 8 shows the error distribution of the uncalibrated ensemble forecasts compared to observations for the extreme precipitation. The brown color represents the mean of the ensemble forecast and green color is the upper limit of the sorted ensemble forecast. In case of extreme rainfall, the ensemble mean underestimated the quantity of precipitation. In this case the systematic error cannot be seen, but the under- and overestimation occur approximately in the same proportion.

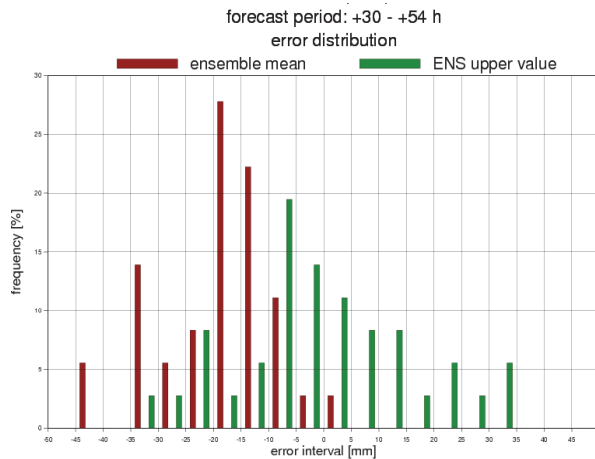


Fig. 8. Error distribution of the uncalibrated ensemble forecasts for the extreme precipitations in the 2008–2013 interval.

For the verification of ENS forecasts, the Talagrand diagram is widely used (Persson, 2011). The number of outlier cases decreased, but wider ensemble spreads were given by the model, thus increasing the standard deviation of the ensemble system. The calibration could reduce the number of outliers and did not increase the ensemble deviation at the same time.

Fig. 9 shows the uncalibrated and calibrated frequencies of the outliers in ensemble forecasts of 24h precipitation for different forecast ranges. In both forecasts the outliers presented the underestimation. However, it can be seen that the frequency of outliers decreased with the calibration. The forecast of extreme precipitation was improved by the calibration method.

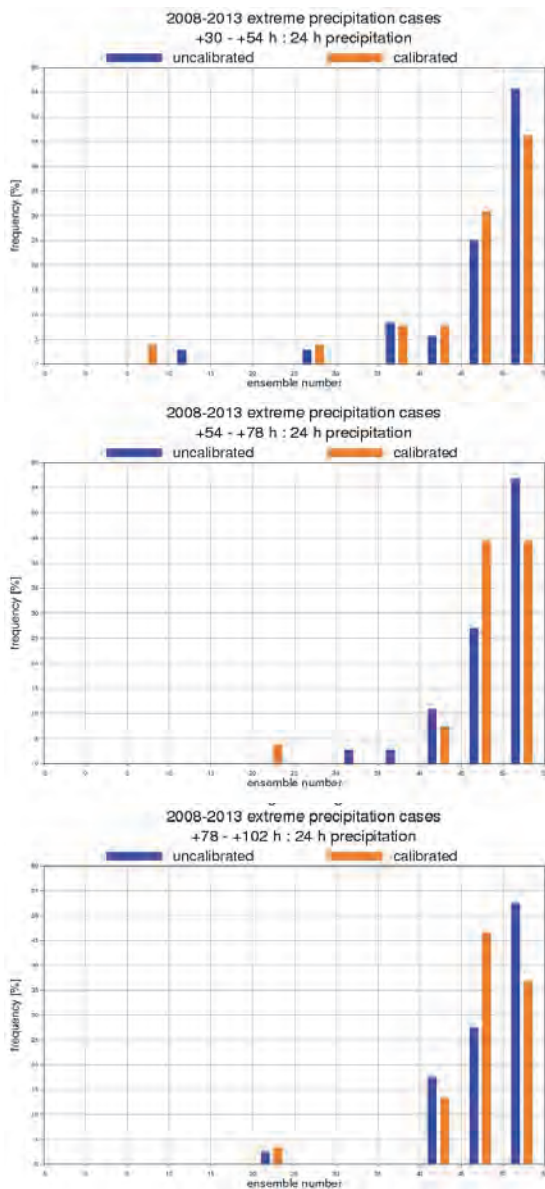


Fig. 9. Talagrand diagrams for 24-hour precipitation amount for different forecast ranges.

#### ***4. Application of limited area numerical prediction models***

For several local hydrological applications, meteorological fields of higher temporal and spatial resolution are needed than what is provided by global numerical weather prediction models. In these cases, limited area NWP models (LAMs) might be used, which could have the following advantages:

- They have higher temporal and spatial resolution;
- More – especially remote sensing – observations could be used for the generation of initial conditions;
- Local climatological characteristics could be taken into account during model development;
- Close interaction between local users of NWP outputs and model developers could be realized.

In this section, these possible advantages of limited area models are reviewed through the example of the ALADIN/AROME modeling system applied at the Hungarian Meteorological Service (OMSZ). Hungary, together with several other European countries, has been participating in the ALADIN (Aire Limitée Adaptation Dynamique Développement International) consortium since 1991. The ALADIN consortium was initiated by Météo France and currently has 16 participating countries. The aim of this consortium is to develop a short-range limited area numerical weather prediction model. As a result of this collaboration, the ALADIN/AROME model family has emerged, and it is constantly being developed in the participating countries. As of the beginning of 2017, the ALADIN/AROME operational suite at OMSZ consists of three models: the hydrostatic ALADIN model (with ALARO physics) runs at 8 km horizontal resolution, the non-hydrostatic AROME model (*Szintai et al., 2015*) runs at 2.5 km horizontal resolution, and the probabilistic ALADIN-EPS system operates at 8 km horizontal resolution with 11 members (*Szűcs et al., 2016*).

For non-hydrostatic NWP models running at a horizontal resolution of 2–3 km, deep convection is supposed to be resolved explicitly, thus no deep convection parameterization is required (*Seity et al., 2011*). In principle, this enables a more accurate prediction of convective events often accompanied by high precipitation amounts. Consequently, limited area models with high resolution could mean an added value from the point of hydrological applications. The advantage of high resolution NWP models as compared to global models could be observed in two precipitation characteristics. First, timing of deep convection is more accurate, secondly, high precipitation events are predicted with better skill in non-hydrostatic models. In the following, some objective verification results are presented to demonstrate these advantages.

During the verification, precipitation forecasts of the high resolution (HRES) global model run at ECMWF are compared with the AROME model. Both of these models are used operationally at OMSZ. The time period of the comparison is the summer of 2016 (June, July, and August). In this period, the HRES model was run at approximately 9 km horizontal resolution, while the AROME model was run at 2.5 km resolution. *Fig. 10* depicts three hourly accumulated area averaged precipitation over Hungary as a function of forecast lead time. For the verification, always the 00 UTC runs of the models were used and forecasts were compared to radar precipitation measurements. Based on the radar measurements, the summer precipitation has a pronounced daily cycle, with a maximum measured during the night. The global HRES model follows this daily cycle, however, the minimum predicted for the afternoon hours is too short and the maximum during the night is too long. The AROME model simulates a more realistic daily precipitation cycle with accurate timing and length of precipitation maximum. It has to be noted that the three-month period (June-July-August of 2016) serving as the basis for verification was somewhat extraordinary, with July 2016 giving the second highest precipitation amounts since 1901. The three-month averaged scores are very much affected by three high precipitation days in July, which are all influenced by large scale forcing (convection generated by cold front passages). As all of these three cold fronts arrived during the night, the daily maximum depicted in *Fig. 10* is shifted towards the early morning hours, contradicting the usual afternoon maximum of deep convective precipitation.

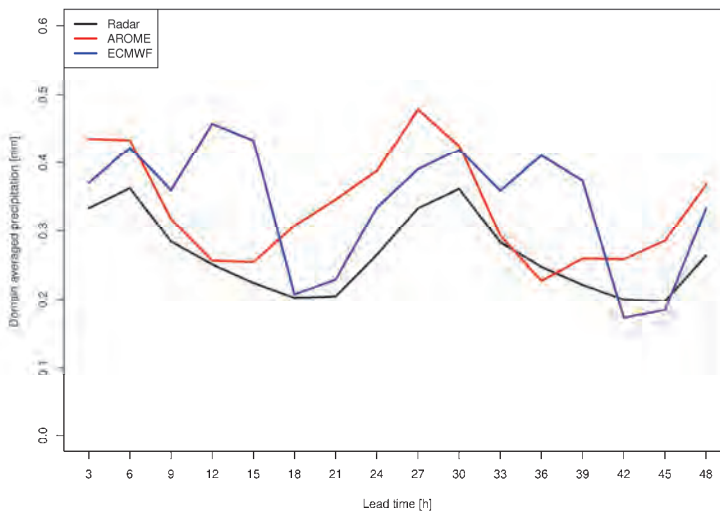


*Fig. 10.* Forecasts of three hourly accumulated precipitation averaged over Hungary as a function of lead time for summer 2016. Red: AROME model, blue: HRES model run at ECMWF, black: radar observation.

Averaged precipitation rates over a country are important to drive hydrological applications on a large scale (e.g., calculate discharge rates of main rivers), however, for local applications (e.g., flash flood warnings), it is crucial to accurately forecast the location and intensity of high precipitation events. The symmetric extremal dependence index (SEDI) was developed in order to have a reliable score which has good statistical properties even for rare events (*Ferro and Stephenson, 2011*). To estimate the advantage of limited area NWP models in predicting severe precipitation phenomena, the SEDI score was calculated for the HRES and AROME models for the summer of 2016 using precipitation measurements from the surface observation network in Hungary (*Fig. 11*). It has to be noted that during the summer of 2016, more precipitation was observed than the long-year average, and several severe convective events took place, consequently this three month period is supposed to be enough to draw solid consequences about precipitation forecasts. Results show that low precipitation cases (below 10 mm/day) are better predicted by the HRES model. For days with moderate precipitation (10–30 mm/day), HRES and AROME have similar skills. High precipitation events (above 30 mm/day) are better predicted by AROME, which could be attributed to the higher resolution, the non-hydrostatic dynamics, and the advanced microphysical parameterization of this model. It is important to mention that the SEDI score is independent of the frequency bias of the models. For the HRES model, an underestimation is present for the number of high precipitation cases, while the AROME model tends to overestimate the frequency of these events (not shown).

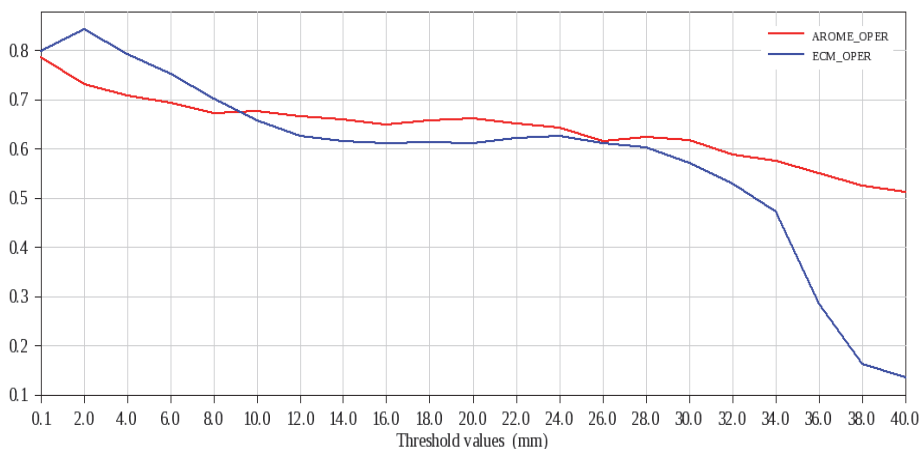


*Fig. 11.* SEDI score of daily precipitation computed for AROME and ECMWF/IFS for summer 2016 for several thresholds. Higher score means better model performance.

Another advantage of limited area models could be the assimilation of local observations to improve the initial conditions of the simulation. Nowadays, the most promising such observation type is the radar. From the radar, both the reflectivity and the Doppler wind measurements can be assimilated, with the former having significant impact on precipitation forecasts. Two approaches are available for the assimilation of radar data. The first approach was the latent heat nudging technique (*Jones and Macpherson, 1997*), used operationally nowadays in the UKMO and COSMO limited area models. In the ALADIN/AROME model family, a radar assimilation technique based on the variational approach was developed (*Caumont et al., 2010*). At the Hungarian Meteorological Service, experiments with radar data assimilation started in 2010 (*Mile et al., 2015*), however, due to several technical problems and the lack of manpower, the development process was slow and the operational application is expected to be realized in 2018. Apart from the application of local observations, another benefit of limited area NWP models could be the increased frequency of model runs. Since the beginning of 2016, the AROME model is run eight times per day at OMSZ. The additional model runs could deliver a benefit for severe weather forecasters in rapidly changing convective conditions.

In the case of limited area models, local climatological characteristics could be taken into account during model development. One example for this is the fine tuning of physical parameterizations like cloud physics. For varying climatological regimes, the frequency of certain weather phenomena is different. For instance, winter low cloud events are more frequent in the Carpathian Basin than in Western Europe. Consequently, in a LAM applied only over Hungary, a different set of tuning parameters can be used than in a LAM applied over France, which could improve the low cloud forecasts (*Szintai et al., 2015*). Although cloud cover is not used directly by hydrological models, it could have a significant impact on soil moisture or snow cover which are important for these applications.

At national meteorological services, a closer interaction could be realized between model users (forecasters, external partners) and model developers, which might not be the case for global model centers. Consequently, special applications could be developed based on LAM models, which satisfy users' needs. One such application which was recently developed at the Hungarian Meteorological Service for a major energy provider company is the probabilistic forecast of freezing rain from the ALADIN-EPS system. Apart from this, specialized forecasts for aviation from limited area models are also being implemented in near future.

Within 3 – 5 years, OMSZ is planning to introduce several developments regarding its ALADIN/AROME limited area NWP suite, which could improve the service related to possible hydrological applications as well. The assimilation cycle of AROME is planned to be increased to an hourly rapid

update cycle (RUC), which would increase the number of observations used and would also enable an hourly integration of AROME. With the increase of computer resources, the horizontal resolution of AROME is planned to be increased to 1 km. The hourly updated model runs at this higher resolution could serve as a basis of an objective flash flood warning system. As the accurate forecast of local convection is challenging even at 1 km horizontal resolution, a non-hydrostatic ensemble prediction system based on the AROME model is also planned to be implemented in the future.

Some of the larger national meteorological services have already implemented the so-called convection-permitting ensemble systems, which are usually based on non-hydrostatic 2–3 km resolution numerical models (Gebhardt *et al.*, 2008; Migliorini *et al.*, 2011; Vié *et al.*, 2011; Nuissier *et al.*, 2016). OMSZ, as an ALADIN consortia member has close collaboration with Meteo France on field of ensemble prediction, and participates together in an ECMWF special project which aim is to test AROME-EPS. This project enabled OMSZ to lunch case studies which can be interesting from hydrological point of view, as well. One of these case-studies represents flash-flood events which occurred on July 31, 2016 and had quite low predictability. In a prefrontal situation, some small-scale storm developed and moved very slowly to northeastern direction. Their slow motion and precipitation made it possible that in given locations, cells were able to restructure again causing big amount of point-wise precipitation. These cells typically occurred along the northern part of the Danube River, near the Hungarian-Slovakian boarder, between 8 and 14 UTC. Usually, such small-scale phenomena cannot be described by hydrostatic models. Non-hydrostatic ones are able to evolve them, but sometimes only with relatively big spatial and temporal uncertainty, which can be misleading for forecasters and end-users. That is essential motivation for taking an ensemble of AROME model integrations in such situations. *Fig. 12* is the highlight of hourly precipitation information from the 11 members of the AROME-EPS. Approximately half of the members predicted the evolution of small-scale storms over the region of interest, and two of them was quite accurate in their localization. For an early-warning system, it is very important to summarize information from all these members and identify the areas where hazardous meteorological events can occur with higher probability.

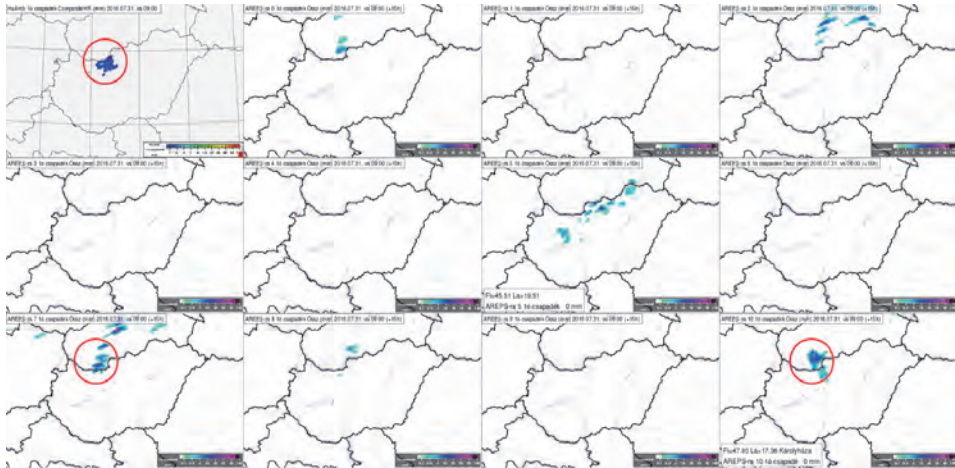


*Fig. 12.* Hourly accumulated precipitation over Hungary at 09 UTC, July 31, 2016. Top left panel shows the radar observation based amount, while other maps belong to the 11 members of an AROME-EPS started at 18 UTC, July 30, 2016. The interesting precipitation pattern is marked with red circle on the radar map and also for the members which were the most successful in the localization.

## 5. Conclusion

Using ensemble forecasts provides contribution to estimate the risk of the high impact meteorological events in hydrological applications. Possibility of reforecast based ensemble calibration was born in 2008. Even if significant developments had been achieved in operational forecasts based on the work done at the ECMWF, locally applied ensemble calibration can improve the quality of the forecasts in extreme situations, too. Any former studies focusing on the influence on forecasting extremes are not known. Benefits of the local developments on regional hydrostatic and non-hydrostatic models were shown, as well. It can be seen that high resolution limited area non-hydrostatic models can predict heavy precipitation during summer more accurately. The importance of the ensemble method was underlined in case of small-scale phenomena with low-predictability and accompanied by heavy precipitation event. Global and regional numerical weather prediction models will be continuously developing in the future. As a result of the ECMWF's 2016–2025 Strategy, the horizontal resolution of ensemble model will likely reach 5km around 2025. OMSZ plans of developments on its ALADIN/AROME operational suite was also detailed.

## References

- Bodolainé, J.E., 1976: Mennyiségi csapadékelőrejelzés a Duna és a Tisza vízgyűjtő területére a csapadékot létrehozó folyamatok találkozási modellje alapján. Manuscript, OMSZ Library, Budapest. (in Hungarian)
- Bodolainé, J.E., 1983: Árhullámok szinoptikai feltételei a Duna és a Tisza vízgyűjtő területén. *OMSZ Hivatalos Kiadványai* 56, Budapest. (in Hungarian)
- Bonta, I., and Újváry K., 2011: Hidrológiai célú mennyiségi csapadékelőrejelzés hazánkban. *Magyar Tudomány* 172, 1449–1458. (in Hungarian)
- Böläni, G., Kullmann, L., and Horányi, A., 2009: Use of ECMWF lateral boundary conditions and surface assimilation for operational ALADIN model in Hungary. *ECMWF Newsletter* 119, 29–35.
- Caumont, O., Ducroq, V., Watterlot, E., Jaubert, G., and Pradier-Varbe, S., 2010: 1D+3DVar assimilation of radar reflectivity data: a proof of concept, *Tellus A* 62, 173–187.  
<https://doi.org/10.1111/j.1600-0870.2009.00430.x>
- Ferro, C.A.T., and Stephenson, D.B., 2011: Extremal Dependence Indices: Improved Verification Measures for Deterministic Forecasts of Rare Binary Events. *Weather Forecas.* 26, 699–713.  
<https://doi.org/10.1175/WAF-D-10-05030.1>
- Gaál, N. and Ihász, I., 2015: Evaluation of the cold drops based on ERA-Interim reanalysis and ECMWF ensemble model forecasts over Europe. *Időjárás* 119, 111–126.
- Gebhardt, C., Theis, S., Krahe, P., and Renner, V., 2008: Experimental ensemble forecasts of precipitation based on a convection-resolving model. *Atmos. Sci. Lett.* 9, 67–72.  
<https://doi.org/10.1002/asl.177>
- Gneiting, T., 2014: Calibration of medium-range weather forecasts. *ECMWF Techn. Memoranda*, 719.
- Hagedorn R., 2008: Using the ECMWF reforecast datasets to calibrate EPS reforecasts, *ECMWF Newsletter*, 117, 8–12.
- Horányi, A., Ihász, I., and Radnóti, G., 1996: ARPEGE/ALADIN: A numerical weather prediction model for Central-Europe with the participation at the Hungarian Meteorological Service. *Időjárás* 110, 203–227.
- Horányi, A., Kertész, S., Kullmann, L. and Radnóti, G., 2006: The ARPEGE/ALADIN mesoscale numerical modelling system and its application at the Hungarian Meteorological Service., *Időjárás* 110, 203–227.
- Horányi, A., Mile, M., and Szűcs, M., 2011: Latest developments around the ALADIN operational short-range ensemble prediction system in Hungary, *Tellus* 63A, 642–651.  
<https://doi.org/10.1111/j.1600-0870.2011.00518.x>
- Ihász, I., 1992: Hogyan működik az első operatív hazai numerikus előrejelző modell? *Léggör* 37, 12–36. (in Hungarian)
- Ihász, I., 2004: Experiments of clustering for central European area especially in extreme weather situations. Proceedings of the Ninth ECMWF Workshop on Meteorological Operational Systems, Reading UK, 10-14 November 2003, 112–116.
- Ihász, I., Üveges, Z., Mile, M., and Németh, Cs., 2010: Ensemble calibration of ECMWF's medium-range forecasts. *Időjárás* 114, 275–286.
- Ihász, I., and Tajti, D., 2011: Use of ECMWF's ensemble vertical profiles at the Hungarian Meteorological Service. *ECMWF Newsletter* 129, 20–24.
- Ihász, I., 2014: Az operatív numerikus modellezés kezdeti éveit Magyarországon: A svéd modell alkalmazása. In Dévényi Dezső emlékkötet 63–69. (in Hungarian)
- Jones, C.D. and Macpherson, B., 1997: A latent heat nudging scheme for the assimilation of precipitation data into an operational mesoscale model. *Meteorol. Appl.* 4, 269–277.  
<https://doi.org/10.1017/S1350482797000522>
- Lázár, D. and Ihász, I., 2016: Potential benefit of the ensemble forecasts in case of heavy convective weather situations. *Időjárás* 120, 383–394.
- Mátrai, A., 2015: A csapadék előrejelezhetőségének vizsgálata a dunai és a tiszai vízgyűjtőkre vonatkozóan valószínűségi előrejelzések alapján Master thesis, Eötvös Loránd University, Budapest. (in Hungarian).

- Mátrai, A. and Ihász, I., 2017: Calibrating forecasts of heavy precipitation in river catchments, *ECMWF Newsletter*, 152, 32–35.
- Migliorini, S., Dixon, M., Bannister, R., and Ballard, S., 2011: Ensemble prediction for nowcasting with a convection-permitting model. I: Description of the system and the impact of radar-derived surface precipitation rates. *Tellus 63A*, 468–496. <https://doi.org/10.1111/j.1600-0870.2010.00503.x>
- Mile, M., Bölöni, G., Randriamampianina, R., Steib, R., and Kucukkaraca, E., 2015: Overview of mesoscale data assimilation developments at the Hungarian Meteorological Service. *Időjárás 119*, 213–237.
- Nuissier, O., Marsigli, C., Vincendon, B., Hally, A., Bouttier, F., Montani, A., and Paccagnella, T., 2016: Evaluation of two convection-permitting ensemble systems in the HyMeX Special Observation Period (SOP1) framework: Evaluation of two convection-permitting ensemble systems. *Quart. J. Roy. Met. Soc.* 142, 404–418. <https://doi.org/10.1002/qj.2859>
- Persson, A., 2011: User guide to ECMWF forecasts products, ECMWF, Reading.
- Richardson, D., Hemri, S., Bogner, K., Gneiting, T., Haiden, T., Pappenberger, F., and Scheuerer, M., 2014: Calibration of ECMWF forecasts, *ECMWF Newsletter 142*, 12–16.
- Seity, Y., Brousseau, P., Malardel, S., Hello, G., Bénard, P., Bouttier, F., Lac, C., and Masson, V., 2011: The AROME-France Convective-Scale Operational Model. *Month. Weather Rev.* 139, 976–991. <https://doi.org/10.1175/2010MWR3425.1>
- Smith, P., Pappenberger, F., Wetterhall, F., Thielen, J., Krzeminski, B., Salamon, P., Muraro, D., Kalas, M., and Baugh, C., 2016: On the operational implementation of the European Flood Awareness System (EFAS), *ECMWF Techn. Memoranda 778*.
- Szépszó, G., 2003: A 80-as és 90-es évek árhullámainak szinoptikus-klimatológiai értékelése. Master thesis. Eötvös Loránd University, Budapest. (in Hungarian)
- Szintai, B., Bazile, E., and Seity, Y., 2014: Improving wintertime low cloud forecasts in AROME: sensitivity experiments and microphysics tuning. *ALADIN-HIRLAM Newsletter 3*. 45–58.
- Szintai, B., Szűcs, M., Randriamampianina, R., and Kullmann, L., 2015: Application of the AROME non-hydrostatic model at the Hungarian Meteorological Service: physical parameterizations and ensemble forecasting, *Időjárás 119*, 241–265.
- Szűcs, M., Sepsi, P., and Simon, A.: 2016: Hungary's use of ECMWF ensemble boundary conditions, *ECMWF Newsletter 148*, 24–31.
- Vié, B., Nuissier, O., and Ducrocq, V., 2011: Cloud-resolving ensemble simulations of Mediterranean heavy precipitating events: Uncertainty on initial conditions and lateral boundary conditions. *Month. Weather Rev.* 139, 403–423. <https://doi.org/10.1175/2010MWR3487.1>



# IDŐJÁRÁS

*Quarterly Journal of the Hungarian Meteorological Service*  
Vol. 122, No. 1, January – March, 2018, pp. 81–99

## Climate change impacts on the water balance - case studies in Hungarian watersheds

**Péter Csáki\***, Márton Miklós Szinetár, András Herceg,  
Péter Kalicz, and Zoltán Gribovszki

*Institute of Geomatics and Civil Engineering, University of Sopron,  
Bajcsy-Zs. u. 4., 9400 Sopron, Hungary*

*\*Corresponding author E-mail: csaki.peter@uni-sopron.hu*

*(Manuscript received in final form December 18, 2017)*

**Abstract**—Climate change will alter various components of the water balance on global, regional, and local scales; these changes will be measurable mainly through alterations of the spatial distribution and temporal trends of temperature, precipitation, and evapotranspiration. We analyzed the water balance of two Hungarian watersheds (Zala and Bácsbokodi-Kígyós) based on a spatially distributed robust hydrological model that was calibrated using actual evapotranspiration values of CREMAP (Complementary-relationship-based Evapotranspiration Mapping Technique). During the model calibration period (2000–2008), evapotranspiration (*ET*) and runoff (or recharge, *R*) were 92% and 8% of the precipitation amount in the Zala watershed, while in the Bácsbokodi-Kígyós watershed it was 75% and 25%. A climate-runoff model was developed to evaluate the effects of climate change on the water balance. Long-term *ET* and *R* averages can be calculated applying a spatially distributed Budyko-model at a resolution of 1 km × 1 km. In the case of the surplus water affected areas where *ET* exceeds precipitation, *ET* and *R* can be calculated with another simple model that works on the analogy of pan evaporation. Using precipitation and temperature results of regional climate model simulations as input data, we calculated the projections of the main components of the water balance. Increasing temperatures in the 21st century are projected to cause a slight increase in evapotranspiration relative to the reference period 1981–2010; this may cause a substantial reduction of long-term runoff. The mean decrease can exceed 53% for the Zala and 38% for the Bácsbokodi-Kígyós watersheds. The decreasing runoff/recharge could limit manageable or extractable groundwater resources, alter agricultural activities, and cause a water deficit in Balaton Lake.

*Key-words:* climate change, evapotranspiration, runoff, Budyko-model, water balance

## 1. Introduction

During the 20th century, there was a worldwide average temperature increase of 0.6°C; even greater increases have been recorded in the recent decades. Without additional mitigation (baseline scenarios), this warming trend will result in a global mean surface temperature increase of 3.7°C to 4.8°C by 2100 compared to pre-industrial levels (IPCC, 2014). There is also general agreement concerning regional climate change projections for Europe that show statistically significant warming for all seasons. The highest temperature increases are expected in the southern Mediterranean region (*van der Linden and Mitchell, 2009*). The climate of Hungary has become warmer and drier as well, with an average annual temperature increase of 0.86 °C during the 20th century (*Nováky and Bálint, 2013*). The warming during the last 30 years was stronger than ever before, especially in the summer periods, during which the average temperature has increased by as much as 2°C (*Bartholy et al., 2011; HREX, 2012*). Depending on climate scenarios, temperatures in Hungary are projected to increase by 2°C to 5°C until the end of the 21st century (*Nováky and Bálint, 2013*).

In addition to rising temperatures, climate change also affects precipitation. Nevertheless, those impacts are less obvious than impacts on temperature, since the higher spatial and temporal variability can hide the average trend of the changes (*Pongrácz et al., 2014*). In Europe, annual precipitation projections point to an increase in the northern regions, but a decrease in the southern regions towards to the end of the 21st century (*Kjellström et al., 2011*). In the transition zone, where Hungary is located, the changes are smaller and statistically insignificant. However, the mean annual precipitation of the entire country decreased by one month of average precipitation (~7%) during the 20th century. Projections show that the transition zone shifts northwards during summer, which results in decreasing precipitation in Hungary. During winter, the transition zone shifts southwards, which leads to increasing precipitation (*Bartholy et al., 2008; Nováky and Bálint, 2013; Gálos et al., 2015*).

The most significant effect of climate change is its impact on the water cycle through the alteration of precipitation patterns and evapotranspiration processes at multiple scales (*Szilágyi and Józsa, 2008; Sun et al., 2011; Nováky and Bálint, 2013; Pongrácz et al., 2014*). In arid climates, the hydrological balance will move toward evapotranspiration, while in more humid climates, it will move toward runoff (*Keve and Nováky, 2010*).

The global evapotranspiration rate for continental precipitation is 70% (ranging from approximately 60% in Europe to over 90% in Australia) (*McMahon et al., 2013*). In Hungary, the evapotranspiration rate is 90%, while the remaining 10% is runoff (*Szilágyi and Kovács, 2011*). Evapotranspiration determines water availability on land surfaces and thus controls the large scale distribution of plant communities and primary production (*Vörösmarty et al., 1998*). The necessity of modeling and attaining a quantitative understanding of the evapotranspiration

process is unquestionable, particularly in the context of climate change projections (Dingman, 2002). In practice, situations such as rainfall-runoff modeling, small irrigation areas, irrigated crops within a large irrigation district, and catchment water balance studies require evapotranspiration estimations with different time steps (McMahon *et al.*, 2013).

A robust Budyko-type model that is able to estimate hydrological changes (evapotranspiration and runoff) in Hungary in high spatial resolution has not been developed so far. However, hydrological projections would prove useful in analyzing the water balance of the Balaton Lake. They could also be applied to agriculture, a major economic sector in the Carpathian Basin that is highly vulnerable to droughts (Antofie *et al.*, 2015). This paper presents a spatially distributed climate-runoff model. A further aim is to analyze the hydrological projections for selected watersheds in Hungary that could be useful in decisions concerning water resources management.

## ***2. Materials and methods***

### *2.1. Study areas*

The watershed is the most appropriate unit to analyze the possible hydrological impacts of climate change. The Zala and Bácsbokodi-Kígyós watersheds in Hungary were selected for comparison in this study, because they met two important criteria: the availability of regular streamflow data, and differing climatic and land use properties.

#### *2.1.1. Zala watershed*

The Zala River watershed is located in the western part of Hungary (Fig. 1) and it provides the largest inflow of water to the Balaton Lake (Virág, 1997). The area above the “Zalaapáti gauging station” (Fig. 2) covers 1520.7 km<sup>2</sup> with a main channel length of 104 km. The long-term (1980–2008) mean discharge is 4.6 m<sup>3</sup>s<sup>-1</sup>. The climate of the watershed is characterized as moderately cool and moderately humid with a mean annual temperature of 10.4 °C and an annual precipitation of 730 mm. The altitude ranges from 100 m a.s.l. to 334 m a.s.l.; the average is 195 m a.s.l.

The dominant land use is agriculture (57.5%; Fig. 2, Table 1), followed by forest and semi-natural areas (36.5%), and artificial surfaces (5.1%). The areas belonging to wetlands and water bodies are rather small: 0.3% and 0.6% of the total area, respectively.

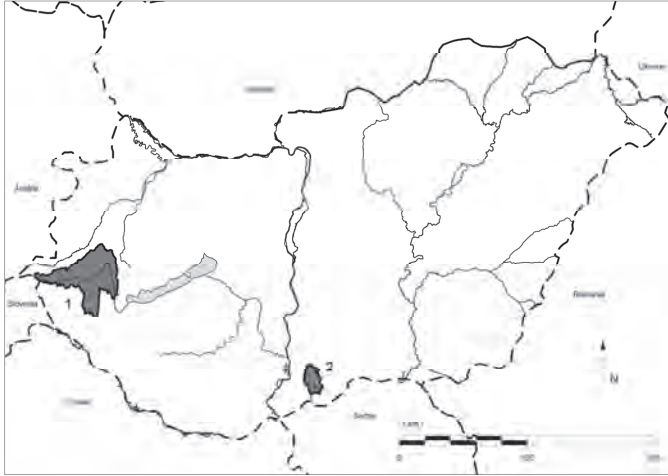


Fig. 1. Location of the study areas within Hungary.  
 1: Zala River watershed, 2: Bácsbokodi-Kígyós watershed

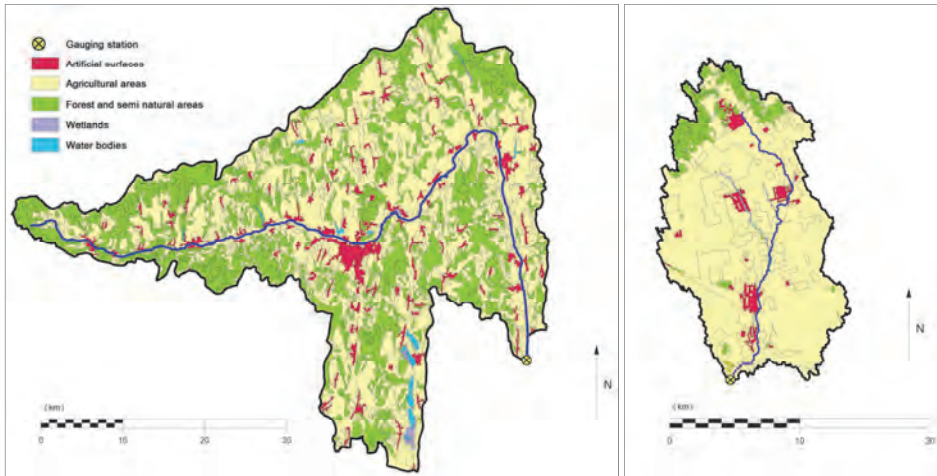


Fig. 2. Land cover (by the Corine Land Cover 2006) and location of the gauging stations of the Zala River watershed (left) and the Bácsbokodi-Kígyós watershed (right).

Table 1. The land cover distribution of the study areas based on the Corine Land Cover types (CLC, 2006): AS - Artificial surfaces, AA - Agricultural areas, FS - Forest and semi-natural areas, WL - Wetlands, WB - Water bodies

<b>Watershed name:</b>	<b>Zala</b>		<b>Bácsbokodi-Kígyós</b>	
<b>Gauging station:</b>	<b>Zalaapáti</b>		<b>Bácsborsód</b>	
<b>Area (km<sup>2</sup>):</b>	<b>1520.7</b>		<b>235.8</b>	
AS (km <sup>2</sup> ; %):	78.0	5.1	8.4	3.6
AA (km <sup>2</sup> ; %):	874.2	57.5	202.4	85.8
FS (km <sup>2</sup> ; %):	554.9	36.5	22.9	9.7
WL (km <sup>2</sup> ; %):	4.3	0.3	1.3	0.6
WB (km <sup>2</sup> ; %):	9.3	0.6	0.8	0.3

### 2.1.2. Bácsbokodi-Kígyós watershed

The Bácsbokodi-Kígyós watershed is located in the southern part of the Great Hungarian Plain, right above the Hungarian-Serbian border (Fig. 1). The water from this area is collected by the Bácsbokodi-Kígyós Canal, from where it discharges to the Tisza through the Ferenc Canal. Long-term discharge data was available from the “Bácsborsód gauging station” at stream-km 9.2 (Fig. 2); therefore, the investigated watershed was delineated above this point, making the area 235.8 km<sup>2</sup> and the length of the canal 30.65 km. The long-term (1964–2008) mean discharge is 0.126 m<sup>3</sup> s<sup>-1</sup>. The area lies on the border of the dry and moderately dry climatic regions. The mean annual temperature is 11.7°C, and the annual precipitation is 590 mm. The area can be described as rather flat with altitude ranges from 104 m.a.s.l. to 171 m.a.s.l., with an average altitude of 132 m.a.s.l.

The area is famous for its outstanding agricultural potential; consequently, the dominant land use is agriculture (85.8%; Fig. 2, Table 1), followed by forest and semi-natural areas (9.7%), artificial surfaces (3.6%), wetlands (0.6%), and water bodies (0.3%).

### 2.2. Spatially distributed evapotranspiration and runoff

Monthly actual evapotranspiration ( $ET_A$ ) rates over Hungary between 2000 and 2008 have been mapped (in a resolution of 1 km × 1 km) by Szilágyi and Kovács (2010) with the Complementary-relationship-based Evapotranspiration Mapping (CREMAP) technique (Szilágyi and Kovács, 2011). It is based on a linear transformation of MODIS daytime land surface temperature values into  $ET_A$  rates (Szilágyi and Józsa, 2009) using the complementary relationship of evaporation (Bouchet, 1963). The CREMAP model has been validated using water balance calculations and eddy-covariance station measurements across Hungary (Kovács,

2011). Using the monthly maps, a nine-year (2000–2008) mean annual  $ET_A$  map has been prepared. Furthermore, nine-year mean annual  $R$  (runoff) has been calculated from the long-term water balance equation as the difference between  $P$  (precipitation) and  $ET_A$ . The spatially distributed precipitation and temperature data was provided by the CarpatClim project (Lakatos *et al.*, 2013); however, the target region of this project does not cover the whole Zala watershed, so data from further stations of the Hungarian Meteorological Service were also involved in the investigations.

### 2.3. Model description and application

In water resources modeling, the Budyko curve (Budyko, 1974) is often used to estimate the actual evapotranspiration ( $ET_A$ ) as a function of the aridity index ( $\phi$ ). It can be derived from two balance equations, the water balance and the energy balance (Csáki *et al.*, 2014). Many studies have been prepared regarding the determination of the  $ET_A - \phi$  relation; some of them are summarized in Gerrits *et al.* (2009). Among these, the Schreiber equation is one of the best known classical studies (Schreiber, 1904).

The potential evapotranspiration by Schreiber is

$$ET_P = -P \left( \ln \left( \frac{P - ET_A}{P} \right) \right), \quad (1)$$

where  $ET_P$  is the potential evapotranspiration ( $\text{mm y}^{-1}$ ),  $P$  is the precipitation ( $\text{mm y}^{-1}$ ), and  $ET_A$  is the actual evapotranspiration ( $\text{mm y}^{-1}$ ).

Potential evapotranspiration can also be expressed as a function of pan evaporation, according to a general relation for Hungary (Nováky, 1985, 2002):

$$ET_P = f(E_{pan}) = \alpha E_{pan} = \alpha \left( 36400 \frac{T}{P} + 104 \right), \quad (2)$$

where  $E_{pan}$  is the pan evaporation ( $\text{mm y}^{-1}$ ; class U pan: 3  $\text{m}^2$  water surface area, 0.5 m depth),  $T$  is the mean annual temperature ( $^{\circ}\text{C}$ ), and  $\alpha$  is a calibration parameter. This parameter aggregates all the factors affecting evapotranspiration, dominantly the surface cover (Keve and Nováky, 2010).

From the above equations,  $\alpha$  can be calculated as

$$\alpha = \frac{ET_P}{E_{pan}} = - \frac{P \left( \ln \left( \frac{P - ET_A}{P} \right) \right)}{\left( 36400 \frac{T}{P} + 104 \right)}, \quad (3)$$

In cases where the  $ET_A$  value is higher than the  $P$  value, the  $\alpha$  parameter cannot be determined, because the natural logarithm of a negative number is indeterminable in Eq. (3). For these surplus water affected pixels, an another calibration parameter, the  $\beta$  parameter can be calculated, which gives the relationship between  $E_{pan}$  and  $ET_A$ :

$$\beta = \frac{ET_A}{E_{pan}} = \frac{ET_A}{\left(36400\frac{T}{P}+104\right)}. \quad (4)$$

The  $\alpha$  and  $\beta$  maps can be used for calculating  $ET_A$  and  $R$  in spatially distributed way; for that, only  $T$  and  $P$  data are required (Eqs. (5), (6)).

$ET_A$  calculation with  $\alpha$  is

$$ET_A = P \left(1 - \exp\left(-\frac{ET_P}{P}\right)\right) = P \left(1 - \exp\left(\frac{-\alpha(36400\frac{T}{P}+104)}{P}\right)\right). \quad (5)$$

$ET_A$  calculation with  $\beta$  is

$$ET_A = \beta E_{pan} = \beta \left(36400\frac{T}{P} + 104\right). \quad (6)$$

A more detailed description of the model can be found in *Csáki et al. (2014)*.

The spatially distributed values of the  $\alpha$  and  $\beta$  parameters were determined using  $ET_A$ ,  $P$  and  $T$  maps for the 2000–2008 period with a resolution of 1 km<sup>2</sup>. The parameters were validated for the Zala watershed, using historical precipitation and streamflow (runoff) data (*Csáki et al., 2015*). The validation for the Bácsbokodi-Kígyós watershed – due to its unique hydrogeological features – can only be implemented by accepting the assumptions described in Section 3.1.

We used Eqs. (5) and (6) to calculate spatially distributed future  $ET_A$  for the study areas. The temperature and precipitation data were obtained from 12 regional climate model (RCM) simulations assuming the SRES A1B emission scenario (*IPCC, 2007, van der Linden and Mitchell, 2009*). The original grid size of the RCM maps was 25 km×25 km; therefore, they were disaggregated (downscaled) to 1 km×1 km spatial resolution by the bicubic convolution interpolation technique. The runoff was calculated as the difference between precipitation and  $ET_A$  (long-term water balance equation). We completed estimations for three future time periods (2011–2040, 2041–2070, 2071–2100) and determined the expected changes relative to the reference period (1981–2010).

### 3. Results and discussion

#### 3.1. Evaluation of evapotranspiration and runoff (2000–2008)

The nine-year (2000–2008) mean annual actual evapotranspiration and runoff maps of the Zala and Bácsbokodi-Kígyós watersheds can be seen in *Fig. 3* and *Fig. 4*, respectively. The mean values are summarized in *Table 2*.

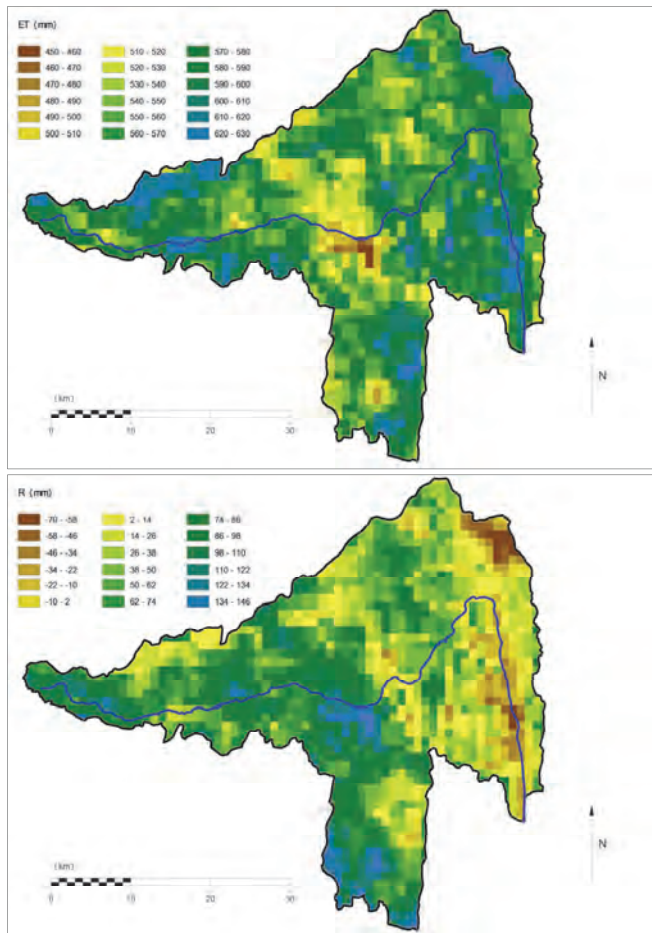


*Fig. 3.* Mean annual actual evapotranspiration (mm, top) and mean annual runoff (mm, bottom) over the Zala River watershed (2000–2008, spatial resolution: 1 km<sup>2</sup>).

During the period of interest, the mean annual  $ET_A$  was 569 mm in Zala, which was 92% of the annual precipitation. Higher values (610–630 mm) can be seen in the forested areas (in the western and eastern parts of the watershed, *Fig. 3*); the artificial surfaces (e.g., the city of Zalaegerszeg in the middle area) are characterized by lower values (450–500 mm). The mean annual  $R$  was 51 mm, which amounted to only 8% of the annual precipitation. Higher  $R$  values (100–140 mm) belonged to higher elevations and slopes (the western half) and lower values (0–30 mm) to lower elevations (the eastern half of the Zala watershed). In the cases of some surplus water affected pixels, the evapotranspiration rates surpassed the precipitation rate the area receives, e.g., the forested areas in the northeastern and southeastern parts of the watershed.

*Table 2.* Daily mean temperature ( $T$ ), annual precipitation ( $P$ ), mean annual evapotranspiration ( $ET$ ) and runoff ( $R$ ) for the study areas (2000–2008)

<b>Watershed name:</b>	$T$ (°C)	$P$ (mm)	$ET$ (mm)	$ET/P$ (%)	$R$ (mm)	$R/P$ (%)
Zala	10.9	619	569	92	51	8
Bácsbokodi-Kígyós	11.7	606	452	75	154	25

The CREMAP  $ET_A$  has been validated for the Zala watershed using the simplified water balance model. The difference between the CREMAP (569 mm  $y^{-1}$ ) and the calculated  $ET_A$  (556 mm  $y^{-1}$ ; the measured streamflow is subtracted from the mean annual precipitation) was only 2.3%. The measured streamflow was available from the “Zalaapáti gauging station” (from the West-Transdanubian Water Directorate).

The mean annual  $ET_A$  for the Bácsbokodi-Kígyós watershed was 452 mm, which was 75% of the annual precipitation (*Table 2*). The highest  $ET_A$  values (550–570 mm) belong to a forested area (in the northwest corner of the watershed, *Fig. 4*). The artificial surfaces (e.g., Rém village in the north) and agricultural areas (on the two sides of the watershed) are characterized by lower  $ET_A$  values (400–450 mm). From there, it gradually increases towards the channel system. The mean annual  $R$  was 154 mm, which was 25% of the annual precipitation amount. The  $R$  map (*Fig. 4*) can be considered as the inverse of the  $ET_A$  map; thus, there are low  $R$  values (50–90 mm) in the case of the forested area (in the northwest corner), while higher values (150–200 mm) belong to artificial surfaces and agricultural areas. There is a significant difference between the runoff (154 mm) and the measured streamflow (16 mm) values, which was available from the “Bácsborsód gauging station” (from the Lower Danube Valley Water Directorate). The special soil and

topological features of the area cause this deviation. The unbounded sandy soil that covers the majority of the watershed combined with the almost flat surface allows the rainwater to rapidly infiltrate the soil; thus, surface runoff occurs only in extreme situations (Pálfi, 2010). The rainwater reaching the surface can be divided into 3 categories, namely: (i) channel flow - water that reaches the channel (stream) through groundwater, (ii) vertical percolation, and (iii) deep percolation. The channel flow, as described above, was  $16 \text{ mm y}^{-1}$  between 2000 and 2008. The deep percolation has been induced by the increased water abstraction from the underlying confined aquifers. It was estimated to be  $0 \text{ mm y}^{-1}$  in the period of 1951–1970 and has increased to  $28 \text{ mm y}^{-1}$  during the period 1971–1992 (Szilágyi and Vörösmarty, 1997). Projection of this linear increment to 2000–2008 results in an annual deep percolation of  $63 \text{ mm}$ . The vertical subsurface seepage was estimated based on two factors. One is that the value of the horizontal seepage has stayed constant (about  $30 \text{ mm y}^{-1}$ ) between 1951 and 1992. The other is that the hydraulic gradient of the groundwater surface in this area is about 2.3 times higher than the average gradient of the Danube-Tisza plateau (Szilágyi and Vörösmarty, 1997). According to Darcy's Law, the 2.3 times higher gradient implies equally higher seepage velocity resulting in  $66 \text{ mm}$  annual value for the horizontal seepage. Summing up, these three values give a  $145 \text{ mm y}^{-1}$  runoff (or recharge) value for the period 2000–2008, which differs by only  $9 \text{ mm}$  from  $R$  value determined by the CREMAP  $ET_A$  ( $154 \text{ mm y}^{-1}$ ).

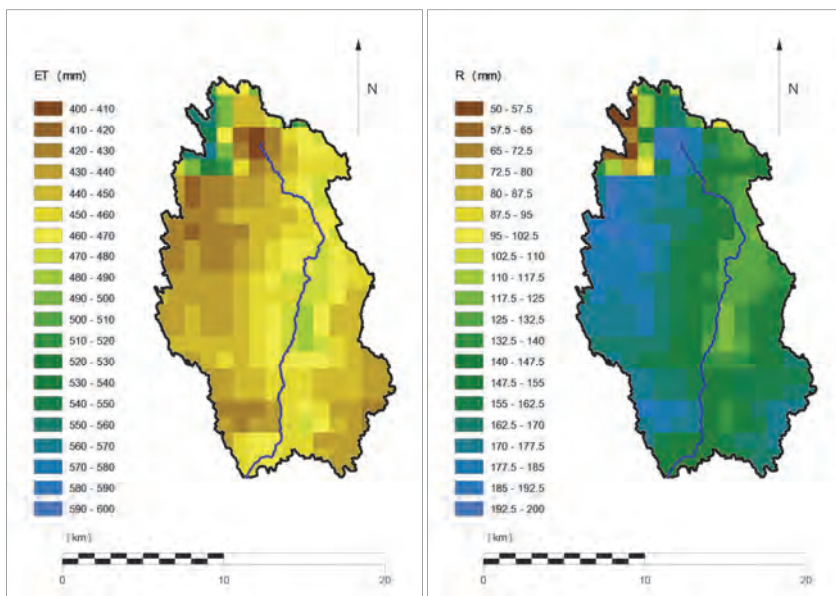


Fig. 4. Mean annual actual evapotranspiration (mm, left) and mean annual runoff (mm, right) over the Bácsbokodi-Kígyós watershed (2000–2008, spatial resolution:  $1 \text{ km}^2$ ).

The CREMAP  $ET_A$  has been validated for the Bácsbokodi-Kígyós watershed using the simplified water balance model. The difference between the CREMAP ( $452 \text{ mm y}^{-1}$ ) and the calculated  $ET_A$  ( $461 \text{ mm y}^{-1}$ ; the measured streamflow is subtracted from the mean annual precipitation) was only 2.0%.

### 3.2. Evaluation of $\alpha$ and $\beta$ parameters

The  $\alpha$  and  $\beta$  parameters have been calculated with the help of Eqs. (3) and (4). The parameter maps for the Zala watershed can be seen in *Fig. 5*. Higher  $\alpha$  values appear where the land cover is mainly forest and semi-natural areas (see *Fig. 2*), e.g., in the western part of the Zala watershed. The  $\beta$  parameter pixels (surplus water affected areas with higher evapotranspiration than precipitation) are situated for a forested area (in the northeast) and in the valley of the Zala River in the southeastern part of the watershed. For the Bácsbokodi-Kígyós region, we calculated only the  $\alpha$  map (*Fig. 6*), because there were no surplus water affected pixels. The highest  $\alpha$  values belong to the forested area in the northwest. In a previous study concerning the water balance of Bácsbokodi-Kígyós watershed, *Keve and Nováky (2010)* used a spatially distributed Budyko model for runoff estimation. They calibrated their model with the streamflow data without taking deep and horizontal percolating water into consideration. Therefore, their  $\alpha$  varies in a different range, but the tendency of how its values increase from artificial areas through agricultural areas to forest areas appears to be similar.

If we compare the  $\alpha$  values of the two watersheds, the values belonging to Zala are much higher than the ones belonging to Bácsbokodi-Kígyós. The main reason for this can be the land cover as the Zala watershed has a larger forested area than the other watershed (*Fig. 2, Table 1*).

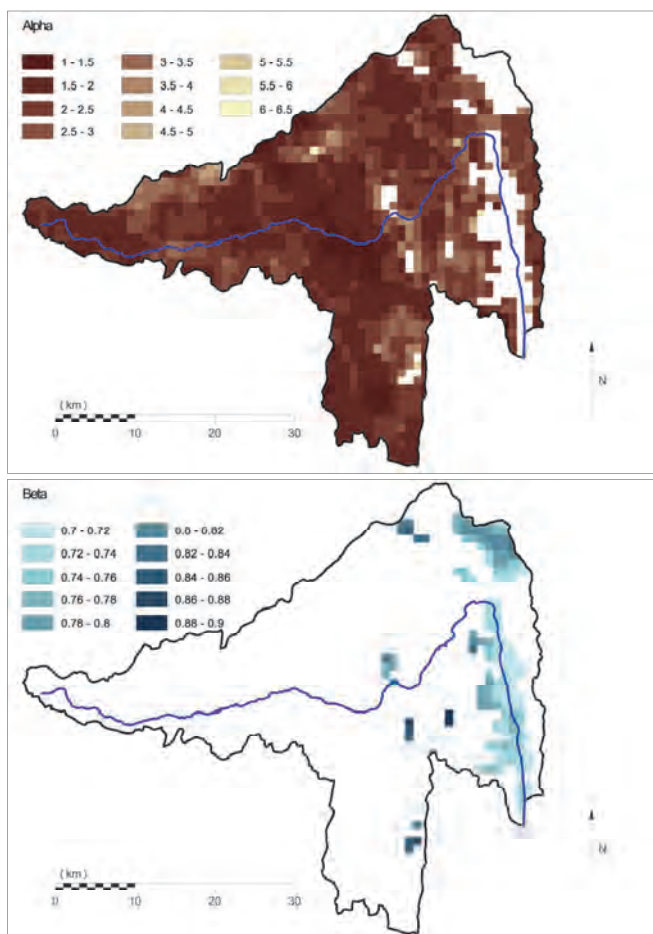


Fig. 5. The calculated Budyko-type  $\alpha$  parameter (top) and the  $\beta$  parameter (bottom) over the Zala River watershed (spatial resolution: 1 km<sup>2</sup>).

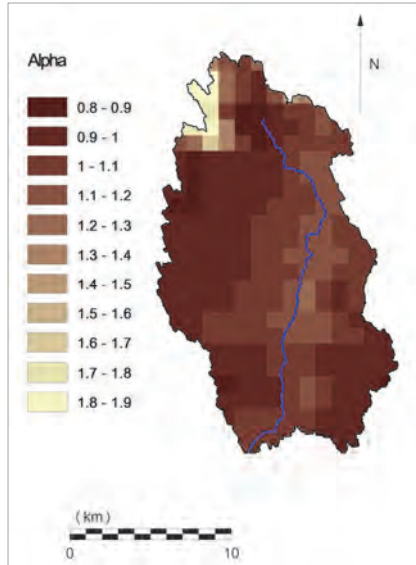


Fig. 6. The calculated Budyko-type  $\alpha$  parameter over the Bácsbokodi-Kígyós watershed (spatial resolution: 1 km<sup>2</sup>).

### 3.3. Evapotranspiration and runoff projections

As described above, we calculated the projected evapotranspiration using the  $\alpha$  and  $\beta$  parameter maps (Eqs. (5) and (6)). The temperature and precipitation values for the calculations were acquired from 12 regional climate model simulations. The long-term runoff ( $R$ ) projections were calculated as the difference between precipitation and evapotranspiration. The results for three periods (2011–2040, 2041–2070, 2071–2100) were compared to a reference period (1981–2010). Table 3 contains the mean of the projected changes (based on the 12 simulations) in mm, while Figs. 7 and 8 illustrate the projected changes of  $ET_A$  and  $R$  in percent as box and whiskers plots (Venables and Ripley, 1999). According to the projections, the mean annual temperature will be higher and higher from period to period (Table 3). It is projected to be more than 3 °C higher in 2071–2100 relative to the reference period for both study areas. However, the mean change of the annual precipitation sum is not significant; a small increase is projected for 2041–2070, and a decrease by 9 and 12 mm for 2071–2100, relative to the time period 1981–2010. (Compared to the period 2000–2008, this amount of decrease – 9 and 12 mm – means about 1.5% and 2.0% of the annual precipitation in Zala and Bácsbokodi-Kígyós watersheds, respectively.)

Table 3. The mean projected changes (based on the simulations using the 12 regional climate models and the  $\alpha$ - $\beta$  parameter maps) of the annual temperature ( $dT$ ), annual precipitation sum ( $dP$ ), annual evapotranspiration ( $dET$ ), and runoff ( $dR$ ) for the study areas. Reference period: 1981–2010

Watershed name:	Period*	$dT$ (°C)	$dP$ (mm)	$dET$ (mm)	$dR$ (mm)
Zala	2011–2040	0.9	1.2	10.7	-9.5
	2041–2070	2.0	9.7	28.1	-18.4
	2071–2100	3.2	-9.1	32.6	-41.7
Bácsbokodi-Kigyós	2011–2040	0.9	-4.0	5.2	-9.2
	2041–2070	2.1	4.8	20.0	-15.2
	2071–2100	3.3	-12.2	19.5	-31.7

\* Relative to the reference period (1981–2010).

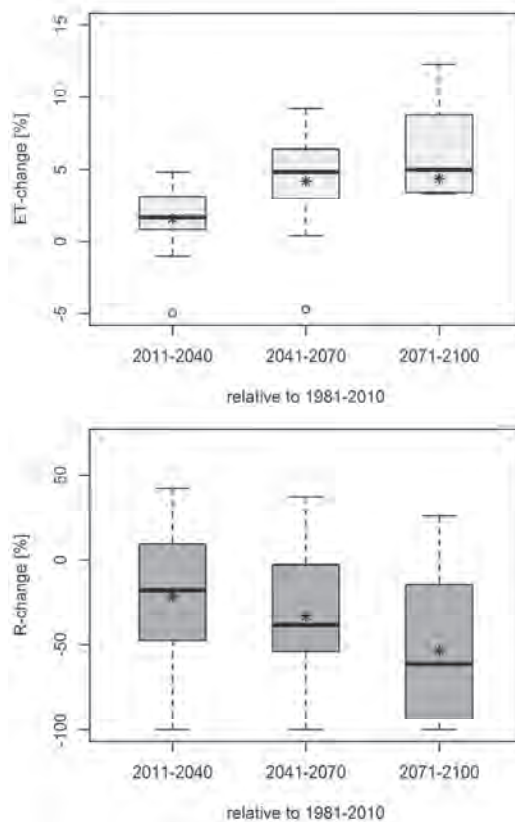
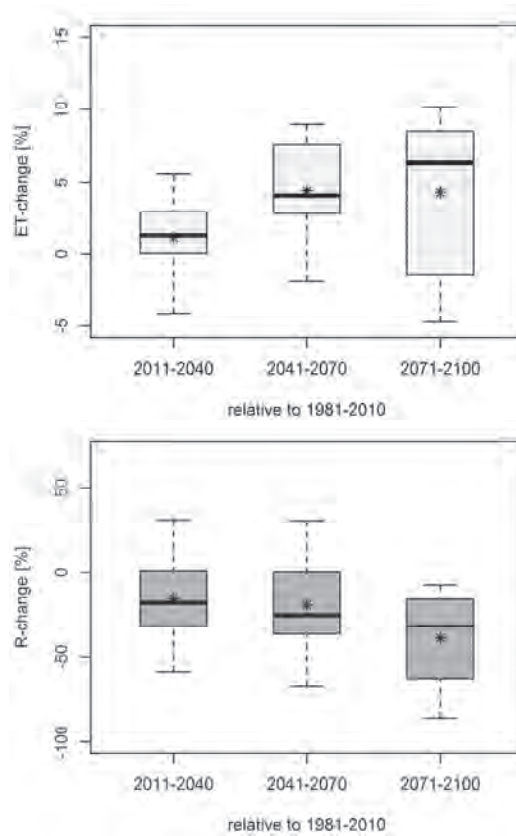


Fig. 7. The projected changes of the mean annual actual evapotranspiration (left) and runoff (right) for the Zala watershed based on the results of 12 regional climate model simulations. Reference period: 1981–2010. (Box: 50% of the results. Bars: minimum and maximum. Star: mean. Thick line: median.)



*Fig. 8.* The projected changes of the mean annual actual evapotranspiration (left) and runoff (right) for the Bácsbokodi-Kígyós watershed based on the results of 12 regional climate model simulations. Reference period: 1981-2010. (Box: 50% of the results. Bars: minimum and maximum. Star: mean. Thick line: median.)

In the case of the Zala watershed (*Fig. 7*), the mean  $ET_A$  change – compared to the reference period (1981–2010) – shows 1.6%, 4.2%, and 4.4% increase in the first, second, and third future time period, respectively. According to the projections, the maximum increase of the  $ET_A$  change can reach 12.0% by the end of the century. The spread of the  $ET_A$  projections based on the simulation results of the 12 RCMs shows an increase from period to period. For  $R$ , a significant decrease can be detected in the investigated future climate periods; the mean values may decrease by 21.2%, 33.2% and 53.4% relative to the reference period. In some extreme projections, the  $ET_A$  of  $\beta$ -type pixels were reduced in consideration with the general rule that the long-term water balance cannot be

negative. The intensified  $ET_A$  increase of the  $\beta$ -pixels can lead to possible serious consequences, such as the risk of the wetlands (e.g., Little-Balaton wetland area) drying out. The tendency is similar to Nováky's projections (Nováky, 2008), where the decreasing runoff and inflow from the catchments may not be enough to balance the increasing evaporation from the Balaton Lake.

The projected changes of  $ET_A$  and  $R$  for the Bácsbokodi-Kígyós watershed are shown in Fig. 8. The  $ET_A$  compared to the reference period shows 1.1%, 4.4%, and 4.3% mean relative increase in the first, second, and third future climate period, respectively. Spread of the  $ET_A$  and  $R$  results (due to the range of the 12 regional climate model simulation results) is the largest in the last period of interest. For  $R$ , the arithmetic mean of the 12 projections shows a decrease by 15.0%, 18.5%, and 38.7%, in the investigated future periods relative to the period 1981–2010. The maximum decrease can reach 85.3% by the end of the century. The decrease likely not will be as strong as in the case of the Zala watershed – where the intensified  $ET_A$  increase of the  $\beta$ -pixels will dominate –, but the decreasing usable water stock may limit agricultural activities and changes may be necessary (e.g., more irrigation, fewer water demanding crops).

#### 4. Summary

The aim of this study was to examine the possible effects of climate change on the water balance in Hungary (for two selected watersheds), and to present a hydrological model that is able to estimate long-term evapotranspiration and runoff changes. The selected study areas were the Zala (which is the most important part of the Balaton Lake watershed) and Bácsbokodi-Kígyós watersheds.

The analysis was based on a spatially distributed robust hydrological model (1 km × 1 km resolution) which was calibrated using actual evapotranspiration values of CREMAP. In the period of 2000–2008, the evapotranspiration ( $ET$ ) and runoff ( $R$ ) were 92% and 8% of the precipitation in the Zala watershed, and 75% and 25% in the Bácsbokodi-Kígyós watershed. Higher  $ET$  rates were valid for the Zala due to the larger forest cover. The differences between the CREMAP and the watershed calculated  $ET$  (for the calibration period) for the Zala and for Bácsbokodi-Kígyós watershed were only 2.0% and 2.3%, respectively.

A climate-runoff model for evaluating the effects of climate change on  $ET$  and  $R$  was presented. The parameters of the Budyko model ( $\alpha$ ) were calculated for pixels without surplus water. For the extra water affected pixels, where the evapotranspiration exceeded the precipitation (e.g., by surface or subsurface inflow), a linear model with  $\beta$  parameters (actual evapotranspiration / pan evaporation) was introduced.

Since the development of the climate-runoff model includes some general relations for Hungary, it can be adapted only for places with similar climatic

conditions. The  $\alpha$  and  $\beta$  model parameters can be calculated if spatially distributed (long-term) evapotranspiration, temperature, and precipitation data are available. Then  $\alpha$  and  $\beta$  can be used with regional climate models data for calculating  $ET$  and  $R$  projections in a spatially distributed way. The uncertainties of the projections stem from the following sources: uncertainty of the CREMAP  $ET$  and the measured meteorological data (used for calculating  $\alpha$  and  $\beta$ ), and the uncertainty of the climate projections. The model ignores the land cover change in the future because there are only assumptions available about this (e.g. the extra water affected areas may decrease; there may be more artificial surfaces).

Hydrological projections for the Zala and Bácsbokodi-Kígyós watersheds have been achieved using the  $\alpha - \beta$  climate-runoff model. According to the projections, the mean annual temperature will be higher in the 21st century (by the end of the century more than 3 °C higher relative to the period 1981–2010), while the projected change of the annual precipitation sum is not significant. Although the spread of the projections increases with time, the tendency is clear: the hydrological balance will move toward evapotranspiration, resulting in a decrease of the long-term runoff. By the end of the 21st century, the mean annual evapotranspiration is expected to increase by more than 4% for the Zala and Bácsbokodi-Kígyós watersheds relative to the reference period (1981–2010). Due to the increasing temperature, the climate will be drier, a slight increase in evapotranspiration and a significant decrease in the long-term runoff can be detected; the mean decrease for the investigated watersheds can exceed 53% and 38%, respectively. This runoff decrease could lead to serious consequences for the Zala watershed including the risk of the wetlands drying out and the worsening of the average water balance of the Balaton Lake. Aridity may also increase in the Bácsbokodi-Kígyós watershed, where a reduction in utilizable water resources may limit or alter agricultural activities. These results can help provide long-term plans in several fields (water management, agriculture, forestry, etc.) and help decision makers recognize the necessary courses of action.

**Acknowledgements:** The research was supported by the “Agroclimate 2 (VKSZ\_12-1-2013-00-34)” EU-national joint funded research project. The research of *Péter Csáki* was supported by the ÚNKP-17-3-III New National Excellence Program of the Ministry of Human Capacities. This paper was also supported by the János Bolyai Scholarship of the Hungarian Academy of Sciences. The research of *Zoltán Gribovszki* was supported by the European Union and the State of Hungary, co-financed by the European Social Fund in the framework of TÁMOP 4.2.4. A/2-11-1-2012-0001 'National Excellence Program'.

## References

- Antofie, T., Naumann, G., Spinoni, J., and Vogt, J., 2015: Estimating the water needed to end the drought or reduce the drought severity in the Carpathian region. *Hydrol. Earth Syst. Sc.* 19.1, 177–193. <https://doi.org/10.5194/hess-19-177-2015>
- Bartholy, J., Bozó, L., and Haszpra, L., 2011: Klímaváltozás – 2011, Klímaszcenáriók a Kárpát-medence térségére. MTA- ELTE Meteorológiai Tanszék. (in Hungarian)
- Bartholy, J., Pongrácz, R., Gelybó, Gy., and Szabó, P., 2008: Analysis of expected climate change in the Carpathian basin using the PRUDENCE results. *Időjárás* 112, 249–264.
- Bouchet, R.J., 1963: Evapotranspiration réelle et potentielle, signification climatique. *IAHS Publ.* 62, 134–142.
- Budyko M.L., 1974: *Climate and Life*. Academic, Orlando, Fla.
- CLC, 2006: Corine Land Cover. European Environment Agency, European Topic Centre for Spatial information and Analysis, Copenhagen, Denmark. Online: <http://www.eea.europa.eu/data-and-maps/data/clc-2006-vector-data-version>.
- Csáki, P., Gyimóthy, K., Kalicz, P., Kisfaludi, B., and Gribovszki, Z., 2015: Development and validation of a climate-runoff model for the Zala River Basin. In: (Eds. Gribovszki, Z., Hlavčová, K., Kalicz, P., Kohnová, S., Carr, G.) *HydroCarpath-2015, Catchment processes in regional hydrology: Linking experiments and modelling in Carpathian drainage basins*. Vienna, Austria, University of West Hungary Press. Paper 3, 7 p.
- Csáki, P., Kalicz, P., Brolly, G.B., Csóka, G., Czimmer, K., and Gribovszki, Z., 2014: Hydrological impacts of various land cover types in the context of climate change for Zala County. *Acta Silvatica et Lignaria Hungarica* 10, 115–129. <https://doi.org/10.2478/aslh-2014-0009>
- Dingman, S.L., 2002: *Physical Hydrology* (2nd edition). Prentice Hall.
- Gálos, B., Führer, E., Czimmer, K., Gulyás, K., Bidló, A., Häsler, A., Jacob, D., and Mátyás, Cs., 2015: Climatic threats determining future adaptive forest management – a case study of Zala County. *Időjárás* 119, 425–441.
- Gerrits, A.M.J., Savenije, H.H.G., Veling, E.J.M., Pfister, L., 2009: Analytical derivation of the Budyko curve based on rainfall characteristics and a simple evaporation model, *Water Resour. Res.*, 45.4, W04403. <https://doi.org/10.1029/2008WR007308>
- HREX, 2012: Éghajlati szélsőségek változásai Magyarországon: Közel múlt és jövő. (eds. Lakatos, M., Szépszó, G., Bihari, Z., Krüzselyi, I., Szabó, P., Bartholy, J., Pongrácz, R., Pieczka, I., Torma, Cs.) [http://www.met.hu/doc/IPCC\\_jelentes/HREX\\_jelentes-2012.pdf](http://www.met.hu/doc/IPCC_jelentes/HREX_jelentes-2012.pdf) (in Hungarian)
- IPCC, 2007: Climate change 2007: Synthesis Report. Contribution of Working Groups I, II and III to the Fourth Assessment Report of the Intergovernmental Panel on Climate Change (eds. Pachauri, R.K. and Reisinger) AIPCC, Geneva, Switzerland, 104 pp. <http://www.ipcc.ch>.
- IPCC, 2014: Climate Change 2014: Synthesis Report. Contribution of Working Groups I, II and III to the Fifth Assessment Report of the Intergovernmental Panel on Climate Change (eds. Core Writing Team, Pachauri R.K., Meyer L.A.). IPCC, Geneva, Switzerland.
- Keve, G., and Nováky, B., 2010: Klímaváltozás hatásának vizsgálata a Bácsbokodi-Kígyós csatorna vízgyűjtőjén Budyko modell alkalmazásával. XXVIII. National Conference of Hungarian Hydrological Society, Sopron, 7–9th July, 2010. (in Hungarian)
- Kjellström, E., Nikulin, G., Hansson, U.L.F., Strandberg, G., and Ullerstig, A., 2011: 21st century changes in the European climate: uncertainties derived from an ensemble of regional climate model simulations. *Tellus A*, 63, 24–40. <https://doi.org/10.1111/j.1600-0870.2010.00475.x>
- Kovács, Á., 2011: Tó- és területi párolgás becslésének pontosítása és magyarországi alkalmazásai. PhD thesis, Budapest University of Technology and Economics. (in Hungarian)
- Lakatos, M., Szentimrey, T., Bihari, Z., and Szalai, S., 2013: Creation of a homogenized climate database for the Carpathian region by applying the MASH procedure and the preliminary analysis of the data. *Időjárás* 117, 143–158., [www.carpatclim-eu.org](http://www.carpatclim-eu.org)
- van der Linden, P., and Mitchell, J.F.B. (eds.), 2009: ENSEMBLES: Climate Change and its Impacts: Summary of research and results from the ENSEMBLES project. Met Office Hadley Centre, FitzRoy Road, Exeter EX1 3PB, UK.

- McMahon, T.A., Peel, M.C., Lowe, L., Srikanthan, R., and McVicar, T.R., 2013: Estimating actual, potential, reference crop and pan evaporation using standard meteorological data: pragmatic synthesis, *Hydrol. Earth Syst. Sci.* 17, 1331–1363. <https://doi.org/10.5194/hess-17-1331-2013>
- Nováky, B., 1985: A lefolyás éghajlati adottságai a Zagyva-Tarna vízrendszerben. *Vízügyi Közlemények* 1, 78–93 (in Hungarian)
- Nováky, B., 2002: Mapping of mean annual actual evaporation on the example of Zagyva catchment area. *Időjárás* 106, 227–238.
- Nováky, B., 2008: Climate change impact on water balance of Balaton Lake. *Water Science and Technology* 58, 1865–1869. <https://doi.org/10.2166/wst.2008.563>
- Nováky, B., and Bálint, G., 2013: Shifts and Modification of the Hydrological Regime Under Climate Change in Hungary. INTECH Open Access Publisher. <https://doi.org/10.5772/54768>
- Pálfai, I., 2010: Water-balance characteristics of the Danube-Tisza interfluvial region. *Hidrol. Közl.*, 90, 40–44. (In Hungarian)
- Pongrácz, R., Bartholy, J., and Kis, A., 2014: Estimation of future precipitation conditions for Hungary with special focus on dry periods, *Időjárás* 118, 305–321.
- Schreiber, P., 1904: Über die Beziehungen zwischen dem Niederschlag und der Wasserführung der Flüsse in Mitteleuropa, *Z. Meteorol.* 21, 441–452.
- Sun, G.K., Alstad, J., Chen, S., Chen, C.R., Ford, G., Lin, C., Liu, N., Lu, S.G., McNulty, H., Miao, A., Noormets, J.M., Vose, B., Wilske, M., Zeppel, Y., and Zhang Z., 2011: A general projective model for estimating monthly ecosystem evapotranspiration. *Ecohydrol.* 4, 245–255. <https://doi.org/10.1002/eco.194>
- Szilágyi, J. and Józsa, J., 2008: Klímaváltozás és a víz körforgása. *Magyar tudomány*, 2008, 698–703. (In Hungarian)
- Szilágyi, J. and Józsa, J., 2009: Estimating spatially distributed monthly evapotranspiration rates by linear transformations of MODIS daytime land surface temperature data. *Hydrology and Earth System Sciences*, 13, 629–637. <https://doi.org/10.5194/hess-13-629-2009>
- Szilágyi, J. and Kovács, Á., 2010: Complementary-relationship-based evapotranspiration mapping (cremap) technique for Hungary. *Periodica Polytechnica. Civil Engineering*, 54, 95. <https://doi.org/10.3311/pp.ci.2010-2.04>
- Szilágyi, J. and Kovács Á., 2011: A calibration-free evapotranspiration mapping technique for spatially-distributed regional-scale hydrologic modeling, *J. Hydrol. Hydromech.* 59, 118–130.
- Szilágyi, J. and Vörösmarty, C., 1997: Modelling unconfined aquifer level reductions in the area between Danube and Tisza rivers in Hungary, *J. Hydrol. Hydromech.* 45, 328–347.
- Venables, W.N., and Ripley, B.D., 1999: Modern Applied Statistics with S– PLUS. Third Edition. New York: Springer. <https://doi.org/10.1007/978-1-4757-3121-7>
- Virág, Á., 1997: A Balaton múltja és jelene. Egri Nyomda Kft., Eger. (in Hungarian)
- Vörösmarty, C.J., Federer, C.A., and Schloss, A.L., 1998: Potential evaporation functions compared on US watersheds: Possible implications for global-scale water balance and terrestrial ecosystem modeling, *Journal of Hydrology* 207(3-4), 147–169. [https://doi.org/10.1016/S0022-1694\(98\)00109-7](https://doi.org/10.1016/S0022-1694(98)00109-7)







## INSTRUCTIONS TO AUTHORS OF *IDŐJÁRÁS*

The purpose of the journal is to publish papers in any field of meteorology and atmosphere related scientific areas. These may be

- research papers on new results of scientific investigations,
- critical review articles summarizing the current state of art of a certain topic,
- short contributions dealing with a particular question.

Some issues contain “News” and “Book review”, therefore, such contributions are also welcome. The papers must be in American English and should be checked by a native speaker if necessary.

Authors are requested to send their manuscripts to

*Editor-in Chief of IDŐJÁRÁS*  
P.O. Box 38, H-1525 Budapest, Hungary  
E-mail: [journal.idojaras@met.hu](mailto:journal.idojaras@met.hu)

including all illustrations. MS Word format is preferred in electronic submission. Papers will then be reviewed normally by two independent referees, who remain unidentified for the author(s). The Editor-in-Chief will inform the author(s) whether or not the paper is acceptable for publication, and what modifications, if any, are necessary.

Please, follow the order given below when typing manuscripts.

*Title page* should consist of the title, the name(s) of the author(s), their affiliation(s) including full postal and e-mail address(es). In case of more than one author, the corresponding author must be identified.

*Abstract:* should contain the purpose, the applied data and methods as well as the basic conclusion(s) of the paper.

*Key-words:* must be included (from 5 to 10) to help to classify the topic.

*Text:* has to be typed in single spacing on an A4 size paper using 14 pt Times New Roman font if possible. Use of S.I.

units are expected, and the use of negative exponent is preferred to fractional sign. Mathematical formulae are expected to be as simple as possible and numbered in parentheses at the right margin.

All publications cited in the text should be presented in the *list of references*, arranged in alphabetical order. For an article: name(s) of author(s) in Italics, year, title of article, name of journal, volume, number (the latter two in Italics) and pages. E.g., *Nathan, K.K.*, 1986: A note on the relationship between photo-synthetically active radiation and cloud amount. *Időjárás* 90, 10–13. For a book: name(s) of author(s), year, title of the book (all in Italics except the year), publisher and place of publication. E.g., *Junge, C.E.*, 1963: *Air Chemistry and Radioactivity*. Academic Press, New York and London. Reference in the text should contain the name(s) of the author(s) in Italics and year of publication. E.g., in the case of one author: *Miller* (1989); in the case of two authors: *Gamov and Cleveland* (1973); and if there are more than two authors: *Smith et al.* (1990). If the name of the author cannot be fitted into the text: (*Miller*, 1989); etc. When referring papers published in the same year by the same author, letters a, b, c, etc. should follow the year of publication. DOI numbers of references should be provided if applicable.

*Tables* should be marked by Arabic numbers and printed in separate sheets with their numbers and legends given below them. Avoid too lengthy or complicated tables, or tables duplicating results given in other form in the manuscript (e.g., graphs). *Figures* should also be marked with Arabic numbers and printed in black and white or color (under special arrangement) in separate sheets with their numbers and captions given below them. JPG, TIF, GIF, BMP or PNG formats should be used for electronic artwork submission.

*More information* for authors is available: [journal.idojaras@met.hu](mailto:journal.idojaras@met.hu)

Published by the Hungarian Meteorological Service

---

Budapest, Hungary

**INDEX 26 361**

**HU ISSN 0324-6329**